

CALIFORNIA PATH PROGRAM
INSTITUTE OF TRANSPORTATION STUDIES
UNIVERSITY OF CALIFORNIA, BERKELEY

Development of Requirement Specifications for Transit Frontal Collision Warning System

**Xiqin Wang, Joanne Lins, Ching-Yao Chan,
Scott Johnston, Kun Zhou, Aaron Steinfeld,
Matt Hanson, Wei-Bin Zhang**

**California PATH Research Report
UCB-ITS-PRR-2003-29**

This work was performed as part of the California PATH Program of the University of California, in cooperation with the State of California Business, Transportation, and Housing Agency, Department of Transportation; and the United States Department of Transportation, Federal Highway Administration.

The contents of this report reflect the views of the authors who are responsible for the facts and the accuracy of the data presented herein. The contents do not necessarily reflect the official views or policies of the State of California. This report does not constitute a standard, specification, or regulation.

Final Report for MOU 3018

November 2003

ISSN 1055-1425

Development of Requirement Specifications for

Transit Frontal Collision Warning System

Task Order 3018 Final Report

Xiqin Wang, Joanne Lins, Ching-Yao Chan, Scott Johnston, Kun Zhou,
Aaron Steinfeld¹, Matt Hanson, and Wei-Bin Zhang

California PATH Program
University of California at Berkeley

In collaboration with

Federal Transit Administration
San Mateo Transit District
California Department of Transportation
Gillig Co.



¹ Formerly associated with PATH

Acknowledgement

This project was sponsored by the U.S. Department of Transportation, Federal Transit Administration (FTA) under the National Intelligent Vehicle Initiative Program. The contents of this report reflect the views of the authors, who are responsible for the facts and the accuracy of the data presented herein.

The project team would like to thank Denso Co. for its contribution and costshare of the lidars used for the prototype collision warning system. The authors of this report would also like to express our appreciation to Brian Cronin of FTA for his guidance and support, Dave Nelson, Paul Kretz, Dan Empey, Bart Duncil, Thang Lian, Mark Miller, Doug Cooper and Steven Shladover of PATH, Sonja Sun and Ron Deleon of Caltrans, Frank Burton, Chuck Harvey, Jerie Moeller and James Castagno of SamTrans and Gail Ewing and Brian Macloed of Gillig for their technical assistance and support, and the Advisory Committee members for their active participation in the project.

Introduction

The U.S. Department of Transportation (US DOT) initiated the Intelligent Vehicle Initiative (IVI) Program with the goal of improving safety through the application of advanced technologies. The frontal collision warning function has been identified as one of the key safety improvement measures for the transit vehicle platform of the IVI Program. Frontal collision, defined as a bus colliding with a vehicle in front of the bus, is a frequent incident in transit bus operations and the cause of property damage, personal injuries, and interruption to bus operations. A team that includes San Mateo County Transit District (SamTrans), the University of California PATH Program (PATH), California Department of Transportation (Caltrans), and the Gillig Corporation has been selected by the US DOT to develop and validate performance and technical requirement specifications for Frontal Collision Warning Systems (FCWS) for transit buses. Additionally, a group of local transit agencies are participating in the project in an advisory capacity. The project began in January 2000 with a planned duration of two years.

SamTrans operates a fleet of 316 buses in the counties of San Mateo, Santa Clara, and San Francisco that covers one of the most congested areas in the United States. Crash statistics tracked by SamTrans in recent years indicate frontal collisions can result in significant property damage and liability. In addition to frontal collisions, passenger falls resulting from emergency braking also contribute to an increased potential for passenger injuries and liability. This finding is further supported by the crash data collected by a number of transit agencies in the Bay Area (members of FCWS Bay Area Transit Advisory Committee). The crash data analysis suggests that a FCWS using advanced sensing and computer technologies can potentially reduce frontal collision rates, which will minimize losses and reduce operational interruptions. The collision warning system may also help the driver to adequately respond to the hazard with smoother maneuvers. Furthermore, information collected through sensors can be recorded for the purpose of crash analysis and for avoiding false claims.

The **purpose** of the transit Frontal Collision Warning System (FCWS) under the context of this project are to (a) address imminent crashes, (b) provide warnings for smoother maneuvering, and (c) provide warnings when a bus is too close to a forward vehicle.

Previous studies on collision warning and collision avoidance have focused on highway applications, freight trucks, and light-duty passenger cars. The project team has conducted a literature review and found no existing work on FCWS for transit buses, the subject of the current project. The transit bus application environment differs from existing CWS development efforts mainly in the following two ways. First of all, most of the transit frontal collisions occurred in urban areas. The urban and suburban operating environment is dramatically different from those targeted in previous CWS studies, thus presenting considerable challenges with respect to the diversity of obstacles to be detected and the different traffic patterns. The transit FCWS must be able to deal with the environment that current CWS deals with as well as in complicated urban settings. The second major difference is the driver/passenger population. Transit bus drivers are professional drivers who may have different needs from and sensitivities to a FCWS. In addition, operators have expressed concern regarding the presentation of warnings that can be detected by passengers. Bus passengers may find warnings for advance cues of potential threats to be annoying and potentially alarming. There is a lack of past human factors research in FCWS within the transit environment. Topics that need further examination include visual display placement, warning thresholds for both advanced cues and critical warnings, and the impact of transit specific driving tasks.

Despite the differences between the collision warning applications, the FCWS for transit buses requires the same functional elements that are used by other CWS. A principal functional element of a CWS is sensing and detection of presence of a hazardous object. This function must be able to match the environment in which it is intended to be used. A second functional element is the warning generation function that: (1) processes the sensory information to ‘detect’ the targets that may potentially collide with the bus, (2) determines the threat level, and (3) generates warnings at an appropriate time. The third functional element is the Driver Vehicle Interface (DVI) which communicates the warning message to the driver. Figure 1 depicts the functional description of the collision warning system.

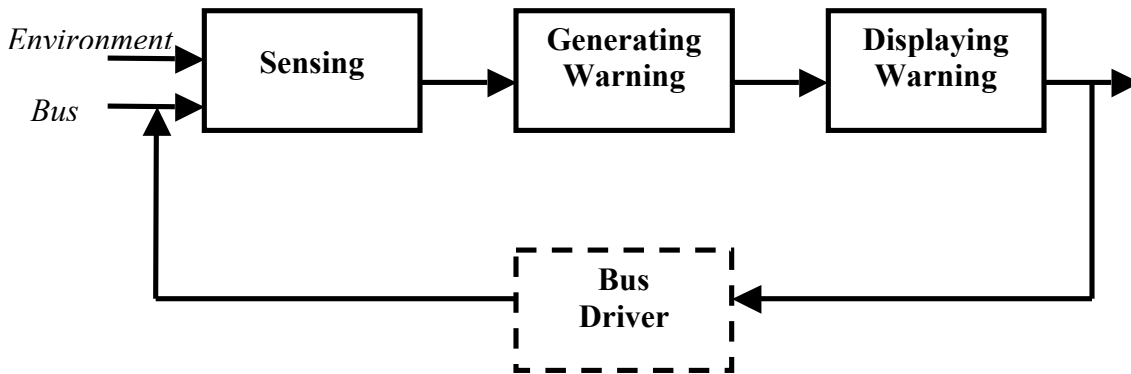


Fig. 0.1 Frontal collision warning system functions

The project team, under the direction of the Federal Transit Administration (FTA) and the support of the FCWS Advisory Committee, conducted research on the requirement specifications for FCWS for transit buses. The scope of the project includes:

1. Perform literature and national data review
2. Analyze frontal collisions
3. Develop a definition of FCWS functions and preliminary functional requirements
4. Develop a data acquisition system for data collection
5. Collect data
6. Study approaches for the FCWS
7. Design collision warning scheme and algorithm
8. Build and test the FCWS
9. Perform field verification and validation tests
10. Develop requirement specifications

In addition, following the requirement analysis process defined under the System Engineering Process (SEP), the team emphasized the following aspects of the analysis:

(1) Data collection and analysis: In order to define the operational environment and the bus operation scenarios, a thorough data collection and analysis effort was conducted, which established a foundation for the determination of sensor performance and system specifications and for the definition of the performance requirements.

(2) Study of driver needs: As bus drivers are the intended users of the transit FCWS, it is important to form the requirements and to develop the FCWS to meet the driver’s needs. To do

so, the FCWS team has closely interacted with SamTrans drivers to understand their needs, expectations, operational environment and to define system boundaries.

(3) Verification of requirements through field testing: In order to verify that the performance requirements developed under this project are indeed within a reasonable and reachable range, a prototype FCWS was developed and instrumented on three SamTrans buses. Field testing of the system under regular service provides valuable inputs to the development of the requirements.

This report summarizes the development efforts conducted in conjunction with the development of performance specifications for FCWS for transit buses.

BACKGROUND

In order to understand the goal of the IVI program and the status of the development of a Frontal Collision Warning System (FCWS), the project team has been conducting a continuous literature review.

Transit IVI

The Transit IVI Committee, composed of the FTA, representative transit agencies, manufacturers, and academia, have identified four user services as high priority transit IVI services, using systems that enable drivers to process information, make better decisions, and operate vehicles more safely:

- 1) Lane Change and Merge Collision Avoidance
- 2) Forward Collision Avoidance
- 3) Rear Impact Collision Mitigation
- 4) Tight Maneuvering/Precision Docking

These services focus particularly on the safety of the driver (and indirectly both passengers and pedestrians) and the vehicle in preventing crashes.

Following a recommendation by the Transit IVI Steering Committee, a study was conducted by Volpe Center to identify and prioritize transit industry requirements and problems involving IVI technologies [4]. This study concluded that although the total number of crashes involving transit buses is relatively small within the national crash data statistics, crashes involving transit buses do result in significant social and economic consequences. The study further indicated that the largest single cost component among the economic cost of crashes of all vehicles, is property damage, which accounted for over one third of total costs. Of equal or greater importance is the safety of the bus passenger and pedestrian public. Among the transit-related IVI applications that have potential to boost safety and efficiency, in-vehicle collision avoidance/warning systems, and in-vehicle obstacle and pedestrian warning systems are listed as highest priority.

The Volpe study further pointed out that the transit industry, with increasingly restricted funding, finds itself bearing the cost of expensive technologies and infrastructure necessary to support their systems. Transit managers cannot afford to be adventurous. There tends to be a reluctance to “be the first” or to be the testing ground in public arenas. There is also a perception in the transit industry that the deployment of new technologies is high-risk. Additionally, there is the need to obtain acceptance from unions where implementing technology changes will affect individuals’ jobs. The importance and uniqueness of the existing transit infrastructure must be recognized. Any deployment of new technologies should be synergistic with existing infrastructure, thus eliminating the need to create new infrastructure accoutrements. Recognizing these unique transit characteristics, it is important for the IVI program to develop collision warning technologies that meet specific transit needs and to conduct field testing to demonstrate system feasibility and cost effectiveness.

Status of development of FCWS

From recent literature, it was found that significant studies have been conducted in various aspects of CWS designs for transportation applications. Research and development efforts have been conducted in the industrial, academic, and governmental sectors. In the last five years, the publications have been quite extensive, indicating that research and development results have gradually materialized and that systems have been commercially deployed. Among the topics of research and development within this review, there are studies across a diverse range of subject areas. Research and development are documented in the following areas:

Crash statistics in publications

Wilson [1] stated that data from the General Estimates System (GES) and the NHTSA Fatal Accident Reporting Systems (FARS) showed that frontal collisions are 23% of all police reported crashes per year. Among them, 77%-84% are caused by driver inattention, and 7%-18% are caused by following too closely.

In another publication [2], statistics showed that 85% of frontal collisions involved two vehicles; equal occurrence at intersection and non-intersection; 91% on straight road, 60% on dry roads; 75% in well-lit conditions; 67% without injuries. GES from 1992 data showed that 59% are caused by the leading vehicle having stopped; 37% by the leading vehicle decelerating; 80% in clear weather and 70% under well-lit conditions; 73% on dry roads; 95% on straight roads.

Asher [3] reiterated that about 20-25% of crashes are frontal collisions and reported that about 60% frontal collisions could be avoided if the driver had an additional 0.5 sec of warning before the incident.

It was estimated in another publication [5] that frontal crashes accounted for 24% of all crashes from NHTSA research. These crashes occurred mostly during the daytime (77%), on straight roads (90%), and under dry weather conditions (79%).

The National Automotive Sampling System (NASS) General Estimates System (GES) provided the most usable data about all types of crashes and related vehicle types. By restricting attention to police-reported crashes, the GES concentrates on those crashes of greatest concern to the safety community and the general public. The GES data was supplemented by direct transit industry input. The five most frequent crash types involving motor coaches are: lane change, intersection, with a parked vehicle, and backing up scenarios. The total for the top five crash categories comprises approximately 87% of crashes involving motor coaches within the United States.

The study by Volpe that focuses on nationwide collision statistics has concluded that the highest-crash-rate-and-severity-rating accident is intersection type of crashes where a bus is struck by another vehicle. The second major scenario is rear-end type of collisions where a bus is struck by another vehicle. These two types of crashes account for almost one third of the top five scenarios. The mid-level types of accidents, which carry a medium range of risk and severity, include the other half of the intersection type of accidents where the bus strikes another vehicle; frontal type where the bus does the striking, and both backing up type of crashes. There remains a critical need for gathering real life data that is transit specific. In order to specifically evaluate the effectiveness of IVI technologies, the crash data needs to be more specific with respect to the crash characteristics, including causal factors. All transit IVI projects should require a detailed crash analysis phase.

Benefits evaluation from selected applications

Farber [6] compared two collision-warning algorithms: Closing Rate Algorithm (CRA) and Stopping Distance Algorithms (SDA). It was estimated that SDA provides advanced warning and eliminates 95-100% crashes, but it also produces a substantial volume of incorrect warnings. CRA provides last moment warnings and only eliminates 65-70% of crashes, but it produces fewer incorrect warnings. This illustrates that a compromise may be necessary between frequent warnings and false alarms.

In a study [7] of CWS for commercial trucks, it was found that a 37% reduction of hard braking of $0.25g$ ($1g = 9.8m/s^2$) or greater could be achieved. This led to a 2-10% reduction in fuel consumption. In one test, fuel savings as high as 20% was obtained. In a separate field review [8] of CWS for heavy-duty trucks, it was revealed from a survey of 171 drivers that 80% changed their way of driving, which had a positive effect.

Even though these evaluation studies have been conducted for different settings and applications, they show that the deployment of CWS potentially can reduce crash numbers and fatalities. It is also significant that by alerting the driver to obstacles ahead there might be a reduction in hard braking which will result in smooth maneuvers, thus leading to fewer passenger falls in the case of transit bus operations.

Sensors

Most collision warning systems demand the use of radar or optical sensing devices. The descriptions of the sensor performances or their design issues have been examined in numerous reports, such as those in [10,8,11,12,13,14]. Wilson [1] gave a comprehensive review of performance guidelines for radar or other forward-looking sensors in the requirements for range, and lateral and vertical field of view. However, those guidelines are given for passenger cars and mainly highway applications.

Human factors research

Past human factors explorations of forward collision warnings have emphasized scaled time-based headway [15 & 16] and binary warnings [17 & 18]. Time-based warnings, often formulated using Time-To-Collision (TTC), have been championed as they are less affected by speed when compared to distance-based warnings. Furthermore, they relate well to models of how drivers maintain longitudinal separation [19].

Binary warnings are more often used for critical scenarios where early warnings would not be possible. For example, a simulator study on how people responded to vehicles cutting in from parked positions compared icons, text commands ("Swerve Left"), and the baseline case of no warning [18]. In some scenarios it will be impossible for sensors to provide advance cues to alert the driver to potential threats. In these events, the system will need to proceed directly into a full warning state, thus emulating a binary warning interface. The aforementioned study did find that drivers were able to gain some benefit from the binary warning.

Recent work on snowplows has used distance-based displays [20] as they were deemed easier to transition to should a sudden period of low visibility (e.g., a white-out) obscure an actively watched forward obstacle. As low visibility is a rare event for a bus, a time-based approach is probably more suitable. The research on snowplows also deemed binary warnings unsafe given

the likelihood of low traction, a scenario that is also conceivable for transit during adverse weather. Furthermore, sharp braking or swerving actions are not desirable within the transit community due to passenger falls. This suggests that binary warnings requiring fast intervention are not preferable for transit applications.

In fact, most literature on visual warnings for CWS applications suggests a graded approach to warnings [21,22,16,23,20]. This commonly involves a scale of some sort implying increased danger. Also commonly suggested is the use of auditory warnings when TTC has reached a critical point and braking action is sorely needed. In fact, auditory tones are incorporated into the Eaton-Vorad CWS, which is offered by several truck OEMs as an option. Research on strictly auditory warnings has also shown beneficial results [17]. Extending this notion was a government-funded study on the value of localized auditory warnings to assist drivers in identifying the location of hazards [24]. While the results suggested that such a feature is promising, the authors also found that such a system requires special care with respect to speaker location and sound choice.

References

1. Intelligent Vehicle Initiative Needs Assessment, FTA-TRI-11-99-33, DOT-VNTSC-FTA, November 1999.
2. T. Wilson, et al., "Forward-Looking Collision Warning System Performance Guidelines," SAE No. 970456, 1997.
3. T. Wilson et al., IVHS Countermeasures for Rear-End Collisions, Task1, Volume II: Statistical Analysis, DOT HS 808 502, 1994.
4. H. Asher, B.A. Galler, "Collision Warning Using Neighborhood Vehicle Information," Proceedings of ITS America, 1996.
5. S. K. Kenue, "Selection of Range and Azimuth Angle Parameters for a Forward Looking Collision Warning Radar Sensor," Proceedings of Intelligent Vehicles, 1995.
6. E. Farber, "Using the REAMACS Model to Compare the Effectiveness of Alternative Rear End Collision Warning Algorithms," Proceedings of IVHS America, 1994.
7. J. Woll, editor, "Radar-based Adaptive Cruise Control for Trucks," 1998.
8. H. Fukuhara, K. Kuniyuki, "Essential Issues involved in Radar-Based Collision Warning/Avoidance System," Proceedings of IVHS America, 1994.
9. Omit.
10. R. Tribe, et al., "Collision Warning," Prometheus – Future Systems, C462/9/183, 1993.
11. W. Ulke et al., "Radar Based Automotive Obstacle Detection System," SAE 940904, 1994.
12. M. Hirschke, "Collision Warning Radar Interference," Proceedings of Intelligent Vehicles, 1995.
13. M. Hirschke, "Interference Resistance Signals for Collision Avoidance Radar," Mark Hirschke, TRB IDEA ITS-21, 1996.
14. C. Eckersten, et al., "A High Performance Automotive Radar for Adaptive Cruise Control and Collision Warning/Avoidance," Proceedings of IEEE ITS Conference, 1997.
15. A.D. Horowitz, "Warning Signal Design: A Key Human Factors Issue in an In-Vehicle Front-to-Rear-End Collision Warning System," Proceedings of the Human Factor Society 36th Annual Meeting, 1992.
16. T. Dingus, et al., "Human Factors Field Evaluation of Automotive Headway Maintenance/Collision Warning Devices," Human Factors, 39, 216-229, 1997.
17. M. Vercruyssen, et al., "Automobile Braking Response Speed: Age Differences and Effects of Collision Warnings," Proceedings of the 1996 Annual Meeting of ITSA (pp. 958-965), 1996.
18. H. Yoo, et al., Automotive Collision Warning Effectiveness: A Simulator Comparison of Text vs. Icons (Technical Report UMTRI-96-29), Ann Arbor, MI: The University of Michigan Transportation Research Institute, 1996.
19. J.A. Misener, et al., "A Focused Examination of Critical Factors and the Emergence of a Cognitive Car Following Driver Model for Rear-End Crashes with a Stopped Lead Vehicle," Transportation Research Board 79th Annual Meeting, 2000, Accepted for Transportation Research Record.
20. Steinfeld, A. H-S. Tan, "Development of a Driver Assist Interface for Snowplows Using Iterative Design," accepted for Transportation Human Factors. Intelligent Vehicle Initiative Needs Assessment, FTA-TRI-11-99-33, DOT-VNTSC-FTA, November 1999.
21. R. Graham, S. Hirst, "The Effect of a Collision Avoidance System on Drivers' Braking Responses," Proceedings of the 4th Annual Meeting of IVHS America (pp. 743-749), 1994.
22. T. Wilson, et al., "IVHS countermeasures for rear-end collisions, driver warning system performance guidelines," Proceedings of the 1996 Annual Meeting of ITSA (pp. 949-957), 1996.

23. T. Dingus, et al., "Human Factors Design Issues for Crash Avoidance Systems," in W. Barfield & T. Dingus (Eds.), *Human Factors in Intelligent Transportation Systems* (pp. 55-93). Mahwah, NJ: Lawrence Erlbaum Associates, 1998
24. A.K. Tan, N. Lerner, *Acoustic Localization of In-Vehicle Crash Avoidance Warnings as a Cue to Hazard Direction* (DOT HS 808 534). Washington, DC: National Highway Traffic Safety Administration, 1996.

1.0 Crash Data Analysis

Frontal collisions account for a significant portion of all collisions. Data from both the National Automotive Sampling System (NASS) General Estimate System (GES) and the NHTSA Fatal Accident Reporting Systems (FARS) showed that frontal collisions are 20-25% of all police reported crashes per year [2,4,5]. Further studies [3,5] showed that frontal collisions occurred mostly during the daytime (~75%), on straight roads (~90%), and under dry weather conditions (60-79%). These studies revealed that 85% of frontal collisions involved two vehicles with equal occurrence at intersection and non-intersection, 77%-84% are caused by driver inattention, and 7%-18% are caused by following too closely, 67% without injuries. Asher [3] reported that about 60% of frontal collisions could be avoided if the driver had an additional 0.5 sec of warning before the incident, which indicated that a collision warning system may offer great potential for reducing frontal collisions.

Both NHTSA and GES accident statistics also included the crash data involving buses. The statistics in NHTSA *Traffic Safety Facts 2000* [5] offers some insights into the types of crashes. Roughly, frontal collisions and rear collisions each account for one-fourth and side collisions half of all crashes. The following table outlines the distribution of crashes by the initial point of impact:

Initial Point of Impact	Number	Percentage
Front	16,000	28.2
Left Side	14,000	24.3
Right Side	13,000	23.3
Rear	13,000	22.9
Non-collision	*	0.3
Other/Unknown	1,000	1.0
Total	56,000	100

**Less than 500 or 0.5 percent.*

The GES data have indicated that the five most frequent crash types involving motor coaches are: lane change, rear end, intersection, parked, and backing up scenarios. The total for the top five crash categories comprises approximately 87% of crashes involving motor coaches within the United States. GES from 1992 data showed that 59% are caused by leading vehicle stopped; 37% are leading vehicle decelerating; 80% are in clear weather and 70% under well-lit conditions; 73% on dry roads; 95% on straight roads.

Following a recommendation by the Transit IVI Steering Committee, a study was conducted by the Volpe Center to identify and prioritize transit industry requirements and problems involving IVI technologies [4]. This study revealed that the highest-crash-rate-and-severity-rating is for intersection type of crashes where a bus is struck by another vehicle. The second major scenario is rear-end type of collisions where a bus is struck by another vehicle. These two types of crashes account for almost one third of the top five scenarios. The mid-level types of accidents, which carry a medium range of risk and severity, include the other half of the intersection type of accidents where the bus strikes another vehicle; frontal type where the bus does the striking, and both backing up types of crashes. The study concluded that although the total number of crashes involving transit buses is relatively small, they result in significant social and economic consequences. Based on GES data, the five most frequent crash types involving buses are: lane

change, rear end, intersection, hitting parked vehicles, and backing up. Between 1994 and 1997, these accounted for approximately 87% of crashes involving buses within the United States.

Although the national crash data provides statistics of transit crashes, detail accident analysis is still needed for the following reasons. In addition to urban transit buses, the national data includes additional sources of bus crashes, specifically school buses and intercity buses. It is not clear the percentage of each vehicle type and the impact of a particular type of vehicles on category of crashes. Additionally, initial study showed that the crashes involving transit buses often occur in very different environments such as urban areas with different speeds from that of automobiles. Furthermore, there is a critical need for gathering real life data that is transit specific so that crash type and associated cost can be investigated in detail to support the benefits of transit IVI systems and provide inputs for developing and implementing FCWS on transit buses. In order to fully understand the environment that transit buses are operated in, the causal factors of frontal collisions involving buses, the characteristics and consequences of these crashes and potential IVI approaches through which frontal collision warning systems can help to prevent or mitigate the identified accident types, the project team has conducted a series of crash data analysis.

In the first phase of the study of frontal collision warning systems, PATH has been working with the AC Transit, Central Contra Costa Transit Authority (CCCTA), Golden Gate Transit (GGT) and San Mateo County Transit District (SMT) in the San Francisco Bay Area to obtain transit crash data. The focus of this initial study is to determine the scenarios relevant to the design and implementation of frontal collision warning systems on transit buses. In the course of working with these agencies, it soon became clear that obtaining detailed collision cost data would not be a straightforward process. In many cases, costs such as damage repair, injury, legal, and compensation payout are not processed or tracked by a single agency department or division and the retrieval of this information often requires hand processing as the relevant information cannot be accessed by computer. In other cases, the handling of legal claims is out-sourced to private organizations (e.g., John Glenn Adjusters & Administrators (JGAA) in the Bay Area), so the data are not available directly from the transit agencies.

Following the initial crash analysis, PATH has worked with JGAA to conduct a detailed investigation of crash costs to support a cost-benefit analysis of transit IVI systems. The objectives of this effort are (1) to further determine crash scenarios in order to assist the improvement of the design and implementation of transit collision warning systems, and (2) to assess the overall costs of incidents or collisions.

In addition to the crash cost data for the SMT, Santa Clara Valley Transportation Authority (VTA), and GGT, JGAA has maintained cost data for the members of the California Transit Insurance Pool (CalTIP), which is an insurance authority currently serving 32 California transit operators (see [Appendix I](#) for a list of all the 32 members). Given the value of the broader database, it was decided to expand the project to include detail crash analysis for CCCTA and Riverside Transit Authority (RTA) and generalized crash analysis for additional 30 CalTIP agencies.

JGAA provided PATH with electronic copies of the crash data. PATH has developed software to automatically process the cost reports and put the information into data forms so that in-depth crash and cost benefit analysis can be carried out.

1.1. Analysis of Detailed Crash Data from 35 California Transit Agencies

The detailed transit crash data analysis is based on the latest five fiscal years (May 1, 1997 to April 30, 2002) of cost data for 35 transit agencies including three in the San Francisco Bay Area and the 32 CalTIP agencies. Those 35 transit agencies operate buses in different regions and operating environments in California, as shown in Figure 1.1 (not shown are the 3 San Francisco Bay Area agencies, VTA, SMT, and GGT).



Figure 1.1 Service coverage of 35 transit agencies

Each incident or crash is indicated as a claim in JGAA’s database. Each claim involves a transit bus and another party, which could be another vehicle, a pedestrian, a stationary object, and/or a passenger on the bus. JGAA tracks the costs in three categories: “Body Injury”, “Property Damage”, and “Legal and Other Fees.” The cost for a claim is the sum of these three types of costs. For each claim, JGAA includes a simple narrative describing what occurred. Different agencies have different cost report formats (see [Appendix II](#) for a sample JGAA cost report).

JGAA uses 103 loss codes to refer to various types of crashes (see [Appendix III](#) for the loss code descriptions.). The code system is designed from a legal perspective, and provides little information about the cause of the crash. It was found to be impossible to retrieve the initial point of impact from the loss code. Loss code 1, for example, indicates a bus going straight ahead colliding with a vehicle from its left at an intersection. This could be a frontal collision if the bus hit the other vehicle or it could be a side collision if the other vehicle ran into the bus. In order to understand the association between crash cost and the initial point of impact, PATH and JGAA have obtained the initial point of impact information for four transit agencies (two are CalTIP agencies) by reviewing the original driver reports and police reports. Four possibilities

are considered for the initial point of impact: front (F), side (S), rear (R), and not-known (N). The statistics from these four agencies are then extended to other agencies.

The 103 loss codes are categorized into three groups:

1. Collision incident: A collision happened between a transit bus and another party.
2. Non-collision incident: Passenger injured on boarding, alighting, or on board (not caused by a collision).
3. Civil Rights and ADA violations.

Table 1.1 summarizes the crash and cost data for the 35 transit agencies. Agency III and IV are CalTIP members, and CalTIP(30) refers to the other 30 CalTIP agencies. For CalTIP agencies, one collision happened per 22,000 revenue miles, and one non-collision incident per 22,000 revenue miles.

Transit Agency	Collision		Non-collision		Violations	
	Claim	Cost	Claim	Cost	Claim	Cost
Agency I	353	\$2,904,763	182	\$1,188,326	11	\$13,500
Agency II	1,146	\$6,319,107	669	\$1,857,460	13	\$35,953
Agency III	358	\$997,982	474	\$858,162	8	\$2,039,006
Agency IV	261	\$1,032,796	363	\$1,174,749	1	\$285
Agency V	261	\$1,032,796	363	\$1,174,749	1	\$285
CalTIP(30)	1,398	\$4,783,760	1,198	\$5,075,349	7	\$442,993
Total	5,255	\$22,354,203	4,285	\$13,583,368	40	\$2,531,737

Table 1.1 Accident cost data for 35-transit agencies (for 5 years)

On average, each collision cost \$4,254, and each passenger injury crash cost \$3,170. Since cost from Civil Right and ADA violations is not directly related to crashes, it is not being included in this analysis.

1.1.1 Crash Costs of Agency I

Most bus routes of Agency I are operated on relatively congested roads. The crash costs for Agency I by crash type and the initial point of impact are summarized in Figures 1.1 and 1.2.

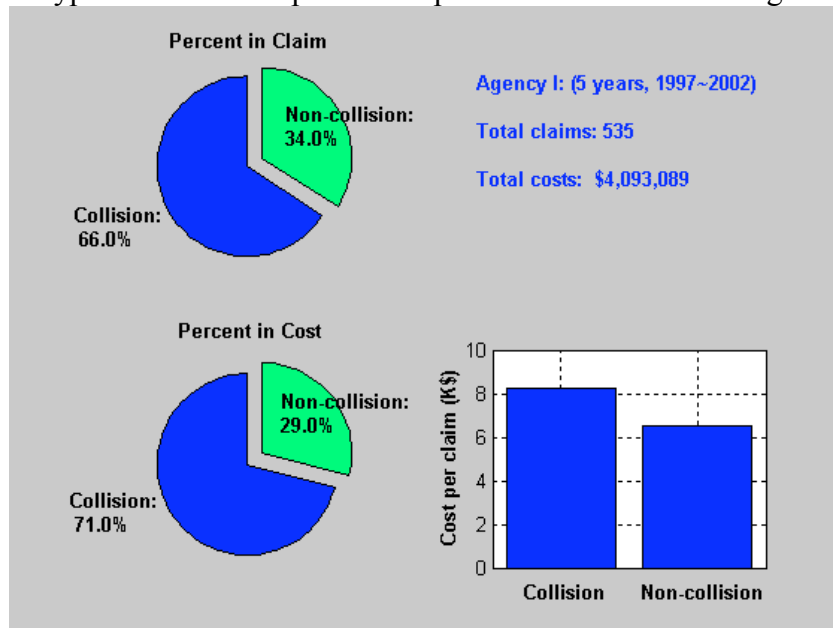


Fig. 1.1 Agency I: Crash costs by incident type

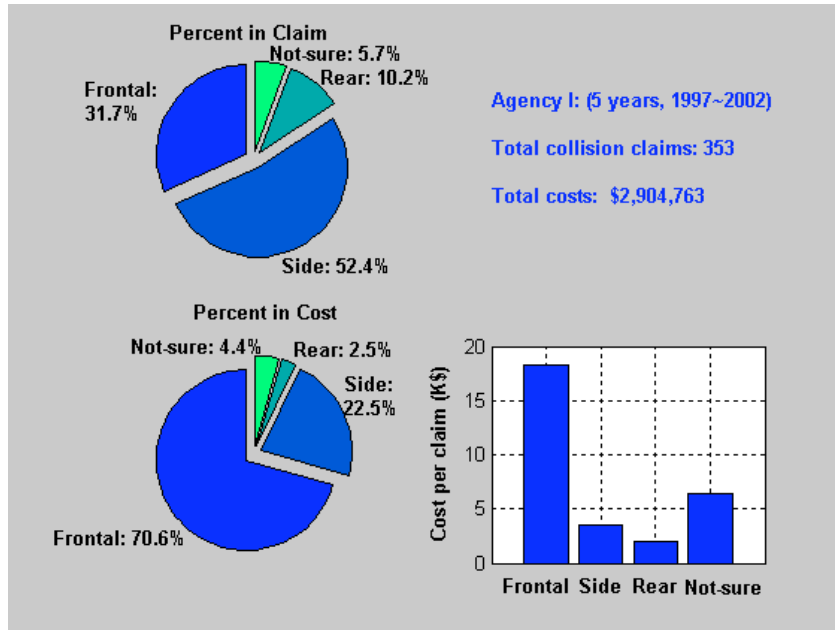


Fig. 1.2 Agency I: Collision costs by initial point of impact

1.1.2 Crash Costs of Agency II

The crash costs for Agency II are summarized in Figures 1.3 and 1.4.

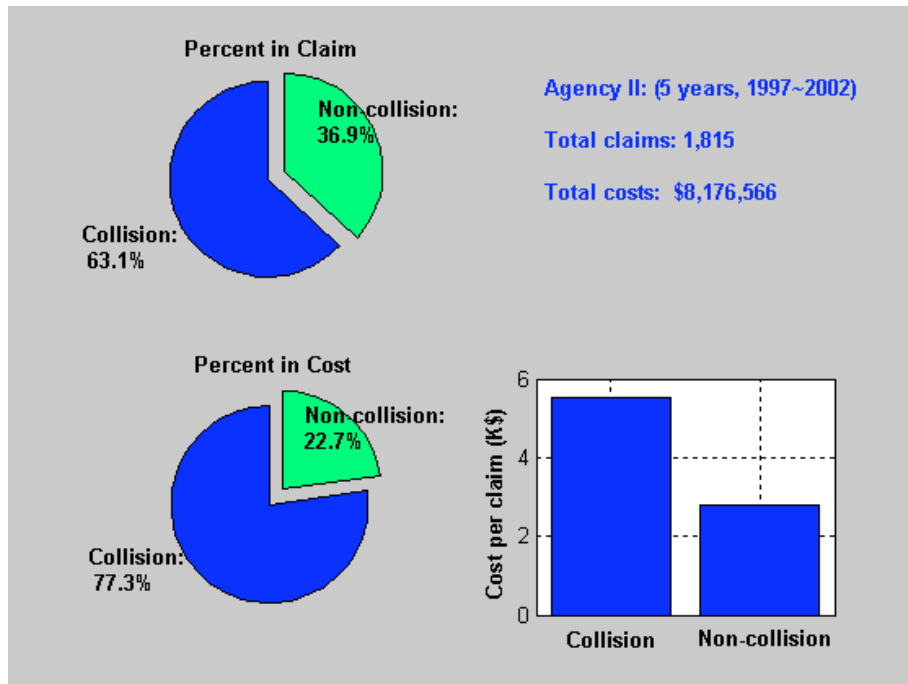


Fig. 2.3 Agency II: Crash costs by incident type

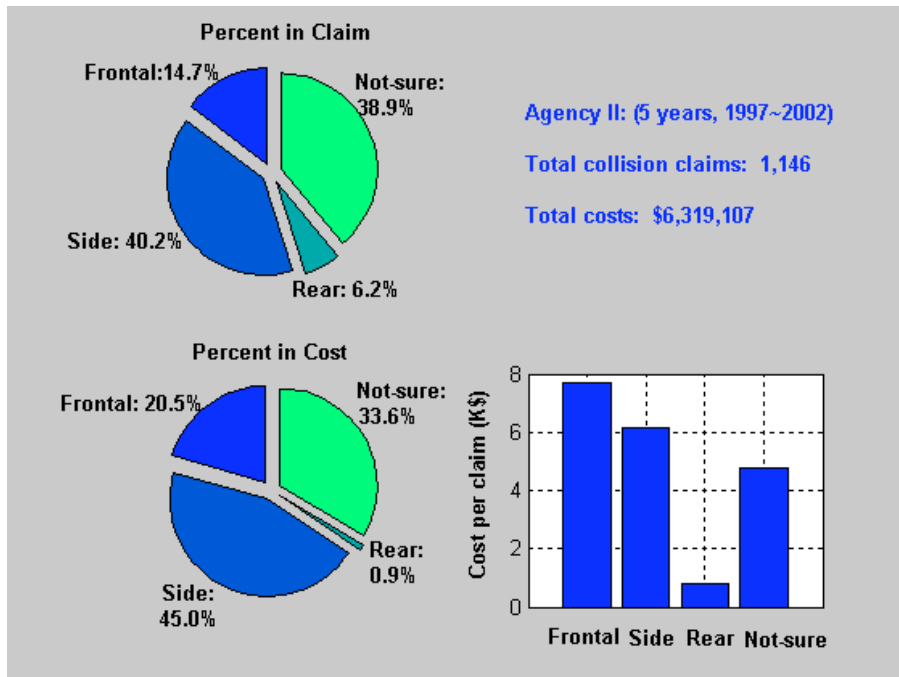


Fig. 1.4 Agency II: Collision costs by initial point of impact

1.1.3 Crash Costs of Agency III

The crash costs for Agency III are summarized in Figures 1.5 and 1.6.

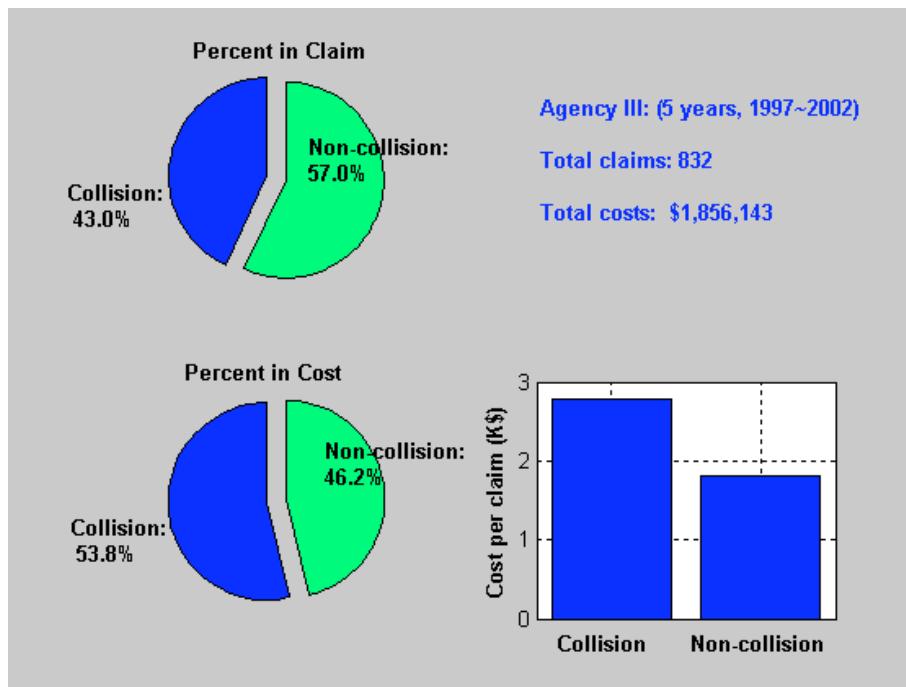


Fig. 1.5 Agency III: Crash costs by incident type

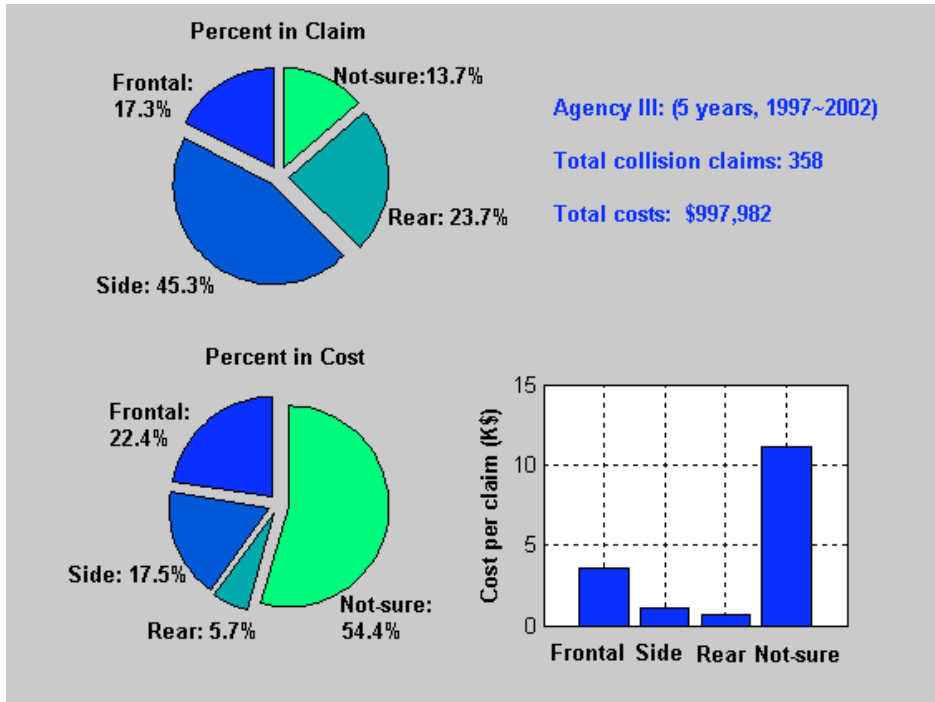


Fig. 1.6 Agency III: Collision costs by initial point of impact

1.1.4 Crash Costs of Agency IV

The crash costs for Agency IV are summarized in Figures 1.7 and 1.8.

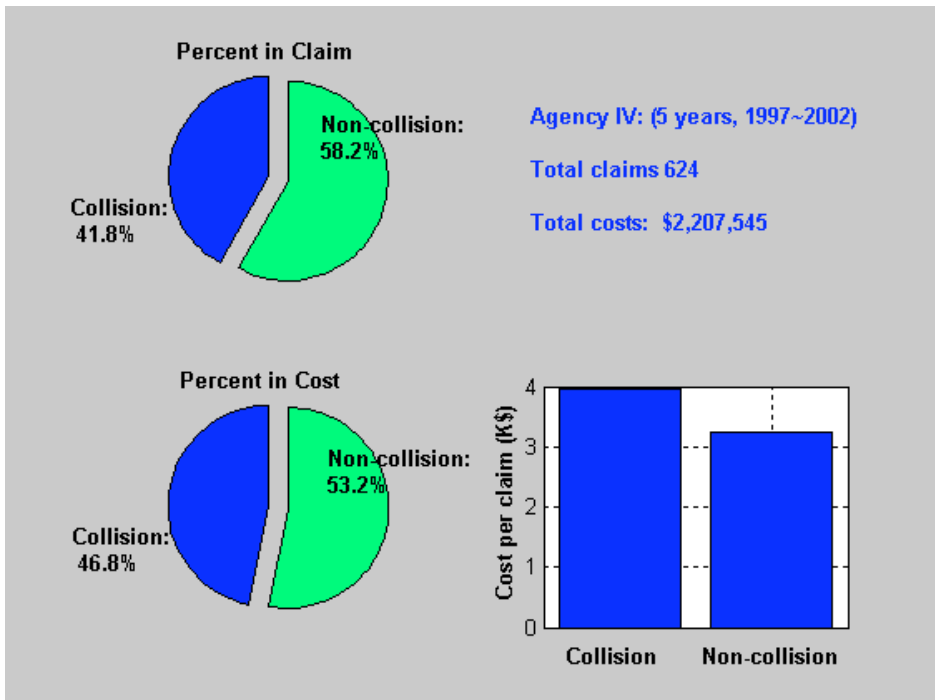


Fig. 1.7 Agency IV: Crash costs by incident type

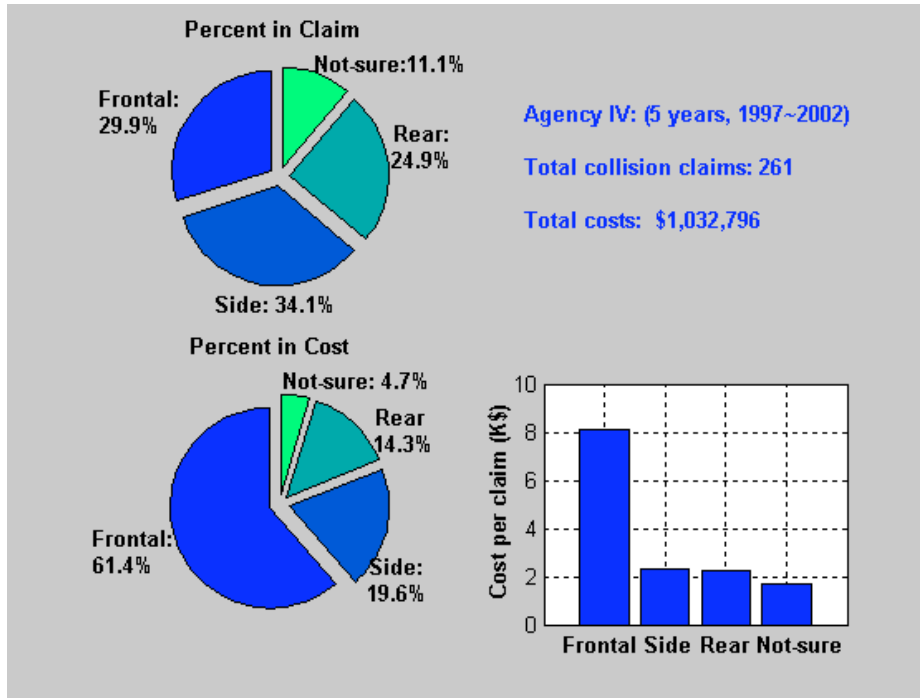


Fig. 1.8 Agency IV: Collision costs by initial point of impact

1.1.5 Distribution of Collision Claims and Costs by Loss Code

As can be seen, the cost distribution by initial point of impact varies from agency to agency. This may be due to the fact that every transit agency has its own driver training program as well as a different operating environment. These can lead to a unique collision pattern and claim distribution. Furthermore, each agency has several severe collisions, each costing more than \$100,000, which can significantly affect the cost statistics.

Although most loss codes cannot be directly associated with an initial point of impact, it was found from the cost data that the claim distribution and cost distribution by loss code and the initial point of impact are very consistent within the four transit agencies for which detailed initial point of impact information was obtained from the original driver and police reports. The data of two CalTIP agencies (agencies III and IV) were selected to generate the claim and cost distributions by loss code and the initial point of impact. These distributions were then applied to the four agencies to verify their accuracy and consistency, and then extended to Agency V and other CalTIP agencies (CalTIP(30)).

There are a total of 47 loss codes that are related to collisions. In order to exclude the affect of severe collisions, only claims costing less than \$10,000 are used to generate the claim distribution, $claim_dist[i][j]$, and cost distribution, $cost_dist[i][j]$, where i refers to the initial point of impact and j refers to the loss code. The original initial point of impact inputs are used for claims costing more than \$10,000. For each transit agency, the generated distributions are applied to claims costing less than \$10,000 as follows

$$claim_est[i] = \sum_j claim[j] \cdot claim_dist[i][j]$$

$$cost_est[i] = \sum_j cost[j] \cdot cost_dist[i][j]$$

where $claim_est[i]$ and $cost_est[i]$ are estimated claim number and crash cost for point of impact i ; and $claim[j]$ and $cost[j]$ are actual claim number and cost by loss code j , which are obtained from the crash data. Finally, the total claims and costs by loss code are given by

$$claim_total[i] = claim_est[i] + claim_review[i]$$

$$cost_total[i] = cost_est[i] + cost_review[i]$$

where $claim_review[i]$ and $cost_review[i]$ are actual claim number and cost by the initial point of impact for claims costing more than \$10,000.

Fig. 1.9 shows the comparison of actual claim and cost distributions by the initial point of impact (top row), and the distributions calculated by using the statistics from Agencies III and IV (bottom row). Again, only crashes with costs less than \$10,000 are considered.

Using the same statistical distributions for crashes costing less than \$10,000, and taking account of those collisions costing more than \$10,000 for which PATH acquired the initial point of impact, Figure 1.10 compares actual cost and claim data (top row) to statistical estimations.

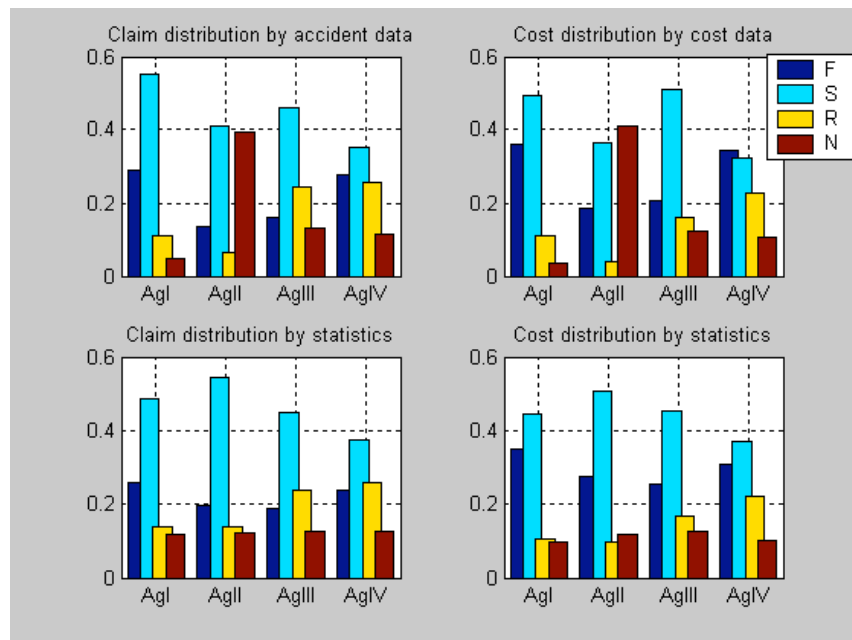


Fig. 1.9 Claim and cost distributions for collisions costing less than 10K

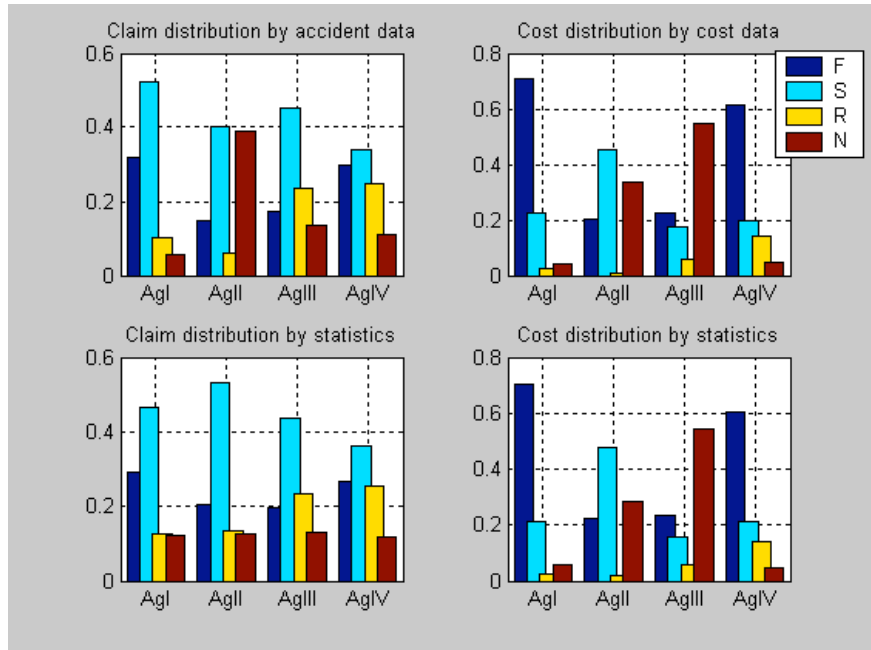


Fig. 1.10 Claim and cost distributions for all collisions

With the exception of Agency II, the derived distributions match the actual distributions quite well (error within 6%). Relatively larger variations can be found for Agency II. This is because 39.5% of its collision accidents have “not-known” initial point of impact due to the information limitation on original reports. This is much higher than other agencies.

1.1.6 Crash Costs of Agency V

The statistics from Agencies III and IV are applied to Agency V for collision claims costing less than \$10,000. PATH has obtained the initial point of impact information for a total of 65 claims which cost more than \$10,000. The results are summarized in Fig. 1.11 and 1.12.

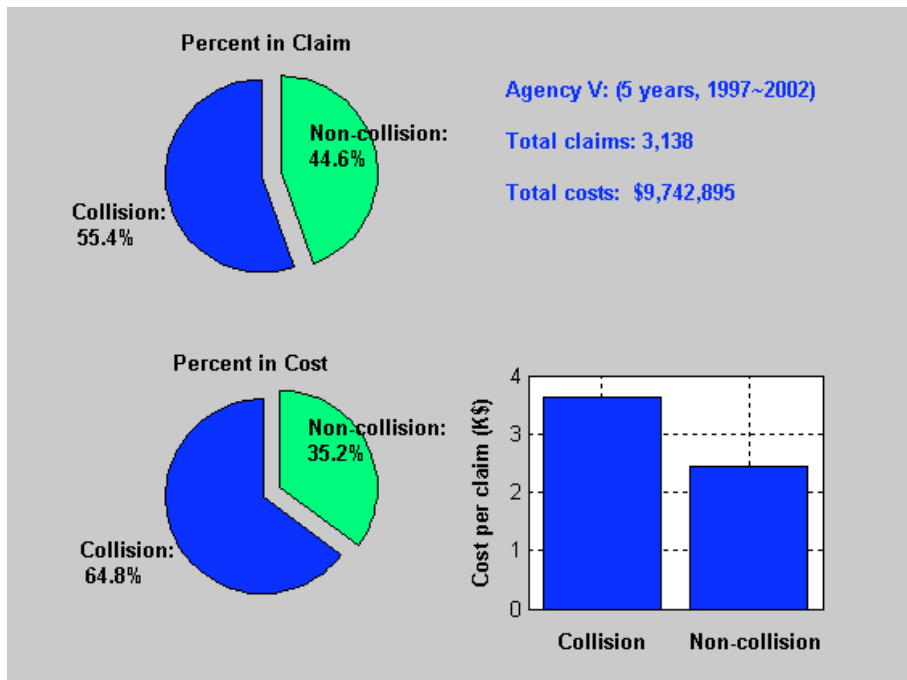


Fig. 1.11 Agency V: Crash costs by incident type

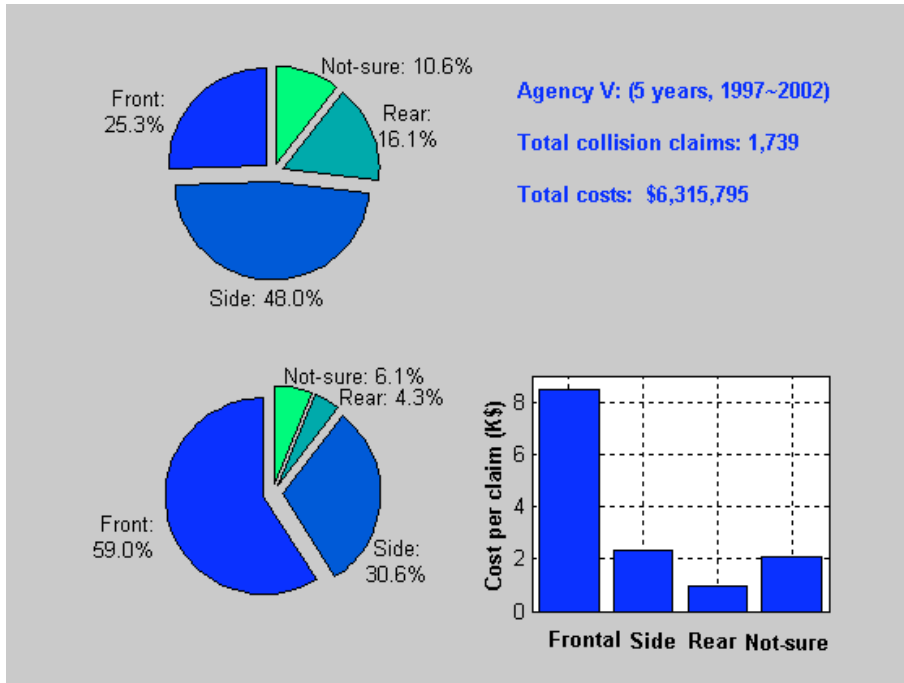


Fig. 1.12 Agency V: Crash costs by initial point of impact

1.1.7 Crash Costs of 30-CalTIP Agencies

Due to the prohibitive cost, in terms of both time and resources, to obtain the initial point of impact information for the 30-CalTIP members, it was decided to apply the statistics from Agencies IV and V to these agencies for collisions costing less than \$10,000. PATH has obtained the initial point of impact information for all the collisions costing more than \$10,000 (a total of 81 accidents). Figures 1.13 and 1.14 summarize the claim and cost data for the combined accident categories of the 30-CalTIP agencies.

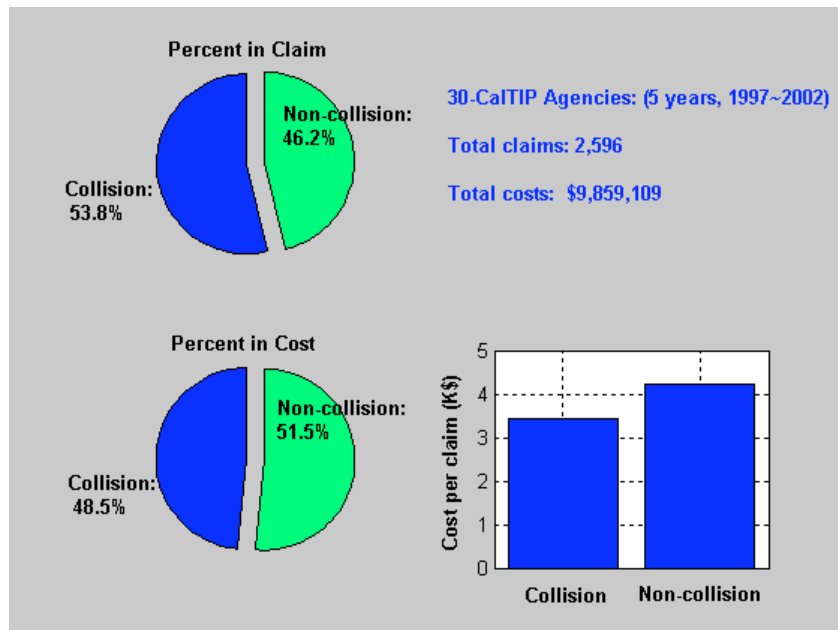


Fig. 1.13 30-CalTIP members: Crash costs by incident type

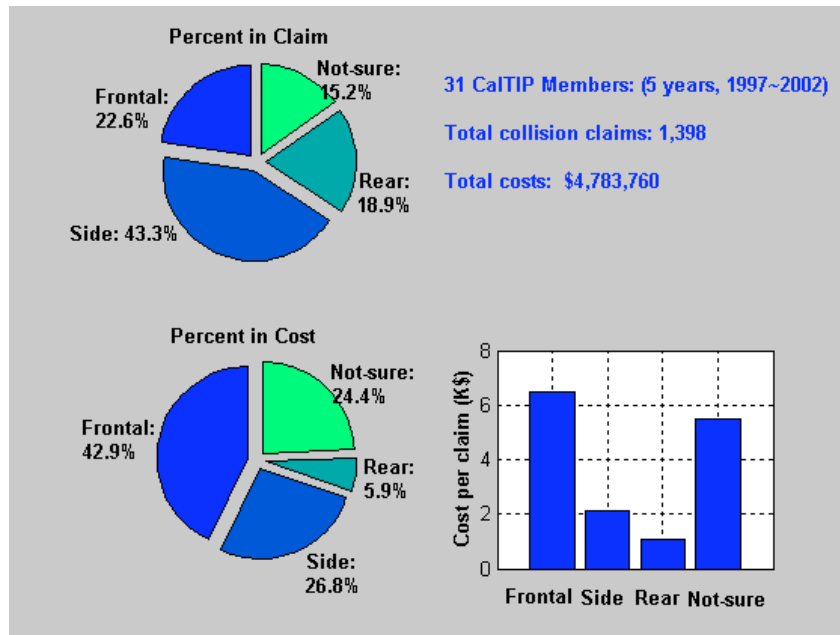


Fig. 1.14 30-CalTIP members: Collision costs by initial point of impact

1.2. In-depth Cost Analysis on Collisions

Two crash severities are defined for collisions: serious casualty (collision costing more than \$100,000), and general collision (collision costing less than \$100,000). Because there are so few fatalities in transit accidents, they are included under serious casualty. Table 1.2 summarizes the cost by crash severity.

Table 1.2 Collision cost data for 35-transit agencies (5 years)

	Claim		Cost	
	Count	Percentage	Amount	Percentage
Serious casualty (Incident costing more than \$100K)	31	0.6%	\$11,563,53	51.7%
General accident (Incident costing less than \$100K)	5,224	99.4%	\$10,790,680	48.3%
Total for 35-transit agencies	5,255	100.0%	\$22,354,203	100.0%

Collisions account for 55.1% of claims and 62.2% of costs among all incidents, as shown in Table 1.3.

Table 1.3 Total accident cost data for 35-transit agencies (5 years)

	Claim		Cost	
	Count	Percentage	Amount	Percentage
Collisions	5,255	55.1%	\$22,354,203	62.2%
Non-collisions	4,285	44.9%	\$13,583,368	37.8%
Total for 35-transit agencies	9,540	100.0%	\$35,937,571	100.0%

1.2.1 Serious Casualty

A few serious casualties account for most costs from collisions. In five fiscal years, there are a total of 31 serious casualties for a total cost of \$11,563,523. They account for 0.6% of claims and 51.7% of costs among all collision accidents. Table 1.4 lists all of the 31 serious casualties which consist of 17 frontal, 7 side, and 7 not-known initial point of impact collisions.

Table 1.4 Serious casualties for 35-transit agencies (5 years)

Claim	Loss Code	Initial Point of Impact	Cost	Crash description
1	2	S	\$195,000	Intersection, going straight bus hit a right turn vehicle
2	9	F	\$162,500	Intersection, bus failure to yield right of way
3	14	S	\$203,300	Sideswipe, bus changing lane
4	19	F	\$130,045	Bus struck a standing vehicle
5	19	S	\$104,727	Bus struck a standing vehicle
6	23	F	\$132,456	Bus rear-ending another vehicle
7	23	F	\$121,335	Bus rear-ending another vehicle
8	23	F	\$127,428	Bus rear-ending another vehicle
9	23	F	\$236,616	Bus rear-ending another vehicle
10	23	F	\$350,640	Bus rear-ending another vehicle
11	23	F	\$158,908	Bus rear-ending another vehicle
12	23	F	\$160,026	Bus rear-ending another vehicle
13	23	F	\$100,207	Bus rear-ending another vehicle
14	24	F	\$172,449	Bus rear-ending another vehicle
15	27	S	\$267,223	Bus pulling from loading zone
16	30	N	\$114,379	Bicyclist veered in front of bus
17	30	S	\$506,313	Bus vs. Bicyclist
18	37	F	\$302,307	Collision, detail unknown
19	37	N	\$258,905	Collision, detail unknown
20	39	N	\$163,542	Bus striking a pedestrian
21	40	S	\$209,278	Bus striking a pedestrian
22	41	F	\$1,642,054	Bus striking a pedestrian
23	42	N	\$429,637	Bus striking a pedestrian (fatal)
24	43	S	\$1,997,950	Bus striking a pedestrian
25	43	N	\$906,025	Bus striking a pedestrian
26	43	F	\$250,000	Bus striking a pedestrian
27	43	F	\$975,000	Bus striking a pedestrian (fatal)
28	43	F	\$298,015	Bus striking a pedestrian
29	43	N	\$106,675	Bus striking a pedestrian
30	43	F	\$326,093	Bus striking a pedestrian
31	48	N	\$454,491	Collision, detail unknown (fatal)
Total			\$11,563,523	

Two scenarios stand out from the others as sources of serious casualties: “bus hitting a pedestrian” (11 claims with 5 front, 2 side and 4 not-known POC), and “bus rear-ending another vehicle” (9 claims, all frontal). They account for 64.5% of claims and 76.7% of costs among all serious casualties.

1.2.2 General Collisions

As shown in Table 1.2, general collisions account for 99.4% of claims and 48.3% of costs among all collisions for the 35-transit agencies.

1.2.3.1 General Collisions by Initial Point of Impact

Figure 1.15 shows the claim and cost distributions by initial point of impact, and Figure 1.16 shows the average cost per claim for each agency. Actual crash and cost data are used for Agencies I, II, III and IV, and the generated distributions by loss code and initial point of impact are used for Agency V and CalTIP(30).

For each agency, side collisions account for the largest number of claims, while frontal collisions account for the greatest cost. Although different agencies have different claim and cost distributions for collisions, in general, frontal collisions account for 15~30% of claims and 30%~50% of costs while side collisions account for 35~50% of claims and 25~35% of costs. On average, each frontal collision costs more than twice as much as a side collision. The point of impact cost ranking, from most costly to least, is frontal, side, then rear collision.

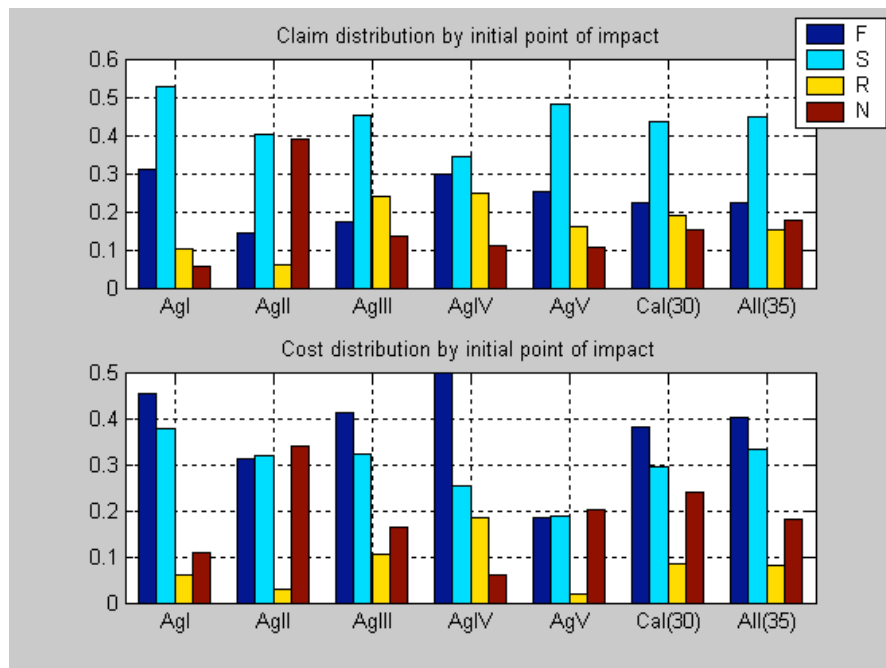


Fig. 1.15 35-transit agencies: General collision costs by initial point of impact

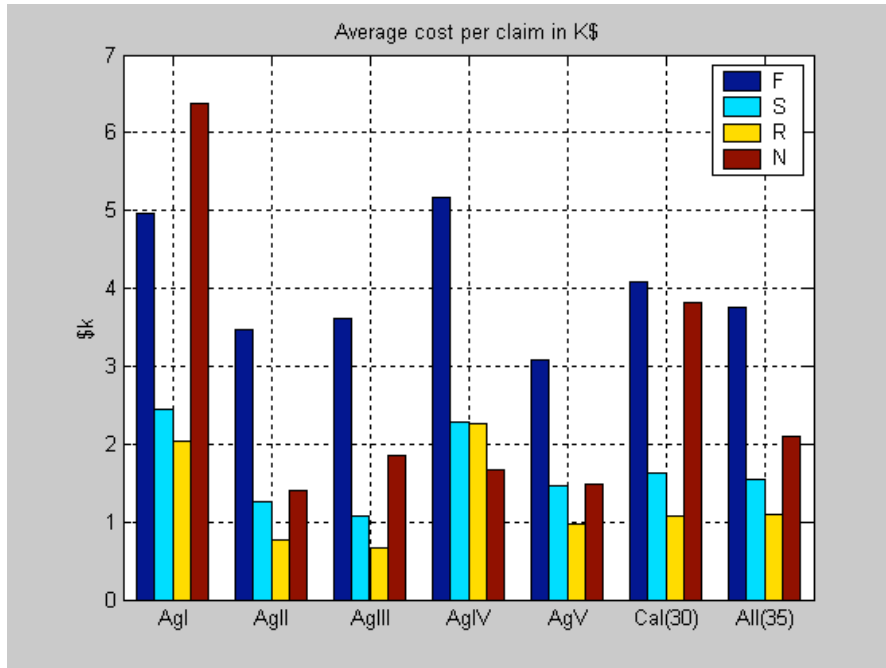


Fig. 1.16 35-transit agencies: Cost per claim by initial point of impact

1.2.2.2 General Collisions by Fiscal Year

Since each transit agency has its own driver training program and operates in a different environment, it is difficult to find crash statistics that are consistent between agencies. The number of crashes and costs by fiscal year do provide interesting detail, however.

Each year, the 35-transit agencies had about 1,000 general collisions which cost \$2 million. Approximately one quarter of these are frontal, and one half are side collisions. The claim costs from these two points of impact account for 40% and 35% of total costs, respectively. This is shown in Figure 1.17 and 1.18.

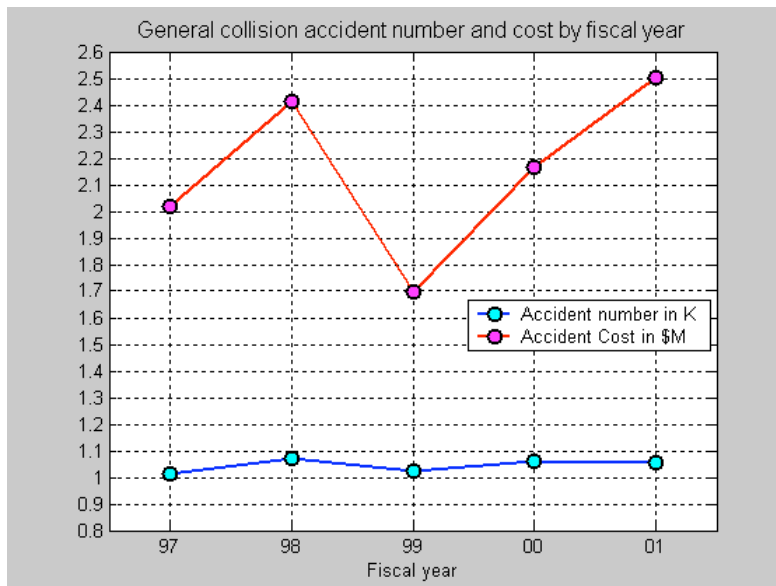


Fig. 1.17 35-transit agencies: General collisions by fiscal year

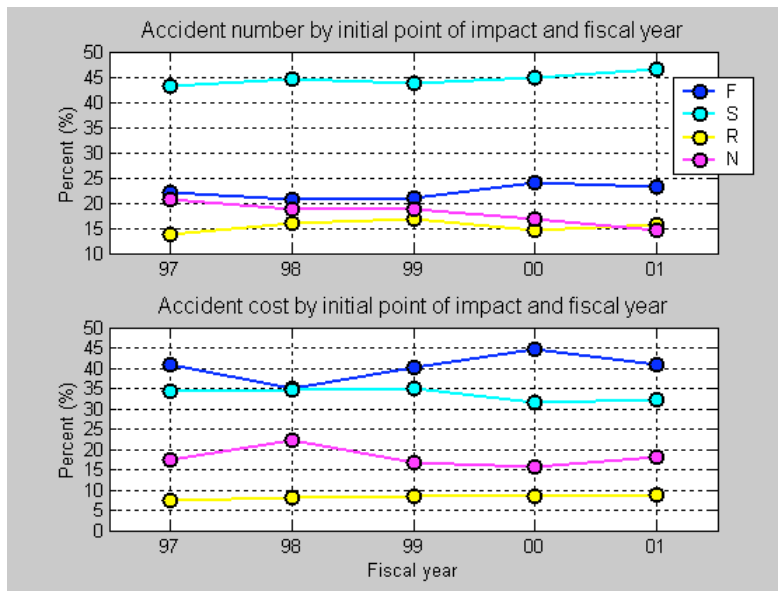


Fig. 1.18 35-transit agencies: General collisions by fiscal year and initial point of impact

1.2.2.3 General Collisions by Collision Object

Collision objects are categorized into three groups: vehicle, pedestrian, and stationary object. Most collisions are vehicle collisions (91.2% of claims and 86.3% of costs). There are only a few pedestrian collisions (3.5% of claims), but they are the most costly. On average, each pedestrian collision cost \$5,583 versus a per vehicle collision cost of \$1,956. The results are shown in Figure 1.19. The ranking of collision objects, from most costly to least, is pedestrian, vehicle, and finally stationary object.

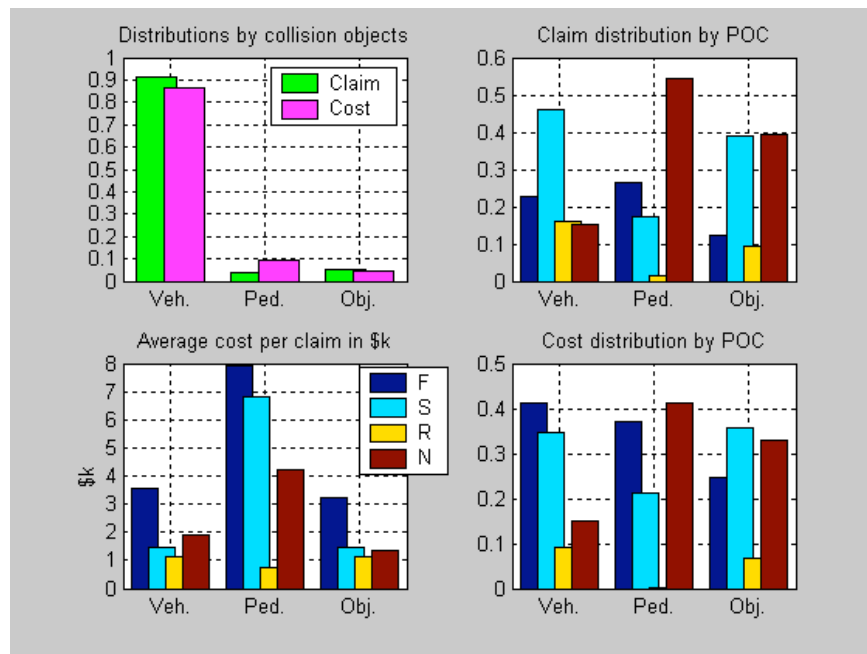


Fig. 1.19 35-transit agencies: General collision costs by collision object

1.2.2.4 Vehicle Collisions by Scenario

Ninety percent of collisions involve a bus colliding with another vehicle. The following eight scenarios have been considered:

Table 1.5 List of accident scenarios

Accident scenario	Stands for
S1	Intersection crash
S2	Bus rear-ending another vehicle (frontal collision)
S3	Collision at bus rear, including bus backing up (rear collision)
S4	Bus hit a standing vehicle
S5	Sideswipe (side collision)
S6	(Other vehicle) Cut-in crash
S7	Loading zone crash
S8	Collision between two buses
S9	Other vehicle collision crash

Five crash scenarios: intersection collision (S1), bus rear-ending another vehicle (S2), bus hitting a standing vehicle (S4), sideswipe (S5), and collision between two buses (S8), account for 65.4% of claims and 74.4% of costs among all vehicle collisions. This is shown in Fig. 1.20.

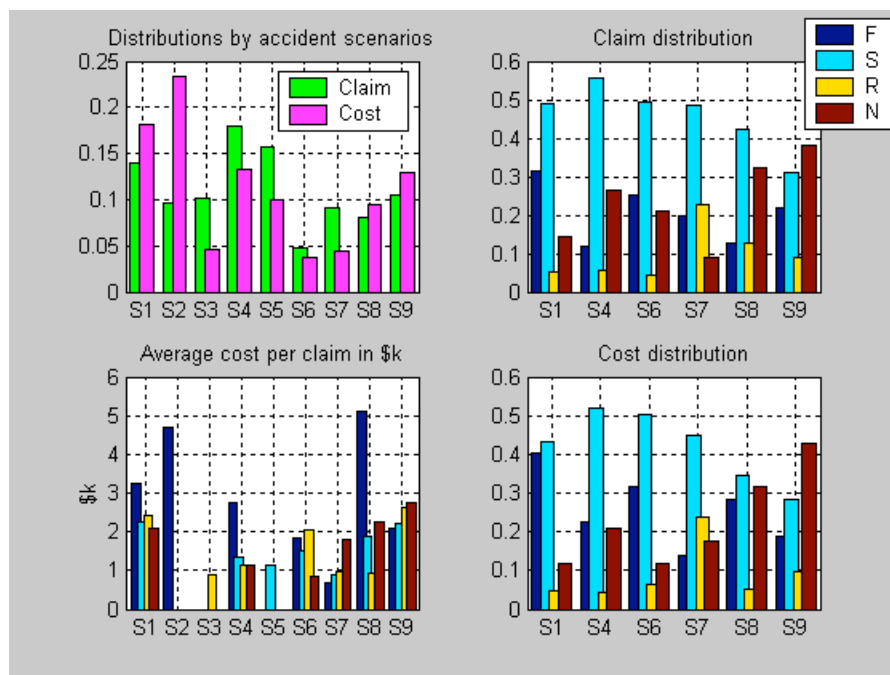


Fig. 1.20 35-transit agencies: General vehicle collision costs by scenario

Thirty-three percent of intersection collisions (S1) occurred while the bus was going straight (30% of costs), while 16% occurred while the bus was turning right (9% of costs) and 18% while the bus was turning left (28% of costs). The subset of crashes in which the bus was turning left and hit another vehicle (as opposed to being hit) made up 3.7% of claims and 16% of costs among all intersection crashes.

Thirty-seven percent of sideswipes (S5) occurred while the bus was passing another vehicle (41% of costs) and 45% occurred while another vehicle was passing a bus (37% of costs). Twelve percent of sideswipe crashes (18% of costs) occurred when a bus hit another vehicle

while trying to turn a corner, confirming the fact that buses have a wide turning radius which often makes it difficult to avoid other vehicles.

Most standing vehicle crashes (S4) and cut-in crashes (S6) are side collisions. Twenty-two percent of loading zone crashes (S7) occurred while the bus was pulling out, accounting for 38% of costs, while 11% of claims and 13% of costs were the result of crashes while the bus was pulling into the loading zone. Two scenarios stand out from the others as sources of loading zone crashes: “bus pulling from zone and hitting a moving vehicle” (16% of claims and 30% of costs), and “bus pulling into zone and hitting a standing vehicle” (6% of claims and 10% of costs).

1.2.2.5 Top Five Vehicle Collision Scenarios by Fiscal Year

Considering crash frequency and cost, the top five collision scenarios involving a transit bus and another vehicle are, from the highest to lowest priority (severity), bus rear-ending another vehicle (S2), intersection collision (S1), collision between transit buses (S8), standing vehicle accident (S4), and sideswipe (S5).

Figure 1.21 shows the percentage of general vehicle collisions and general vehicle collision costs, by fiscal year, for all five scenarios. Figure 1.22 shows the same information broken out by scenario type.

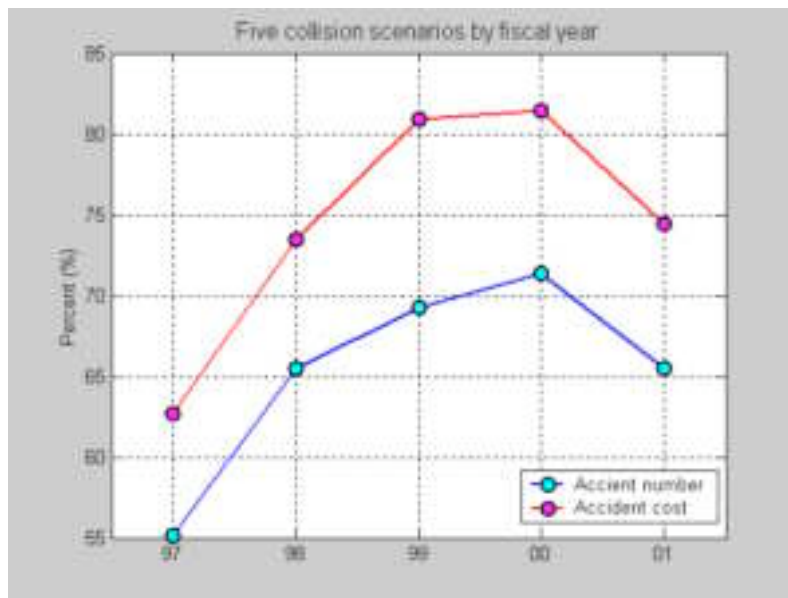


Fig. 1.21 35-transit agencies: Five collision scenarios by fiscal year

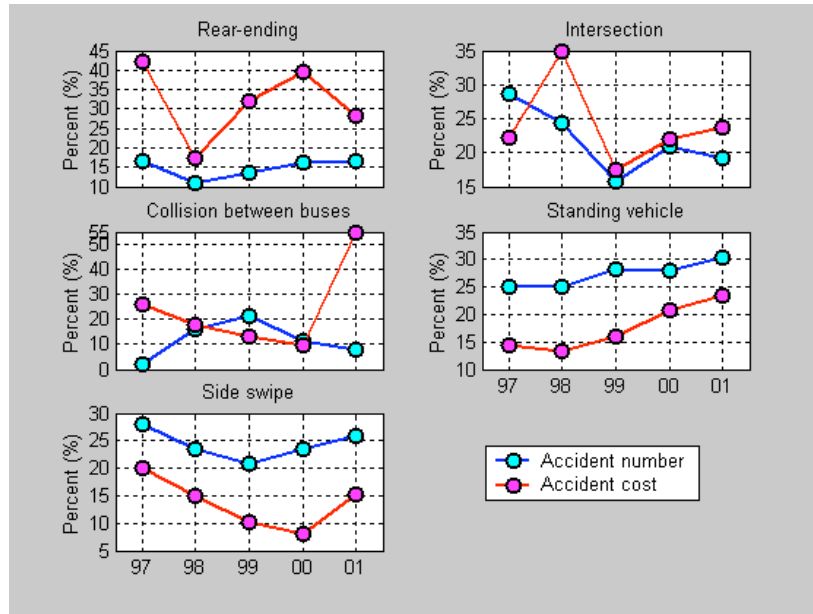


Fig. 1.22 35-transit agencies: Five collision scenarios

1.3 In-depth Cost Analysis of Passenger Injuries

For the 35 agencies, there are a total of 4,285 passenger injury crashes in 5 fiscal years with a total cost of \$13,583,368, and they count for 44.7% in claim and 35.3% in cost among all crashes.

Two severities are defined for passenger injury crashes: severe for passenger injuries which cost more than \$100,000; and general injury otherwise. Table 4.1 lists the 23 severe injuries in the five fiscal years.

Table 1.6 Severe Passenger Injuries for 35-transit agencies (5 years)

Claim	Loss code	Cost	Crash description
1	50	\$125,017	Passenger fell on boarding
2	55	\$179,512	Passenger fell on alighting
3	63	\$110,196	Passenger fell due to abrupt stop
4	63	\$274,079	Passenger fell due to abrupt stop
5	63	\$168,105	Passenger fell due to abrupt stop
6	63	\$134,281	Passenger fell due to abrupt stop
7	63	\$230,531	Passenger fell due to abrupt stop
8	63	\$151,000	Passenger fell due to abrupt stop
9	64	\$104,965	Passenger fell on turning bus
10	65	\$200,000	Passenger fell on going straight bus (walking)
11	67	\$107,910	Passenger leaning out window, hit by sign
12	68	\$177,175	Passenger fell, details unknown
13	68	\$169,493	Passenger fell, details unknown
14	68	\$427,500	Passenger fell, details unknown
15	74	\$500,000	Passenger fell on running for bus
16	74	\$134,494	Pedestrian fell on running for bus
17	78	\$163,593	Details unknown
18	78	\$164,158	Details unknown
19	78	\$150,000	Details unknown
20	78	\$107,500	Details unknown
21	88	\$245,560	Bus vs. bicycle
22	66	\$175,000	Wheelchair rolled backward on board
23	115	\$165,000	Wheelchair rolled backward on board

Total		\$4,365,069	
--------------	--	--------------------	--

Two out of the twenty-three severe injuries happened at loading zones; most severe injuries occurred when passenger were on board. The scenario of “Passenger fell due to abrupt stop” stands out from the others, accounting for about 25% of both number and cost among all severe injuries.

Excluding the 23 severe injuries, the 35-transit agencies had about 900 passenger injuries and spent about \$1.8 million each year. This is shown in figure 1.23.

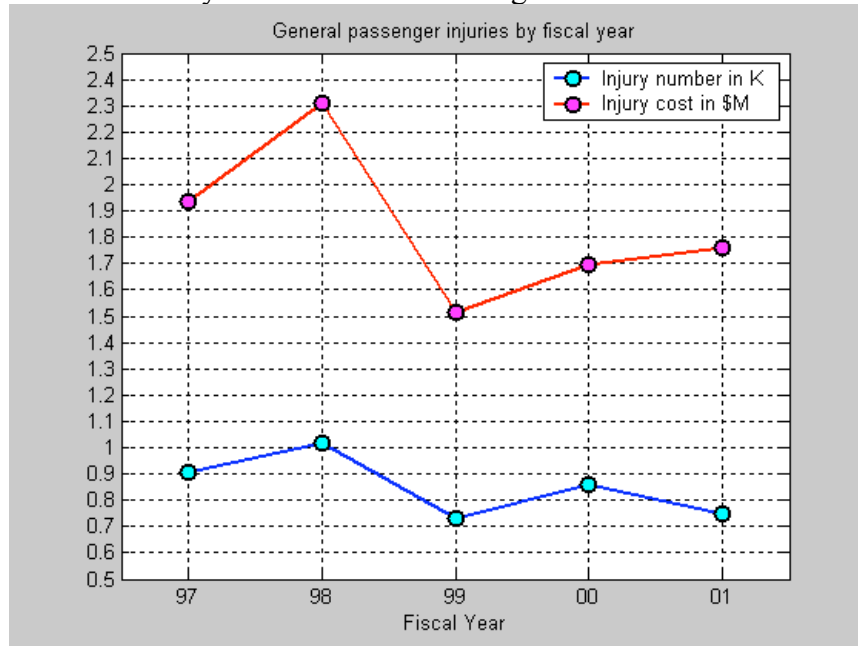


Fig. 1.23 35-transit agencies: General passenger injuries by fiscal year

The following eight maneuvers prior to an incident have been considered for general passenger injuries (excluding the 23 severe incidents)

Bus maneuver	Stand for
M1	Passenger boarding
M2	Passenger alighting
M3	Bus starting
M4	Bus stopping
M5	Bus turning
M6	Bus going straight
M7	Bus moving (others)
M8	Others

About thirty percent of general passenger injuries occurred at loading zones (boarding and alighting), which also accounted for 27.4% of costs. Twenty percent of passenger injuries occurred as a bus was stopping. This type of passenger injury has the highest severity, as it is shown in Figure 1.24.

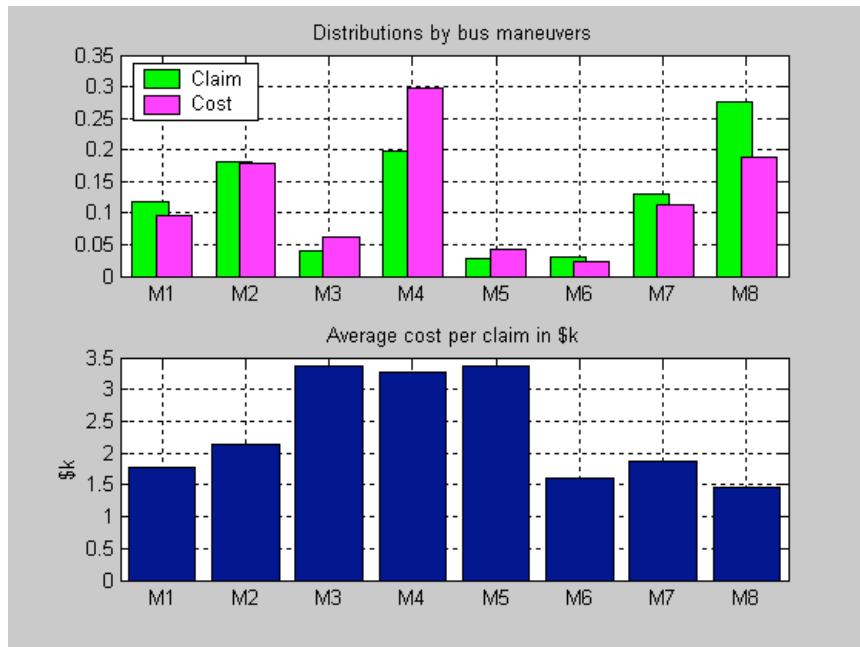


Fig. 1.24 35-transit agencies: Passenger injuries by bus maneuver

During the five fiscal years, there is a steady increase in the percentage of passenger injuries on stopping buses (M4) among all general injuries. This is shown in Figure 1.25.

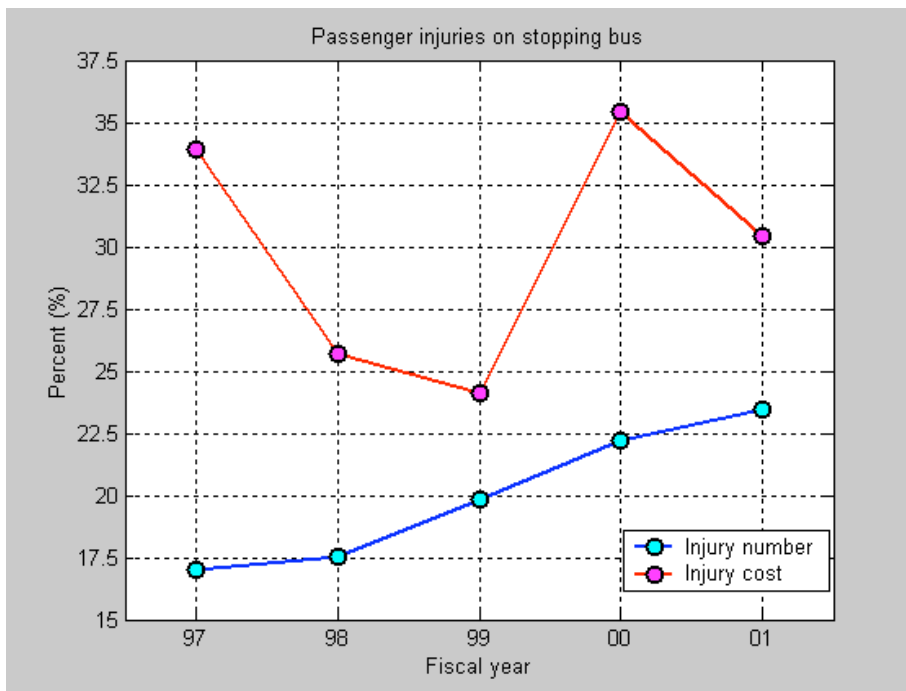


Fig. 1.25 35-transit agencies: Passenger injuries on stopping bus among all general injuries

1.4. System Impacts

As transportation transitions into the information age with the integration of advanced and information technologies, there is a need to examine the potential impacts of new technologies

such as FCWS. The focus of this task is to look at the relationship between frontal (and other) collisions and the corresponding effect(s) at both micro and macro levels. At the macro-level, how can a FCWS make a bus a safer vehicle? And at a system level, how does widespread use of FCWS or other similar technology affect the system? What are the impacts as measured by the costs resulting from death and injury and the costs from increased congestion?

Each of the core participants as well as the associate partners involved with this project has different motivations for participation. As the owner and operator of the state highway system, Caltrans is interested primarily in how vehicle-based systems will affect mobility, transportation operations, and the environment (e.g., the regional and state transportation systems). SamTrans, meanwhile, as a transit property has a greater interest in how Advanced Vehicle Control and Safety Systems (AVCSS) might improve their operations by increasing bus safety and decreasing operating costs.

The original objective of the system impact task was to conduct an analysis of the potential benefit of frontal collision avoidance devices (micro) and the impact of frontal collisions involving transit buses on regional traffic systems (macro). The impact estimates were to include (a) the loss of operation time of individual buses, (b) the loss of revenue, (c) the increase of operational costs due to collisions, and (d) the interruption of traffic flow and resulting congestion.

Because of the lack of data it was difficult or impossible to connect individual incidents to changes in congestion or specific incident related costs, therefore the scope of this task had to be modified to utilize specific crash data along with aggregate state or national data on the cost of crashes and congestion. The potential impacts were categorized into two areas: cost of crashes in terms of fatalities, injuries and property damage and the impact of congestion on society including pollution, energy, health, and personal costs.

Traffic congestion can be divided into two types: recurring and non-recurring. Recurring congestion is predictable and results when the demand for transportation facilities exceeds the supply (i.e., morning and evening commutes). Non-recurring congestion is traffic slowing down as a result of crashes, stalled cars, debris, or driver distracting events adjacent to the highway (such as fires, construction, etc.). It is non-recurring congestion that is of concern in this project.

The benefit estimates will be derived from the impact analysis outlined above as well as the potential reduction of property damage, personal injury, and liability claims. This analysis will provide a foundation for the eventual cost-benefit evaluation of collision warning devices later in this project.

The benefit estimates were derived using the above mentioned baseline data. At a later date, a similar analysis with data from collision warning devices on the local transit buses will be performed correlating the data with the baseline data.

1.4.1 Data source

Data came from several sources:

a) Crash data

Crash data for this analysis was obtained from the California Highway Patrol/Caltrans' Traffic Accident Surveillance and Analysis System (TASAS) [8]. The data includes location, type of crash, type of vehicle(s) involved, time-of-day, weather conditions, pavement conditions, etc.

b) Congestion or traffic volume data

Congestion or Traffic Volume Data was obtained from three sources:

- (1) Texas Transportation Institute's (TTI) 1999 Urban Mobility Study [9]
- (2) Caltrans, the Traffic Volumes Computer Database, and
- (3) The Highway Congestion Monitoring Program [10] (HICOMP) Report.

c) The costs associated with crashes and congestion

The costs associated with crashes and congestion came from a number of sources including:

- (1) TTI's Urban Mobility Study [9],
- (2) The Natural Resources Defense Council/ Resource for the Futures International sponsored study "The Price of Mobility: Uncovering the Hidden Costs of Transportation",
- (3) The National Public Research Institute's report "Highway Crash Costs in the U.S. by Driver Age, Victim Age, Blood Alcohol Level, and Restraint Use"[11], and
- (4) A number of other U.S. government sponsored reports and documents.

1.4.2 Analysis approaches

There were three primary activities as part of this task: 1) a review of current literature; 2) a search for pertinent crash, congestion, and cost data; and 3) an analysis of these data.

TASAS Data was downloaded from Caltrans' mainframe computer system, and converted to worksheet and relational database format for subsequent analysis. Bus crash data versus time-of-day (by hour) was analyzed at three levels: statewide, for the San Francisco Bay Area, and for SR 82 in San Mateo County.

Cost estimates for fatalities, injuries, and property damage were obtained through the literature. The cost of bus crashes for California, the San Francisco Bay Area, and State Route 82 in San Mateo County was then calculated.

1.4.3 Results

a) Cost of crashes

The cost of accidents, taken from the literature, used a comprehensive cost method known as Willingness to Pay to calculate the monetary value of fatalities, injuries, and property damage. While there are other methods used to determine costs associated with crashes, these values were used because they have an acceptance level within Caltrans [12] and within the broader highway transportation community including FHWA and National Safety Council advisory groups.

The comprehensive cost method includes seven cost factor areas: medical, work loss (victim), public services, employer costs, travel delay, property damage, and quality of life. The first six of these categories are self evident (i.e., public services - costs incurred by police, EMT, fire, towing, etc; property damage - costs to repair or replace vehicle or objects struck by vehicles; etc.). The seventh category Quality of Life, however, puts a value to the quality of life by quantifying pain, suffering, and quality of life for a family. The value is computed from the amount people routinely spend in dollars or time to reduce their or a family member's risk of death or injury. The amount people spend is calculated from what is commonly spent on items such as automobile air-bags, anti-lock brakes, and hazard pay for higher risk jobs.

Table 1.7 Crash Unit Costs 1997 Dollars in California Comprehensive Cost Method			
Area	Fatality	Injury	PDO/vehicle
Rural	\$3,123,603	\$45,802	\$2,058
Suburban	\$3,123,603	\$39,745	\$2,058
Urban	\$3,123,603	\$33,688	\$2,058
Average	\$3,123,603	\$39,745	\$2,058

b) Crash involving buses

The number of crashes involving buses and the associated fatalities and injuries on California-owned highways was determined from the TASAS database. Further investigation needs to be done in order to separate out school buses from other buses, although, informal observation indicates that the percentage of accidents involving school buses is relatively small. It also may be possible to determine what vehicle is the hitter and which was hit. This particular analysis would also go a long way toward determining the percentage of frontal collisions versus other types of collisions. The following table shows the breakdown of crashes involving buses on the state highway system.

Table 1.8 Crashes Involving Buses on California State Highways 1996 through 1998 California's Traffic Accident Surveillance and Analysis System (TASAS)			
Region	# of Crashes	Fatalities	Injuries
Statewide	2914	24	1066
Caltrans District 4 (S.F. Bay Area)	858	4	243
State Route 82 (In San Mateo Co.)	66	1	15

c) Cost of crashes involving buses

The cost of crashes involving buses was calculated from the previous two tables and is shown in the following table. The numbers indicate the potential benefit that would be gained by eliminating these crashes. Property damage is calculated assuming damage to two vehicles per accident.

Table 1.9 Cost Estimates of Crashes Involving Buses 1996 through 1998 (For California State Highways Only)				
Region	\$ of Fatalities	\$ of Injuries	\$ of PDO	Total
Statewide	\$75M	\$36M	\$12.M	\$123M
CT District 4 (S.F. Bay Area)	\$12M	\$8.2M	\$3.5M	\$24M
State Route 82 (In San Mateo Co.)	\$3.1M	\$0.51M	\$0.27M	\$3.9M

d) Crashes and congestion

There was a rough proportionality between the number of crashes involving buses and traffic volumes (i.e. morning and evening commutes) in that there more bus crashes occur in higher traffic volumes. While it is obvious that crashes impact traffic flow by reducing the capacity of the highway, it is not apparent whether congested traffic conditions cause more crashes because

they are more hazardous (i.e., speed differentials created by alternating free-flowing and stop-and-go traffic flow) or if the increases are simply due to the fact that there are more vehicles on the road. Many different methods have been used over the years to estimate the cost of congestion.

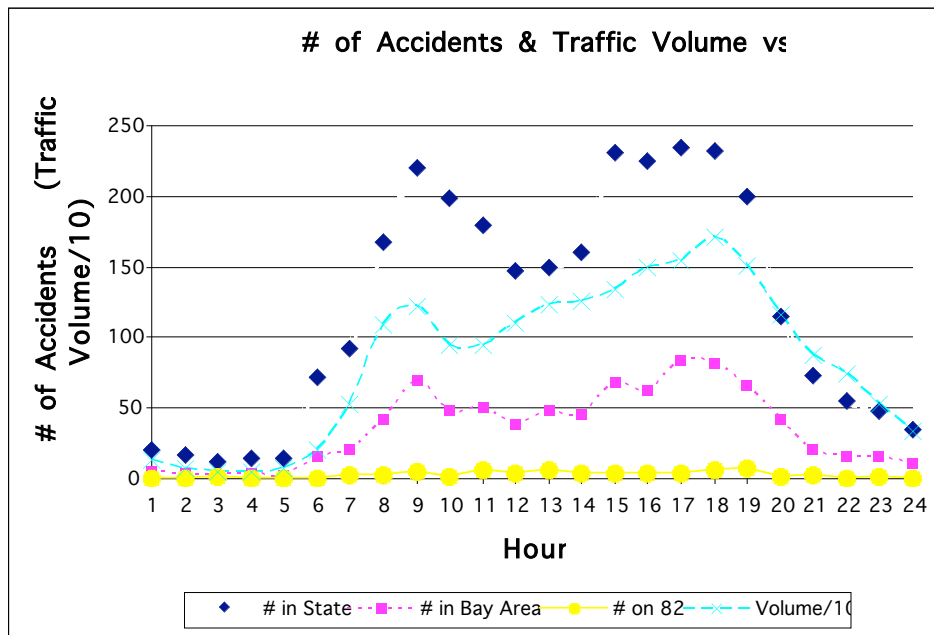


Fig. 1.26 Number of accidents and traffic volume vs. hour

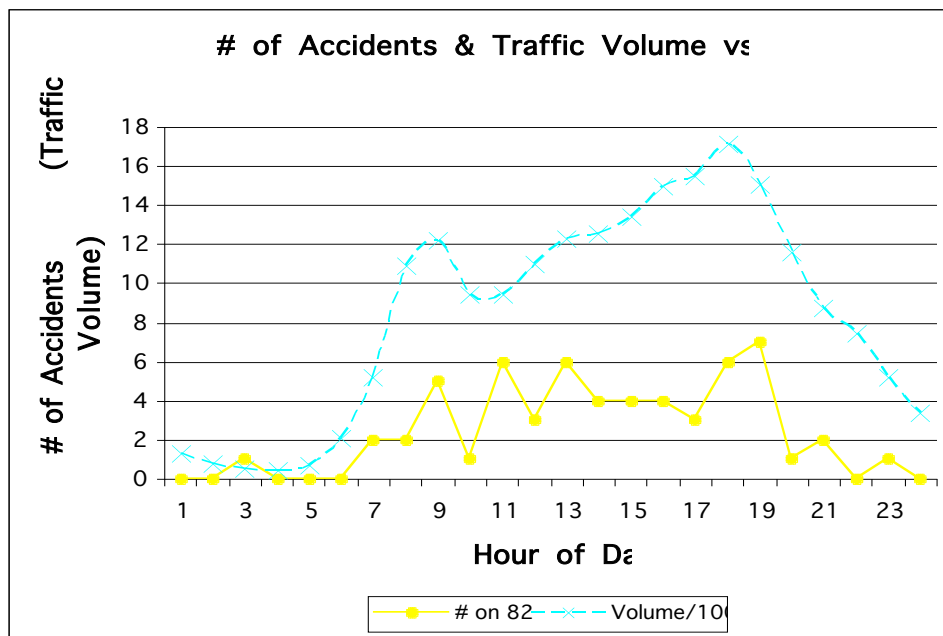


Fig. 1.27 Number of accidents and traffic volume vs. hour

Dealing with lack of data is perhaps the greatest difficulty when trying to perform this type of analysis. In addition to the fact that congestion data is generally aggregate and averaged over days or weeks or months, crash data, whether it be the physical data surrounding the crash or the subsequent medical and legal costs, are considered very sensitive and therefore difficult to

obtain. Additionally, each agency has a different system for collecting and archiving safety data, varying from paper records to archaic computer databases to modern database systems. Also, congestion data was available only for California state highways, whereas, most transit agencies operate their vehicles on local streets and roads. This data was generalized data that was averaged out over weekly or monthly periods so there was no way to correlate what effects specific crashes had on traffic flow.

Regardless of the perspective of the person looking at crash statistics, it is apparent that crashes, especially those leading to death or injury, are very expensive. Also, they get more expensive, at least in terms of dollars, as one transitions from the individual to the transit agency to the insurance company to state and federal governments and to society at large. Although the transit industry has the safest drivers when compared to commercial vehicle operators and the driving public, the costs of bus related crashes warrants the investigation and development of devices or systems to mitigate crashes, which is over one million dollars per year on only one state route in San Mateo County.

Because of the uncertainty in quantifying the costs related to crashes (i.e., congestion, air pollution, pain and suffering, public relations, etc.) it is important to consider measures other than dollars when deciding on whether to research, develop and eventually deploy collision warning and collision avoidance systems.

Baseline statistics proposed as benchmarks in measuring the effectiveness of projects in these areas should include, but not be limited to: frequency and severity of crashes, injuries and fatalities, vehicle role, corrective action, movement prior to critical event, critical event, and damage costs. An effective benchmark would be a reduction in critical factors: overall incidents, injuries/fatalities, and costs.

1.5. Observation and Conclusions

This transit crash and cost analysis was conducted using actual crash data from 35 transit agencies in California for the most recent five fiscal years. These agencies operate buses in a wide range of regions and operating environments, including one of the most congested areas in the United States, the San Francisco Bay Area. We have confirmed that crash claim and cost distributions vary from agency to agency due primarily to the fact that every agency has its own driver training program and a different operating environment. We have also shown that the crash and cost distributions by loss code and the initial point of impact are very consistent between transit agencies.

The statistics obtained are consistent with the national bus crash statistics:

- 0.6% of collisions involved serious casualties of which 54.8% were frontal collisions and 22.6% were side collisions. NHTSA[5] reports 0.6% fatality, of which 68.4% were frontal and 16.8% were on the side for bus collision accidents (school, intercity and transit).
- 91.2% of collisions involved another motor vehicle, 5.3% involved an object, and 3.5% involved pedestrians. NHTSA[5] reported 83.5% with vehicle and 16.2% with an object.
- Excluding not-known initial point of impact collisions, 27.1% of collisions are frontal collisions, 54.3% are side and 18.6% are rear collisions while NHTSA [5] reported 28.2% front, 47.6% side and 22.9% rear.

The cost benefit analysis confirmed the recommendation by the transit IVI Committee on the need for IVI technologies:

- Excluding the costs for serious casualties and not-known point of impact collisions, 49% of collision costs are for frontal collisions, 41% are for side, and 10% are for rear collisions. These numbers may be significantly reduced by frontal/forward, side and rear warnings.
- Passenger injuries (not collision related) account for one third of all incident costs. Passengers injured due to the bus coming to an abrupt stop have the highest priority both in frequency and severity (19.8% of claims and 28.1% of costs). This type of incident may be avoided with smoother operation from FCWS.
- 56% of passenger injury costs are related to moving buses, while 21% are from boarding and alighting. Those numbers may be significantly reduced with Lane assist/precision docking.

This analysis also shows the specific needs for IVI technologies:

- Bus backing crashes are not a critical scenario for the 35 agencies.
- Forty-four percent of serious casualty costs are for pedestrian crashes, which also account for 15% of all crash costs. This shows the critical need for pedestrian detection and avoidance service.
- Considering crash frequency and cost, the top five collision scenarios involving a transit bus and another vehicle are, from the highest to lowest priority (severity): bus rear-ending another vehicle, intersection collision, collision between transit buses, standing vehicle crash, and sideswipe. These five scenarios account for 65.4% of claims and 74.4% of costs among all general vehicle collisions (excluding serious casualties).

Several observations can be concluded from the review of numerous crash reports in the course of this study:

- The speed of buses prior to the crash occurrence was generally modest as recorded in the incident reports, for example below 30 mph. This is due to the fact that the transit buses operate on suburban corridors, local streets, and among transit stations and typically they are not expected to run at high speeds for transportation purposes. For incidents near bus stops, traffic lights, or intersections, the speed can be considerably lower. Since the operating environment of transit buses covers a variety of local streets and corridors in urban and suburban environments, they generally see heavy traffic and frequently encounter street objects such as pedestrians, bicycles, and parked vehicles. It is essential to examine carefully the performance and capability of sensors under these circumstances. Thus, the first phase of data collection and the evaluation of sensing signals and noises will be extremely important.
- Among the reviewed crash reports, many incidents involved the bus making contact with a neighboring vehicle at the front corners at relatively low speeds. This may happen when the bus is pulling out from a stop or turning at an intersection, or an adjacent vehicle is moving aggressively ahead of the bus. The incident may be classified as a frontal or a side impact in reports. This implies that the implementation of corner sensors may be essential to alert the drivers of such obstacle presence. The corner sensors can also be useful for detecting cut-in vehicles.
- The operating speed of buses on local streets, near traffic lights, or bus stops is low and the distance to other vehicles or obstacles are short. Under these operating circumstances, it may be challenging to provide a warning signal that is timely yet not frequent enough to distract the driver.

- In the selection process of warning signal types and driver-machine interface, it should be taken into consideration that transit bus drivers are working under heavy work loads.

1.5 Reference

1. T. Wilson, et al., "Forward-Looking Collision Warning System Performance Guidelines," SAE No. 970456, 1997.
2. T. Wilson et al., IVHS Countermeasures for Rear-End Collisions, Task1, Volume II: Statistical Analysis, DOT HS 808 502, 1994.
3. H. Asher, B.A. Galler, "Collision Warning Using Neighborhood Vehicle Information, Proceedings of ITS America, 1996.
4. Intelligent Vehicle Initiative Needs Assessment, FTA-TRI-11-99-33, DOT-VNTSC-FTA, November 1999.
5. Traffic Safety Facts 2000, NHTSA, December 2001.
6. Ching-Yao Chan, et al., "Studies of Accident Scenarios for Transit Bus Frontal Collisions", Proceeding of ITS America, 2001.
7. Traffic Safety Facts 2000, NHTSA, December 2001.
8. California Highway Patrol/Caltrans' Traffic Accident Surveillance and Analysis System (TASAS)
9. Schrank, David, Lomax, Tim, Texas Transportation Institute's 1999 Urban Mobility Study, November 1999, <http://mobility.tamu.edu/>
10. Caltrans Traffic Operations Program, Office of Traffic Safety, Traffic Volumes Data
11. Miller, Ted R., Spicer, Rebecca S., Lestina, Diane C. (1998) "Highway Crash Costs in the U.S. by Driver Age, Victim Age, Blood Alcohol Level, and Restraint Use", Accident Analysis and Prevention, Vol. 30(2):137-150. National Public Services Research Institute, Landover MD.
12. Peterson, Roy A., Estimated Crash Costs For California, 1999 California Department of Transportation, Traffic Operations Program, Office of Transportation Safety.

2. Field Data Analysis

The crash data provides a knowledge base for determining the type and frequencies of frontal collisions. As transit crash data relies on recall from the parties involved, the data may not accurately describe the cause and time sequence of events in enough detail to enable a detailed crash analysis. In order to better understand the bus operating environment and time sequence of events in potential crashes, the team determined that it was critical to collect field data so that bus crash scenarios can be constructed. Significant efforts were devoted to the development of a data acquisition system.

The objectives of the Data Acquisition System (DAS) are to: (1) help understand the environment that the Frontal Collision Warning Systems will operate in, (2) provide a basis for an analysis using a dynamic vehicle model to predict potential collision courses, (3) facilitate the development of the collision warning system, and (4) enable before-and-after data comparison to determine if there is any change in driving behavior with the introduction of the system. It is understood that the likelihood of the buses instrumented with the data acquisition system being involved in an crash is extremely small. However, the large amount of data collected on these buses will provide an accurate description of the relative movement of buses and the surrounding vehicles. In the absence of collisions, hazardous conditions that potentially can lead to crashes can be identified and driver reactions to these hazardous conditions can be analyzed. In-depth understanding of the bus operating environment and hazardous conditions through collection and analysis of field data is a critical portion in determining the specification of performance requirements for a transit bus FCWS.

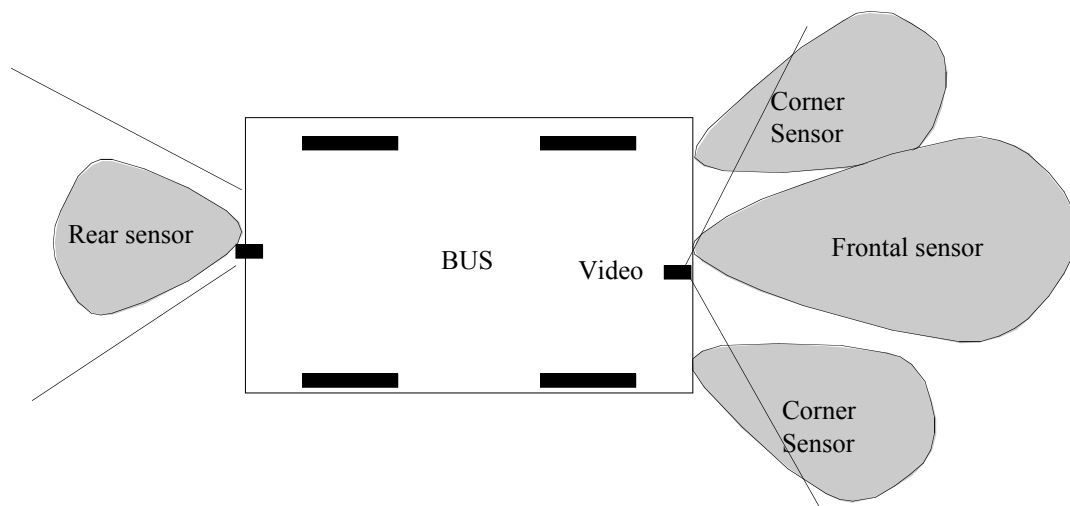


Fig. 2.1. Sensor Arrangements of the Data Acquisition System

Based on the data acquisition needs, a sensor arrangement for the DAS is designed to include sensors to detect frontal and frontal corner obstacles and to monitor steering angle movement, brake and throttle motion, vehicle velocity and acceleration (Figure 2.2 provides the DAS

configuration. Detail description of the development of the data acquisition system can be found in [Appendix V](#).

The hardware configuration of the DAS can also be used as the hardware platform of the FCWS. Minor changes in sensor layout and computer configurations may be required to do this. The data acquisition function and the collision warning function can both be implemented in software. They can run in parallel in a multi-task system. This means the DAS will be still running after the FCWS has been installed on the bus. This allows us to analyze driver adaptations by comparing the data collected before the FCWS is installed with the data after installation.

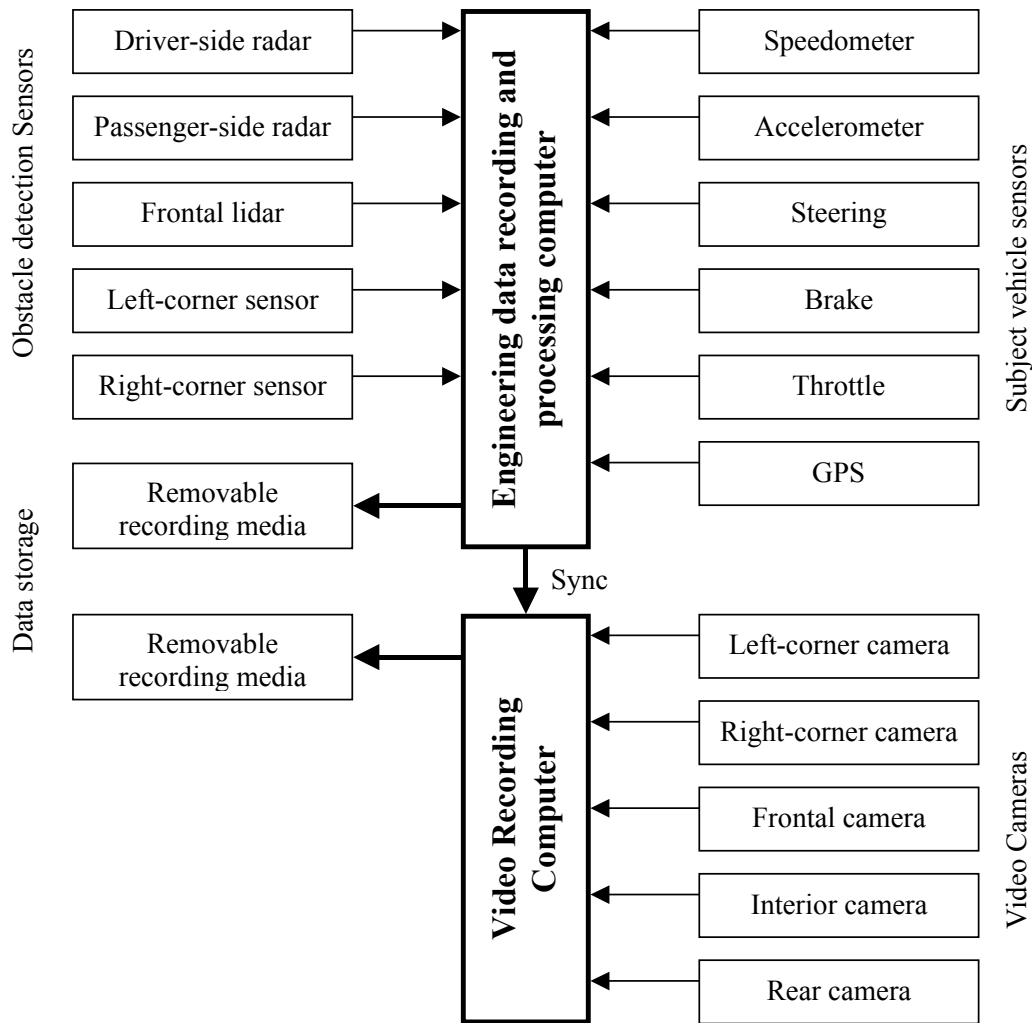


Fig. 2.2 Schematic Diagram of the Data Acquisition System

Using 3 buses instrumented with this data acquisition system, field data were collected since early 2001. The data was analyzed at three different levels: 1) manual review with the data playback tool which is a Windows™ program developed by PATH, 2) histogram analysis of specific parameters by simply counting the numbers of samples in the data, and 3) event-related histogram and clustering analysis by applying filtering algorithms to the data to detect events (e.g. braking onset) and estimate parameters. These approaches are discussed in detail in the following sections.

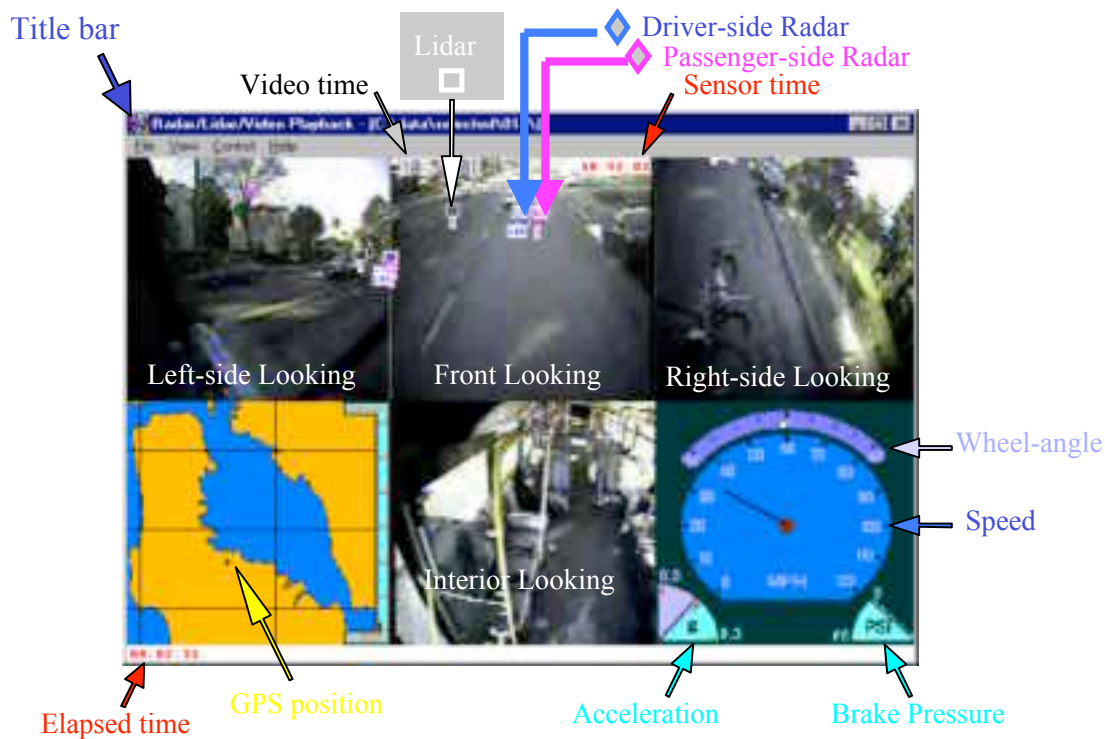


Fig. 2.3 Snapshot of the data playback tool window

To facilitate data analysis, PATH has developed a data playback tool, a program running in a Windows™ environment. The tool was developed in May 2000 and has been updated several times. The tool can decode and play back MPEG movies in Windows™. It displays bus states, such as speed, acceleration, brake pressure, front wheel angle and GPS location, simultaneously during video playback. It projects the radar and lidar targets into the video frames, using simple visual marks to indicate which objects in the frames have been detected by which radars or lidars. Fig. 2.3 is a snapshot of the data playback window. It can be seen that the display is divided into six sub-windows. Video from each camera is displayed in one sub-window. The GPS location and altitude are displayed in the lower left-hand sub-window. Other subject vehicle states, i.e. wheel angle, speed, acceleration and brake pressure, are displayed in the lower right-hand sub-window.

This tool provides the data reviewer a complete view of all the data collected at the same time. The tool provides the ability to understand sensor behavior, traffic scenarios, and the characteristics of targets. For example, the tool has been used to verify different sensor performance; see below for radar and lidar performance assessments derived using the tool:

a) Micro-wave radar disadvantages

1. Nearly stationary targets can not be detected;
2. Target signal drops;
3. Low azimuth accuracy.

b) Micro-wave radar advantages

1. Working well in all weather;
2. Accurate range;

c) Lidar disadvantages

1. Saturation facing sun ;
2. False alarms with rain, fog and grime on lens;
3. range-rate is directly differentiated from range measurement;
4. More stationary roadside targets;
5. Occasional target split.

d) Lidar advantages

1. Able to detect stationary targets;
2. Accurate two-dimensional position measurements;
3. Large view angle;
4. Fewer target drops.

The tool also provided a software platform to develop and test the warning algorithms.

2.1 Analysis of data samples

The field data used for this analysis was recorded on the first bus (SamTrans bus No.600) from August 1, 2000 thru April 16, 2001. There were 80 days of data. The bus was operated for an average of 7.5 hours a day. The experimental bus was on normal service in San Mateo County, California. The drivers who drove the bus were not specified or selected. The bus and the service routes were assigned to them by the dispatch center of SamTrans according to normal crew assignment schedules. The service routes were spread throughout San Mateo County, with connections to the Daly City and Colma BART stations, the San Francisco Airport, several Caltrain stations, and the downtown areas of local cities. Different weather conditions including rain, fog and wind, were encountered. The bus was usually put on service in the early morning before daybreak, until the late afternoon around sunset, with a few scheduled breaks. The 80-day data covers the representative drivers, routes, weather, time-of-day and level of traffic.

2.1.1 Approaches

For each parameter x , the possible distributed value region I was divided into n equidistant intervals I_i ($i = 0, 1, \dots, n-1$). The step size is $\Delta = I/n$. The data is scanned to accumulate the number of samples of x that fall into each interval. This is like generating histogram bins. Since the Data Acquisition System (DAS) has a fixed sampling rate, the number of samples in each bin, b_i , is proportional to the total time that x stays on the value interval. The following normalized parameter (B is the total samples of x):

$$p_i = \frac{b_i}{B \cdot \Delta} \quad i = 0, 1, \dots, n-1$$

is proportional to the total time that x stays on the value interval i . It has the property that:

$$\sum_{i=0}^{n-1} p_i \Delta = 1$$

p_i ($i = 0, 1, \dots, n-1$) is the relative frequency distribution. It is not necessarily an approximation of a Probability Density Function (pdf) of x , because the adjacent samples may not be independent. However it still gives out the probability distribution characteristic of x .

The initial step size, $\Delta = I/n$, is small to preserve the resolution of the relative frequency distribution. In the case that the step size is too small to accumulate sufficient samples in the bins, a moving window average method was used to combine the bins. Assuming the size of the moving window is $(2N + 1)\Delta$, the smoothed relative frequency distribution is defined by:

$$q_i = \frac{\sum_{j=i-N}^{i+N} p_j}{2N+1} \quad i = 0, 1, \dots, n-1.$$

It is also true that:

$$\sum_{i=0}^{n-1} q_i = 1 \quad i = 0, 1, \dots, n-1.$$

In practice, the moving window size is selected by trying different window sizes to smooth p_i .

2.1.2 Bus speed

For bus speed, the value region $I = [0, 40]$ m/s (1m/s = 2.25 mph) was divided into 2000 intervals with step size of $\Delta = 0.02$ m/s. It was found from the data that the minimum speed sensor measurement, except 0, is 0.55m/s, hence a bus stop/running threshold is set at 0.5m/s. Speed above/below this threshold indicates when the bus is moving/stopped.

When the bus is running, the minimum speed measurement is 0.55m/s, and the maximum measurement is 31.3m/s. The maximum speed occurred in the case that a bus was running at highway speed. There are in total 20,890,161 samples. The estimated relative frequency distribution of bus speed, $p(v)$, is shown in Fig. 4 in red with dashed line.

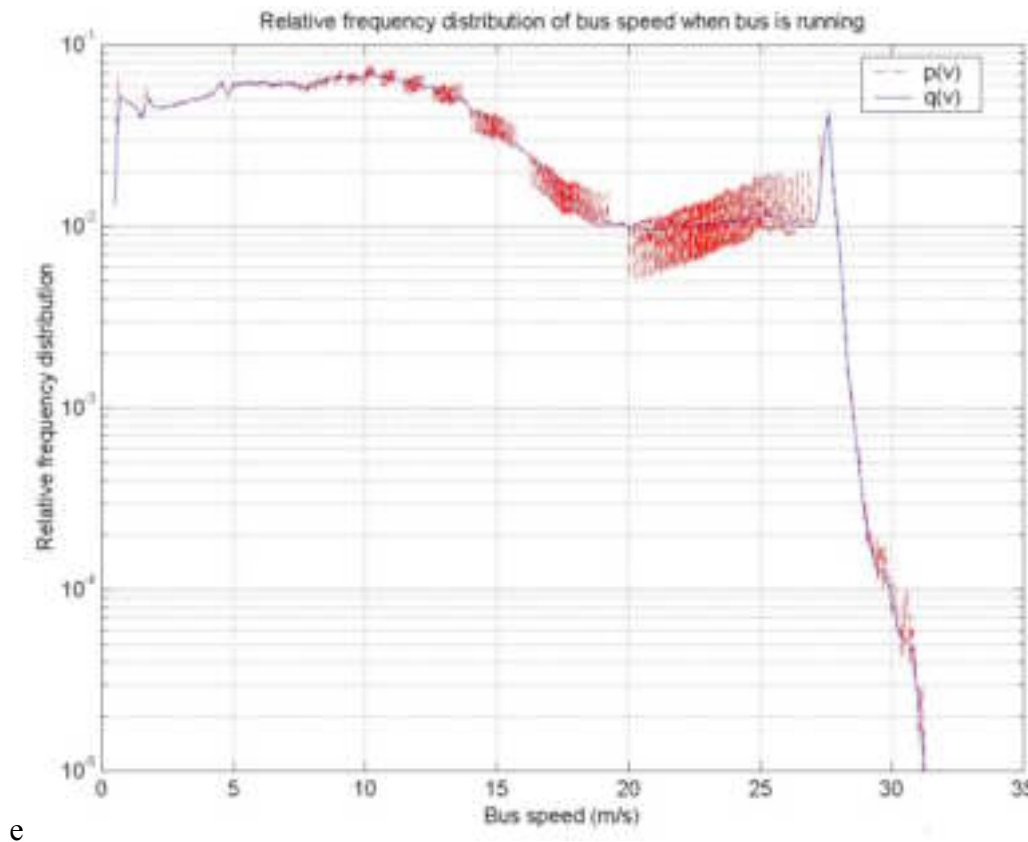


Fig. 2.4 Relative frequency distribution of bus speed when bus is moving

As we can see, the plot of $p(v)$ is quite noisy. To smooth the plot and keep the peak at 27.5m/s, two different window sizes were used. One window with $N = 2$ was applied on the intervals within $[27, 28]$ m/s, and the other window with $N = 5$ was applied to everything else. The smoothed relative frequency distribution $q(v)$ is shown in Fig. with a blue solid line.

As can be seen from Fig. 2.5, the bus mostly travels in four main speed ranges, 8~12m/s, 5~8m/s, 5~8m/s and 12~15m/s.

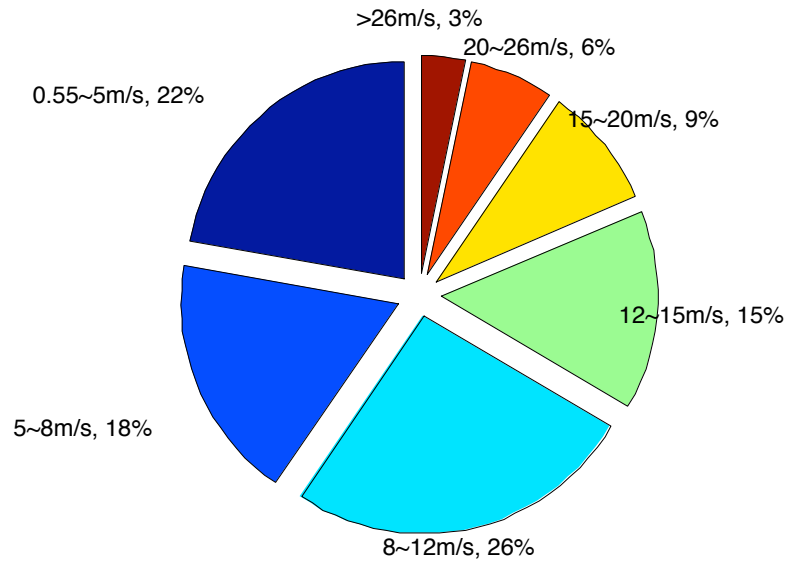


Fig. 2.5 Percentage of time for bus speed

2.1.3 Bus acceleration

For bus acceleration, the value region $I = [-1,1]g$ ($g = 9.8m/s^2$) was divided into 133 intervals with step size $\Delta = 0.015g$. It was found from the field data that the maximum acceleration value is $0.523g$, and the minimum acceleration value is $-0.692g$ (deceleration).

The relative frequency distribution of bus acceleration $p(a)$ is shown in Fig. (in total 20,890,161 samples). Since the plot is pretty clean, no moving widow was applied to it. The highest peak locates at $-0.01g$. In the positive half, there is another peak at $0.028g$. Although the maximum decelerating and accelerating found in the field data are quite large, there is a very limited likelihood that bus has acceleration values below $-0.4g$ ($< 2e^{-13}\%$) in slowing down or greater than $0.4g$ ($< 2e^{-14}\%$) in speeding up. As shown in Fig. , the bus has a higher probability with acceleration valued from $-0.1g$ to $0g$ for decelerating and valued from $0g$ to $0.12g$ for accelerating. Fig. 2.7 shows the percentage of time that the bus is operated with different acceleration levels. The percentage of time that the bus acceleration is greater than $0.2g$ is 0.2% , which is not displayed in the pie chart.

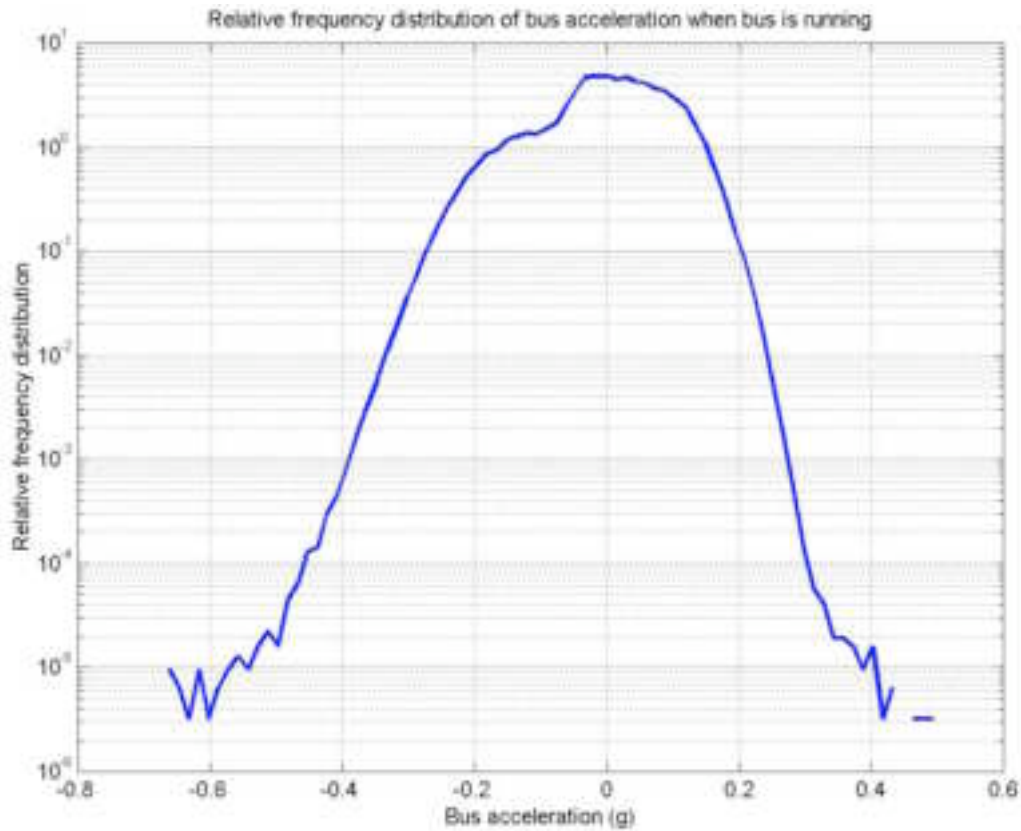


Fig. 2.6 Relative frequency distribution of bus acceleration when bus is moving

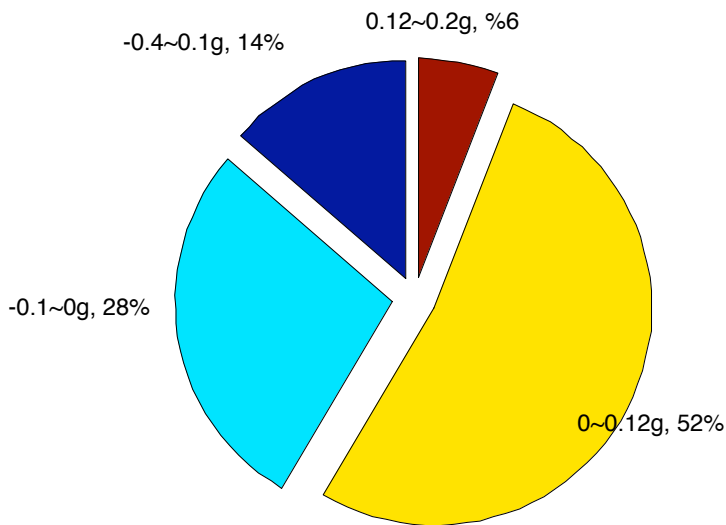


Fig. 2.7 Percentage of time for bus acceleration

The total time spent speeding up is longer than spent slowing down (58%:42%). 67% of deceleration occurs within -0.1~0.0 g, while 90% of acceleration occurs within 0~0.12g.

2.1.4 Brake pressure

For brake pressure, the value region $I = [0,100]$ psi was divided into 1,000 intervals with step size $\Delta = 0.1$ psi. When the bus is stopped, bus drivers sometimes step on the brake harder. This would affect the overall statistics of brake pressure. Hence, only the data from when the bus is moving was considered. There are a total of 20,890,161 samples. It was determined from the field data that 1.3 psi is an appropriate threshold to separate brake-on samples from no-brake data. Fig. 2.8 shows the percentage of time for brake-on vs. no-brake when the bus is moving.

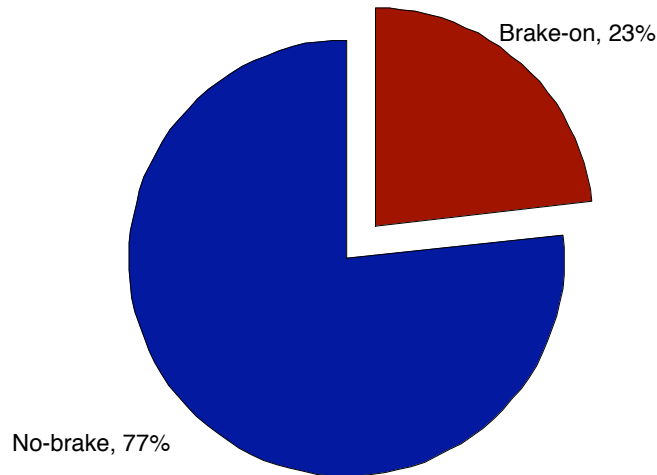


Fig. 2.8 Percentage of time for no-brake vs. brake

The maximum brake pressure in field data when the bus is moving is 81.7 psi, in this case the driver braked in an emergency to avoid hitting a child and a dog that had suddenly run across the street. Fig. 2.9 shows the relative frequency distribution of brake pressure $p(\textit{press})$ (when brake is on) in red with dashed line. A moving window with $N = 10$ was applied to it, the smoothed $q(\textit{press})$ is displayed with a blue solid line.

The highest peak is at 9 psi. When the brake is on the most commonly occurring frequency of brake pressure is 6 to 12 psi. Fig. shows the percentage of time for brake pressure in different levels. It should be noted that brake pressure is above 50 psi less than 0.2% of time.

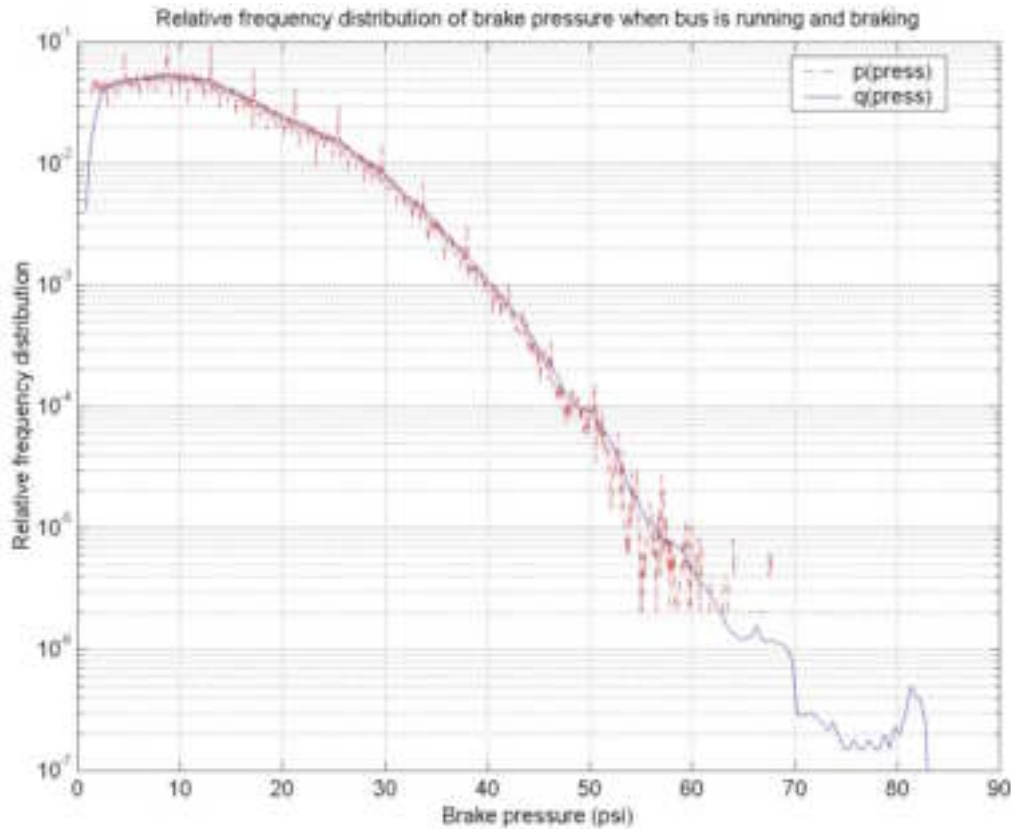


Fig. 2.9 Relative frequency distribution of brake pressure

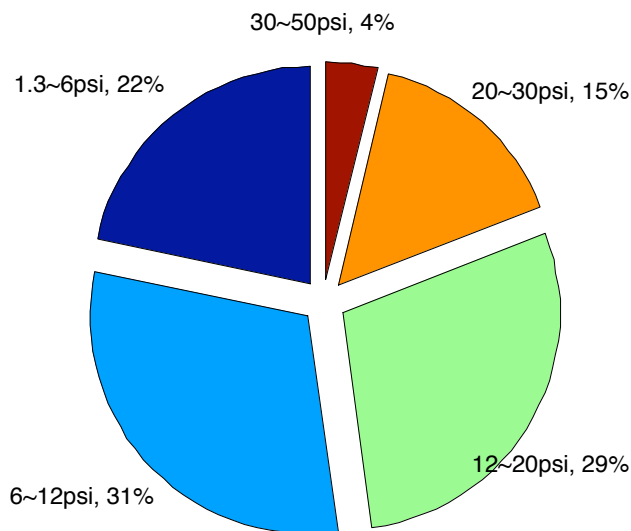


Fig. 2.10 Percentage of time for brake with different pressure levels

2.2.5 Front wheel angle

For front wheel angle, the value region $I = [-60, 60]$ deg was divided into 800 intervals with step size $\Delta = 0.15$ deg. When the bus is stopped, bus drivers sometimes hold the steering wheel at certain non-zero angles. This would affect the overall statistics of wheel angle. Hence, only the data when the bus is moving (speed > 0.5 m/s) was considered. In field data, the maximum front wheel angle is 45.5 deg to the right and 50.1 deg to the left.

The relative frequency distribution of front wheel angle, $p(\text{angle})$, is shown in Fig. 2.11 with a red dashed line. Left is positive and right is negative. To smooth the plot and to maintain the peak at 0 degree, two moving windows were used. One window with $N = 1$ was applied to the region of $-6 \sim +6$ deg, and the other window with $N = 10$ was applied to everything else. The smoothed relative frequency distribution, $q(\text{angle})$, is shown with a solid green line. The highest peak locates at 0 degrees, which indicates that most of time the bus is moving straight forward.

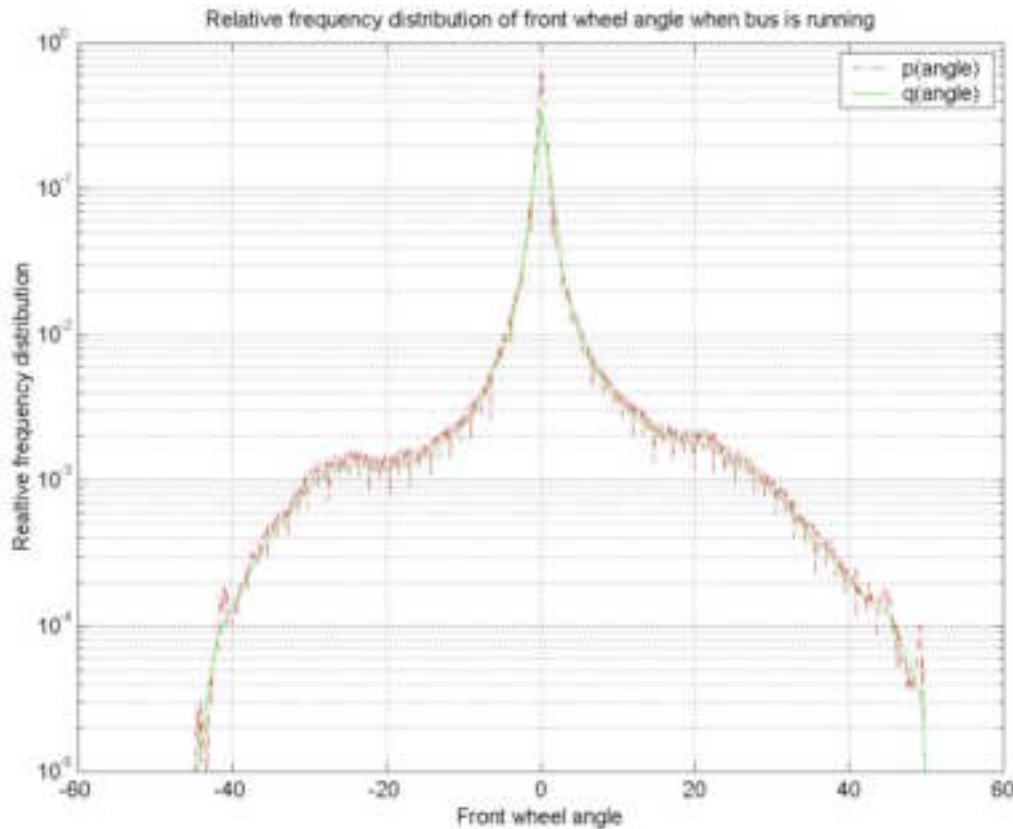


Fig. 2.11 Relative frequency distribution of front wheel angle (+left/-right)

2.1.6 Minimum following distance and cooresponding closing rate

Lidar can detect up to 8 targets simultaneously. Only those targets that are running in the same direction as the bus with 2-meter (about half a lane) or closer lateral distance to the bus center line were picked up. The minimum following distance is the minimum longitudinal distance from the bus frontal bumper to targets. The corresponding closing rate is the closing rate of the target at the minimum distance. Closing rate equals negative range rate. Positive closing rate means that the bus is approaching a forward target.

For minimum following distance, the value region $I = [0, 200]$ m was divided into 2000 intervals with step size $\Delta = 0.1$ m. Again, only those samples from when the bus was moving were considered. There are in total 6,494,755 samples. The closest minimum following distance in the field data is 0.078m, which occurred in a case that bus was following a leading car in stop-and-go movement. The maximum value of minimum following distance found is 160.1m, which is the maximum range that the Lidars can detect.

The relative frequency distribution of minimum following distance, $p(r)$, is shown in Fig. 2.2 with a red dashed line. A moving window with $N = 12$ was applied to it to smooth the plot. The smoothed relative frequency distribution, $q(r)$, is displayed with a blue solid line. The highest peak locates at 22m.

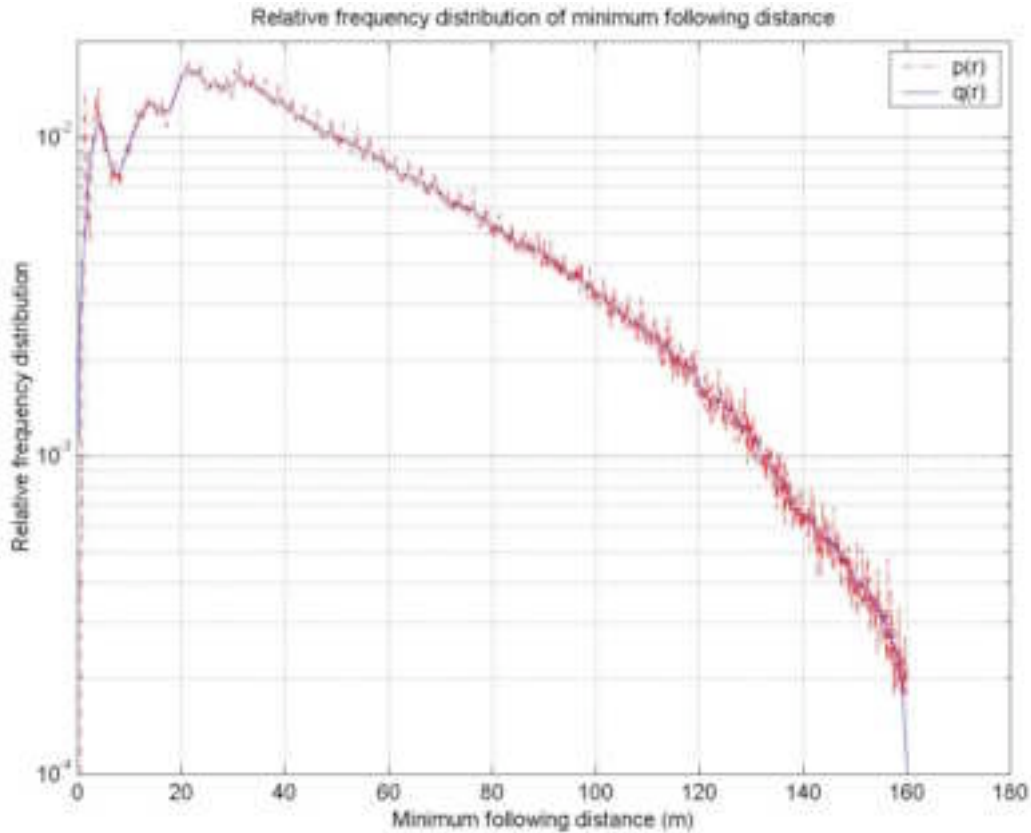


Fig. 2.12 Relative frequency distribution of minimum following distance

For the corresponding closing rate, the value region $I = [-100, 100]$ m/s was divided into 2,000 intervals with step size $\Delta = 0.1$ m/s. The maximum value of closing rate is 29.6m/s, when the bus was approaching a target. The minimum value of closing rate is -65 m/s. This negative closing rate is doubtful because while it is possible it is very rare for a vehicle to move that fast. Furthermore, it is not clear in the video data if there is such a target. However, the Lidar did report such a target with a relative speed of 65m/s. This might be caused by sensor noise, or other targets that are not in the camera's field of view. We are still not sure what caused this problem, and need to do further investigation.

The relative frequency distribution of closing rate, $p(rate)$, is shown in Fig. 2.13 with a red dashed line. The highest peak locates at 0. There is another peak at 2.75m/s. It is also found that there is no data falling in the region of 1.45~2.45m/s. This is another issue that cannot be explained at this moment. Further investigation is needed.

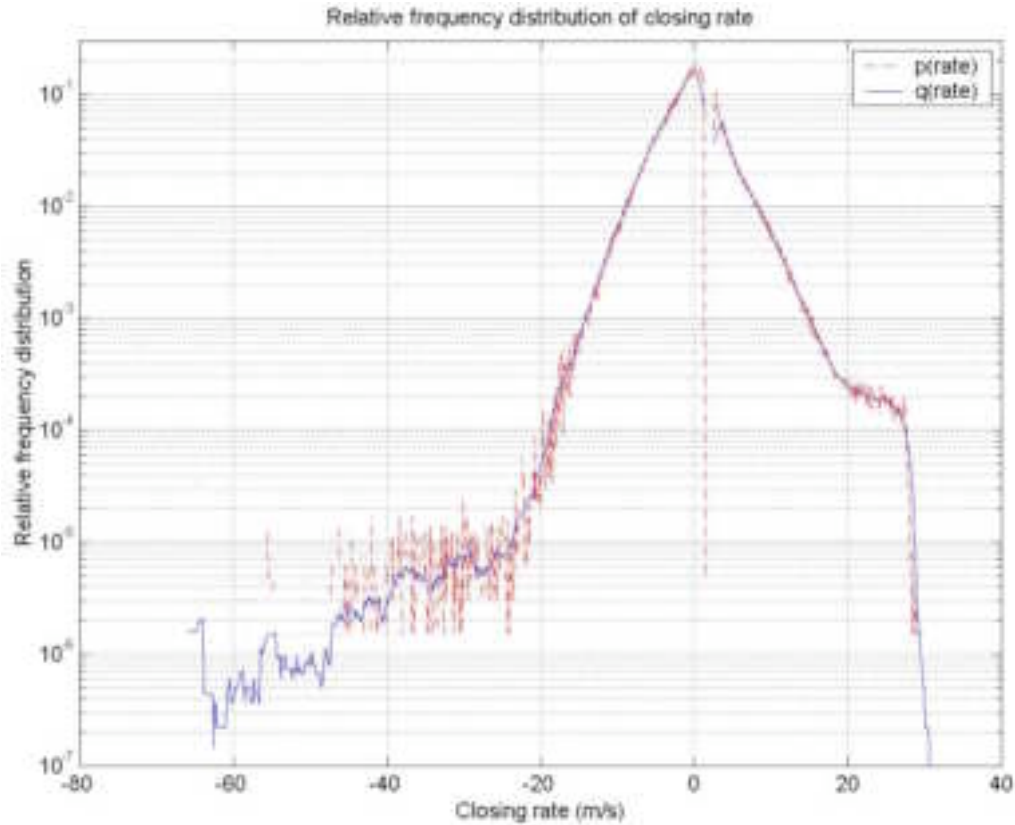


Fig. 2.13 Relative frequency distribution of closing rate

Two moving windows were used to smooth the plot. A window with $N = 0$ was applied to the region of 1.45~2.45m/s, and another window with $N = 10$ was applied to everything else. The smoothed relative frequency distribution is displayed with a blue solid line. Fig. 2.14 shows the percentage of time for different closing rate levels. The percentage of time that closing rate is above 20m/s is 0.15%. The percentage of time that the closing rate is below -20 m/s is 0.02%. Neither of these two closing rates are depicted in the pie chart.

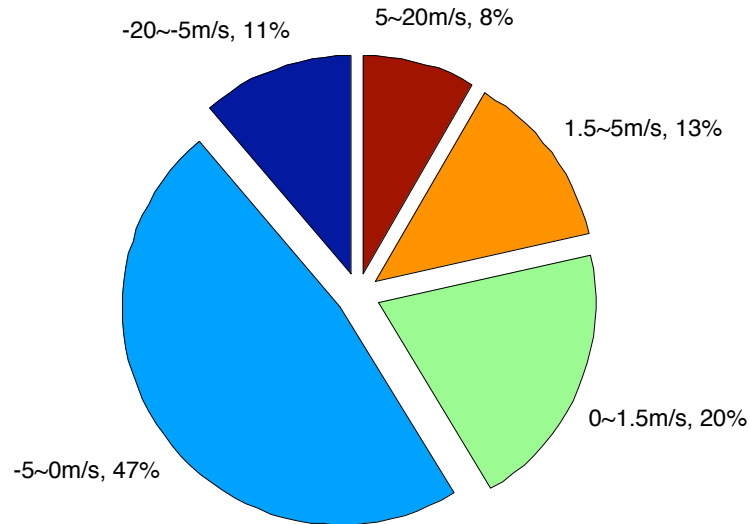


Fig. 2.14 Percentage of time for closing rate

2.2 Braking onset analysis

The data that is used in the braking onset analysis was collected from September 2000 to February 2001, 77 days of data were used. The experimental bus was in normal service in San Mateo County, California. The drivers who drove the bus were not specified or selected. The bus and the service routes were assigned to them by the dispatch center of SamTrans according to normal crew assignment schedules. The service routes spread throughout San Mateo County, with connections to the Daly City and Colma BART stations, the San Francisco Airport, several Caltrain stations, and the downtown areas of local cities. Different weather conditions including rain, fog and wind, were encountered. The bus was usually put on service in the early morning before daybreak, until the late afternoon around sunset, with a few scheduled breaks. The 77-day data covers representative drivers, routes, weather, time-of-day and traffic.

2.2.1 Data pickup

The braking onset data is picked up from the 77-day data set. The lidar data, steering angle and bus speed are all processed with Kalman filtering to remove noise. The steering angle data is converted to the front-wheel angle. The target speed is transformed from relative speed to absolute speed. The time sequence of the braking pressure samples is compared with a threshold of 3 psi, producing a string of 0's (under the threshold) and 1's (over the threshold). Once four 1's are found in five consecutive samples, and the preceding five consecutive samples are all 0's, a braking onset is declared. The first of the five samples containing four 1's is the braking onset. The lidar data at the braking onset is examined to find the closest target in front of the bus. If there is a target in front of the bus, and the bus speed is greater than 1m/s, and the Time-To-Collision (TTC) is smaller than 40s and greater than 0s, then the braking-onset data is picked up and saved in a data file for further processing. TTC is calculated as [1]

$$TTC = R / (Vb - Vt) = R / Vb(1 - Vr) \quad (0.1)$$

where R is the closest range, Vb is the bus speed, Vt is the target speed, and Vr is the Vt -to- Vb ratio. The front wheel angle is sampled five points later than the braking onset.

In total 25,387 braking onset cases were extracted from the data.

2.2.2 Histogram analysis of braking onset parameters

The following pictures are histograms of bus speed, target speed, target range, initial brake pressure and TTC, all at braking onset. Very similar to the data sample analysis in section 0, the features of these quantities can easily be seen in the pictures.

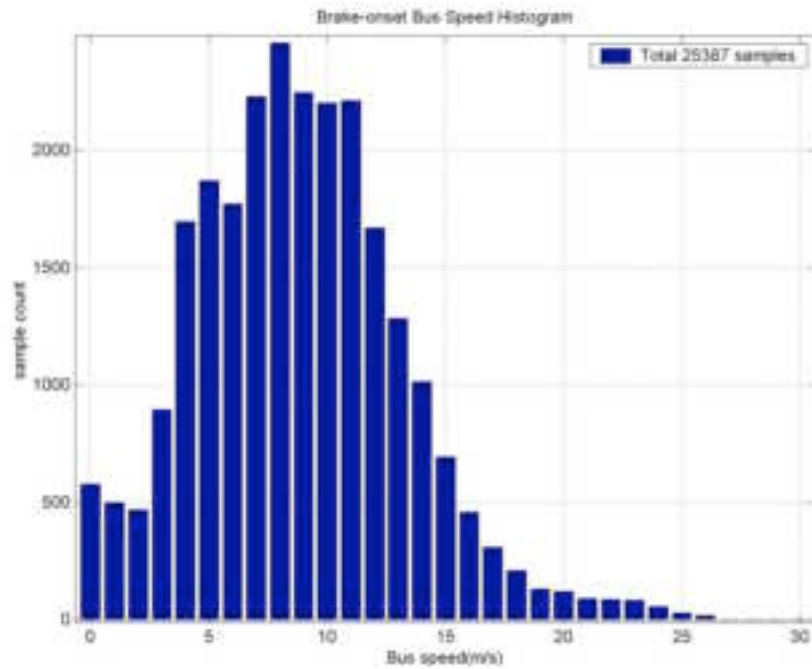


Fig. 2.35. Bus speed histogram at braking onset

Most brakes are initiated at 4~12m/s (9~27mph), see Fig. 2.3. Frequency of brakes at higher speed (over 16m/s or 36mph) is significantly smaller than those at lower speed. For stop-and-go situations when the bus speed is slower than 3m/s (6.5mph), the lower the speed, the higher the number of brake applications.

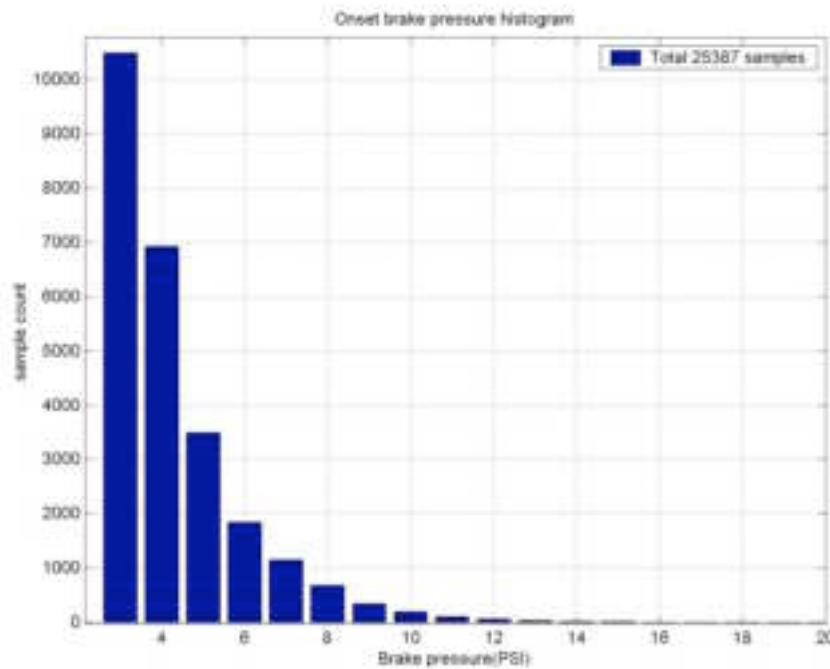


Fig. 2.16 Onset brake pressure histogram

In most cases, the onset (initial) brake pressure is small (<10psi). This indicates that the bus drivers usually brake smoothly.

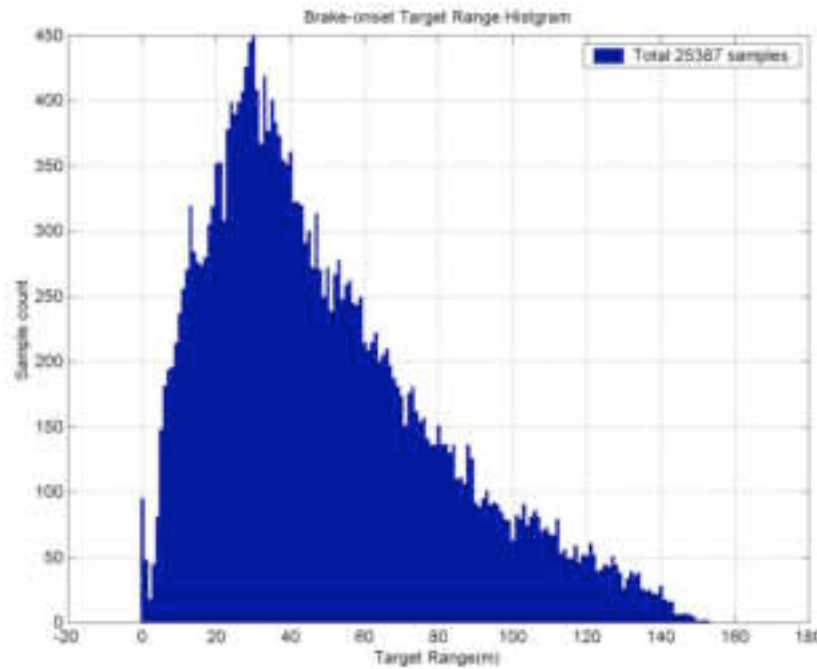


Fig. 2.17. Target range histogram

The most frequent value for of the closest target at braking onset is between 20 and 40 meters. There is a small peak at zero range as shown in Fig. 2.17. The data of those cases were checked. The target is either a very close object or a false target. In most cases the target is a false target (rain or fog).

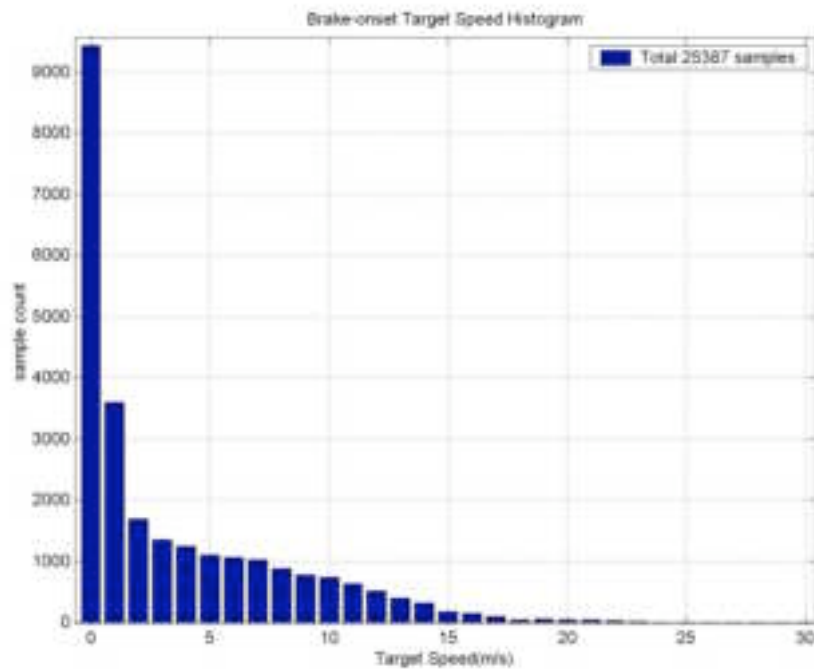


Fig. 2.18. Target speed histogram

In more than half of the cases, the closest target in front of the bus at braking onset was stationary or slowly moving ($<3\text{m/s}$ or $<6.5\text{mph}$), see Fig. 2.18. It should be noted that the

target is not necessarily the direct cause of the brake. In other words, the driver might not be reacting to the target but something else at that moment. One example is where a lead vehicle speeds up after stopping at a stop sign, while the bus driver has to brake to stop at the same stop sign. It is not the lead vehicle but the stop sign that forces the bus driver to brake. Another example is where a car is parked at a corner of a curved road, while the bus driver has to slow down before turning at the corner. It is not the parked car but the curve that forces the bus driver to brake. In both examples, the cars are picked up as targets. But the bus driver is not responding to them.

This point is very important to understand in the TTC histogram of 19. The TTC does not imply the timing of drivers' decision making in braking. It is merely a distribution of TTC at the moment the bus drivers initiate braking. It is informative in that false positives will not be avoided if we use TTC as a measure of severity. Whatever TTC threshold is set, there must be false positives, because in the cases where the TTC is smaller than the threshold, a warning is triggered before the drivers decided to brake, but the drivers would not consider this situation requiring a warning.

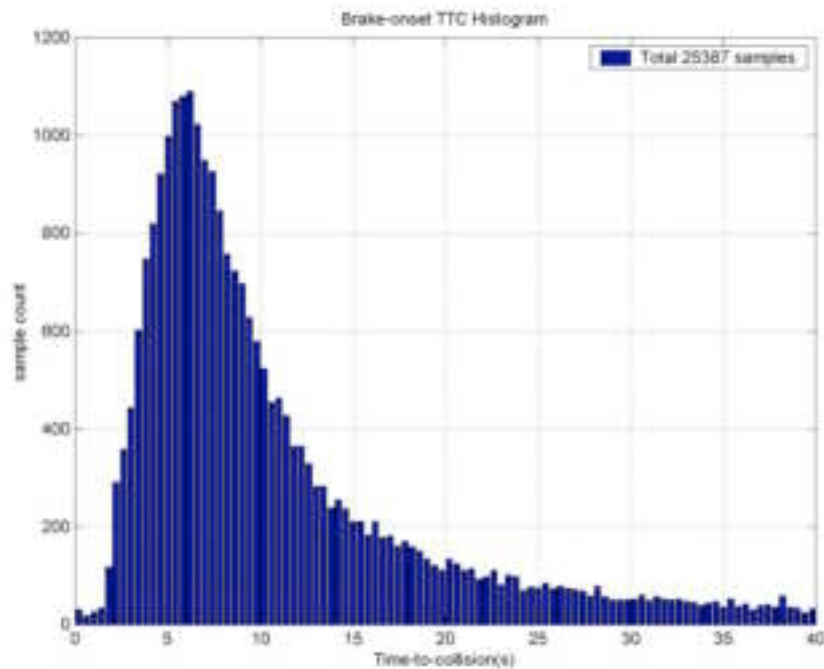


Fig. 2.19. Time-to-collision histogram

2.1.3 Clustering of target following scenarios

In the definition, TTC is proportional to the following range R . If the bus speed and the target speed are given, R is equivalent to TTC in characterizing the braking onset timing. For this reason, we focus on clustering of V_b and V_r hereafter.

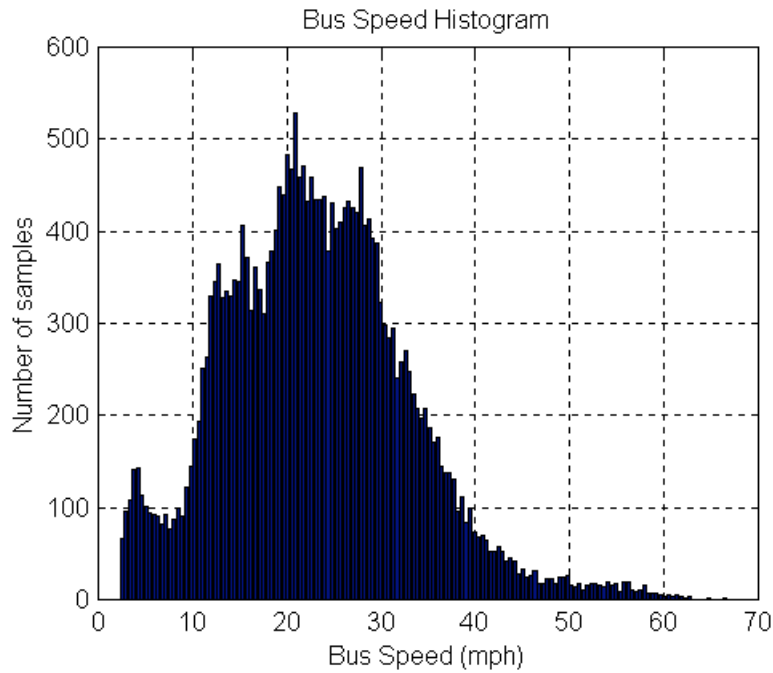


Fig. 2.20 Bus speed histogram

Fig. 2.0 is the refined histogram of V_b . There are several peaks. They are approximately at: 4.0-, 15.0-, 21.0-, 28.0-, 32.5- and 50.0-mph. This is not surprising, because the California speed limits are usually 5mph in congested areas with pedestrians, 15mph at blind intersections or in alleys, 25mph in business or residence areas, 30-, 35-, 40- or 45-mph for broader divided two-ways, and 55-65mph for freeways. The main body of the histogram is between 10- to 40-mph. This says that the bus mainly runs on low speed roads. The frequency that the bus runs below 7.5mph is high. The reason is probably that the bus needs to stop at the bus stations which are usually in congested areas, e.g. BART and Caltrain stations. The frequency becomes zero when bus speed approaches zero. This is because we didn't pick up those data when bus speed is smaller than 1m/s.

We empirically divide the bus speed into five categories in the following table.

Categories of bus speed

Category	B1	B2	B3	B4	B5
$V_b(\text{mph})$	0-7.5	7.5-17	17-31	31-45	>45

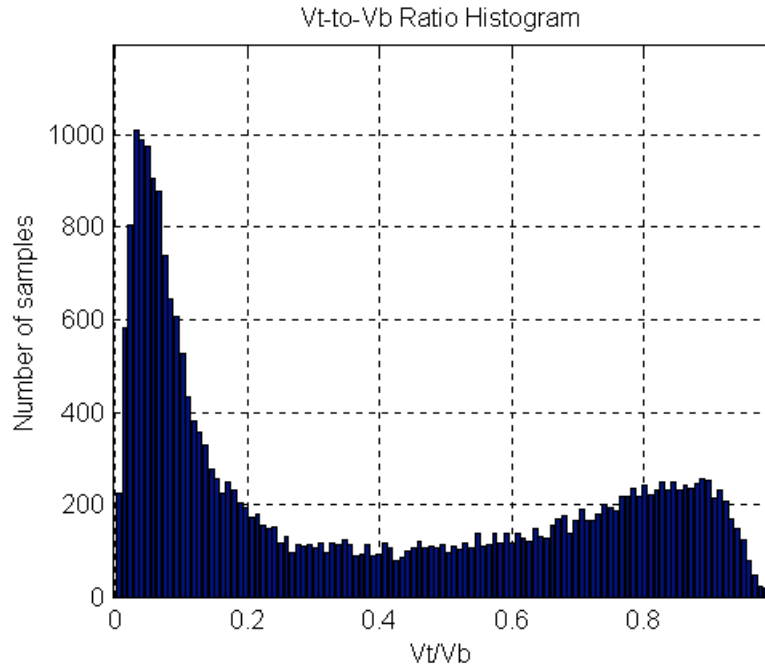


Fig. 2.21 V_t -to- V_b ratio histogram

Fig. 2.21 is the histogram of the V_t -to- V_b ratio. There are two peaks. One is at approximately 0.04, the other is around 0.9. This indicates that most of the targets from which the bus is trying to keep away are either very slow or at the similar speed of the bus. The big peak at 0.04 shows that the bus usually faces a great amount of slow-speed or stationary targets.

We empirically divide the ratio into three categories in the following table.

Categories of speed ratio

Category	T1	T2	T3
V_t/V_b	0-0.25	0.25-0.7	0.7-1

Combining the bus speed categories with those of speed ratio, we get 15 clusters. This is shown in Fig. 2.22. Each braking onset case is represented by a dot in the 2-D plot. The dot density represents the concentration of the clusters. This is a reasonable clustering except the B5-T2 combination. There are too few dots in this region to form a cluster.

The numbers of the cases that fall into each cluster are listed in the following table.

Total number of cases in each cluster

	<i>T1</i>	<i>T2</i>	<i>T3</i>	<i>Subtotal</i>
<i>B1</i>	573	525	138	1,236
<i>B2</i>	3112	1642	1033	5,787
<i>B3</i>	7151	3057	3230	13,438
<i>B4</i>	1761	798	1750	4,309
<i>B5</i>	290	45	282	617
Subtotal	12,887	6,067	6,433	25,387

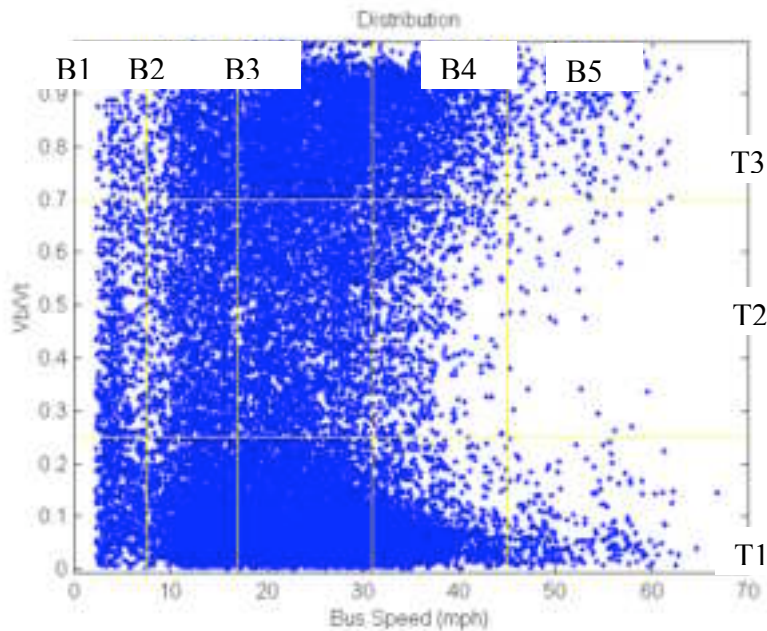


Fig. 2.22 Clusters of target following scenarios

The clustering in Fig. 2.22 provides a natural categorization of braking onset scenarios. Each cluster may follow different statistical characteristics. This provides a way to improve the collision warning performance.

2.14 Future work

Further analysis of the field data requires complex algorithms to pick up specific scenarios or targets. Development of the scenario recognition algorithms will help to improve the performance of the collision warning system. PATH will focus its efforts on algorithm development in the future phase of the project. The data will be reviewed with the improved algorithms.

PATH has developed a prototype CWS on SamTrans buses. PATH is collecting data on these buses. Another task of future data analysis will be to determine drivers' adaptations to the system, i.e. change of drivers' behaviors after cooperating with the FCWS. Future work will also include comparing operators driving performance behavior prior to the introduction of the FCWS to after implementation.

2.1.5 References

1. Hayward J.C., Near misses as a measure of safety at urban intersections. Doctoral dissertation, Pennsylvania State University, 1971.

3.0 Conclusion

Frontal Collisions account for approximately 30% of all transit vehicle related crashes annually. These collisions typically result in property damage, service interruptions and personal injuries while contributing to increased traffic congestion. Transit operators and industry stakeholders recommended that a study be conducted under the US DOT's Intelligent Vehicle Initiative (IVI) to develop a transit frontal collision warning system.

This report provides a summary of the Phase One of the project which entails results from the analysis of crash data and field data.

In order to define the operational environment and the bus operation scenarios, thorough data collection and analysis was conducted. In addition to reviewing national crash statistics, crash records collected by SamTrans and several other Bay Area transit agencies were analyzed. The crash data analysis indicated that frontal collisions can result in significant property damage and liability. In addition to frontal collisions, passenger falls resulting from emergency braking also contribute to an increased potential for passenger injuries and liability.

To further understand the transit operational environment and the conditions under which frontal collisions may occur, field data collection was also conducted using data acquisition systems installed on Samtrans buses. These data acquisition systems were developed by PATH specifically for this project to collect both engineering and video data about movement of surrounding vehicles and obstacles relative to continuous bus movement in a very small time interval. Under this project, diverse initial behavior data from a large pool of drivers were collected. A data processing tool was also developed by PATH to process the large quantity of data. Though no accidents were expected to be recorded through the limited field testing under this project, the relative movement of a bus and surrounding vehicles, particularly at times when brake actions were initiated by the bus drivers, showed that the urban and suburban operating environment is dramatically different from those targeted in other CWS studies. This observation presented a considerable challenge with respect to the diversity of obstacles to be detected and the different traffic patterns in which buses operate.

The field data analysis also helped to establish scenarios under which crashes may occur and a foundation for the determination of sensor performance, system specifications and the definition of the performance requirements.

Further studies are being conducted to design a prototype collision warning system and to conduct field tests in order to better understand how a transit frontal collision warning system needs to be designed in order to be effective in the urban driving environment and to be acceptable by transit drivers. A final report will be produced at the end of the project to summarize the entire study.

Appendixes

Appendix I: List of 32-CalTIP Members

1. AMODOR Regional Transit System
2. City of Arcata & Mad River Transit System
3. City of Auburn
4. City of Azusa
5. Butte County
6. Central Contra Costa Transit Authority
7. Culver City
8. City of Dixon
9. El Dorado County Transit Authority
10. City of Folsom
11. Golden Empire Transit District
12. Humboldt Transit Authority
13. City of Lincoln
14. Livermore Amador Valley Transit Authority
15. City of Lodi
16. Mendocino Transit Authority
17. Monterey-Salinas Transit
18. Morongo Basin Transit Authority
19. Napa County Transportation Planning Agency
20. Nevada County
21. Placer County Transit
22. Riverside Transit Agency
23. San Luis Obispo Regional Transit Authority
24. Santa Cruz Metropolitan Transit District
25. Siskiyou County
26. South Coast Area Transit
27. South County Area Transit
28. City of Vacaville
29. City of Vallejo Transit
30. Western Contra Costa Transit Authority
31. City of Whittier
32. Yolo County Transportation District

Appendix II: Sample JGAA cost report

Div ALL Select Period: As of:
 Activity Period: Printed: 09/11/2002 Page: 1
 07/01/1994 - 09/11/2002 09/11/2002

Incurring from: Selected by: Claims With
 Examiner ID: ALL
 DATE OF LOSS -\$999,999,999
 thru \$99999999999 Leg/Oth: YES Recovs: NO
 Proc Off: ALL ALL CLAIMS IN CLAIM NUMBER ORDER FOR CALENDAR YEARS
 1994-2002 Info-Only: YES Late-Rpt: YES

Maint-Only: YES *HistSumm: N/A

```
=====
=====
Claim Sts Carrier Loss Reported Entry Denied Closed Reopen
Paid in -----TOTALS AS OF: 09/11/2002-----
No No Date Date Date Date Date Date
Pay Period Paid Reserve Incurred
=====
=====
```

```
0053740 C 01/09/00 01/14/00 01/18/00 01/31/01
Loss: 63 ON BRD-STOPPING Desc: ABRUPT STOP PAX FELL

Claimant: VALENCIA, LUCIA Bod Inj:
0.00 400.00 0.00 400.00
Totals:
0.00 400.00 0.00 400.00
---CLAIM SUMMARY--- Totals:
0.00 400.00 0.00 400.00
```

NET: 400.00

```
0053750 C 01/13/00 01/17/00 02/01/00 03/15/00
Loss: 8 TRN LFT-OTH LFT Desc: UNSAFE LANE CHANGE VEHICLE COLLI

Claimant: VITALES, LUZVIMINDA Totals:
0.00 0.00 0.00 0.00
---CLAIM SUMMARY--- Totals:
0.00 0.00 0.00 0.00
```

NET: 0.00

Appendix III: Loss code description

Property damage (code 1~49)

- 1 Intersection: Bus straight ahead - other vehicle from left
- 2 Intersection: Bus straight ahead - other vehicle from right
- 3 Intersection: Bus turning right - other vehicle from ahead
- 4 Intersection: Bus turning right - other vehicle from left
- 5 Intersection: Bus straight ahead - other vehicle from opposite direction turns left
- 6 Intersection: Bus turning right - other vehicle from rear
- 7 Intersection: Bus turning left - other vehicle from ahead
- 8 Intersection: Bus turning left - other vehicle from left
- 9 Intersection: Bus turning left - other vehicle from right
- 10 Intersection: Bus turning left - other vehicle from rear
- 11 Intersection: Other vehicle turns right in front of bus
- 12 Intersection: All other intersection collisions
- 13 Head-on - vehicles from opposite directions
- 14 Sideswipe - bus passing other vehicle
- 15 Sideswipe - other vehicle from opposite direction
- 16 Sideswipe - other vehicle passing bus
- 17 Cutting in - by other vehicle
- 18 Other vehicle pulling from curb hit bus
- 19 Collision with standing vehicle (includes opened doors, parked auto)
- 22 All other accidents between intersections
- 23 Rear end - bus hit vehicle
- 24 Rear end - other vehicle hit bus
- 25 Loading zone: Bus pulling into zone involved with standing vehicle
- 26 Loading zone: Bus pulling from zone involved with standing vehicle
- 27 Loading zone: Bus pulling from zone involved with moving vehicle
- 28 Loading zone: Other vehicle involved with bus standing in zone
- 29 Loading zone: Bus pulling into zone involved with moving vehicle
- 30 Miscellaneous: All other collisions with other vehicles, bikes.
- 31 Scrapes at corners. Intersection sideswipes (includes right turn squeeze)
- 32 Sideswipes between intersections other than opposite direction
- 33 Opposite way sideswipes between intersections
- 34 Collisions between company passenger vehicles: end to end - in loading zones
- 35 Collisions between company passenger vehicles: end to end other than loading zones
- 36 Collision between company passenger vehicles: on company property, yards, terminal company parking
- 37 All other collisions between company passenger vehicles.
- 38 Collision with stationary object while bus backing.
- 39 Pedestrians - Intersection/crosswalks
- 40 Pedestrians - loading zones
- 41 Pedestrians - hit by overhang (bus turning)
- 42 Pedestrians - Between intersections
- 43 Pedestrians - all others
- 44 Miscellaneous collision: alleges - location - division or department unknown
- 45 Collisions with (fixed) stationary objects
- 46 Collision due to bus mechanical failure.
- 47 Collision due to bus leaving road
- 48 Collision not classified
- 49 Bus backing collision with moving vehicle.

Passenger injury (code 50~118)

- 50 Falls boarding
- 51 Miscellaneous boarding
- 52 Struck by front door - boarding
- 53 Falls alighting - front door
- 54 Handi Lift
- 55 Falls alighting - rear door
- 56 Falls alighting - rear door (push type)
- 57 Fall alighting not otherwise classified
- 58 Struck by front door - alighting
- 59 Struck by rear door - alighting
- 60 Struck by rear door - alighting (push type)
- 61 Struck by door not otherwise classified
- 62 On board: bus starting
- 63 On board: bus stopping
- 64 On board: bus turning

65 On board: bus running straight
66 On board: caught/struck by doors
67 On board: injuries from arms, head, etc. out of window
68 On board: accidents not otherwise classified
70 Property damage caused by defective equipment
71 Injuries caused by defective equipment
72 Disturbances, ejections fainting, sickness, fits, deaths on vehicles, etc.
73 Injuries or prop damage caused by other passengers or other person except bus motion
74 Falls - approaching to board or after alighting
75 Clothing soiled off bus (splashed water, etc.)
76 Thrown missiles (injuries/damage)
77 Thrown missiles (no injuries/damage)
78 Incidents not otherwise classified
79 Observation or witness reports (operator's vehicle not involved)
80 Non-operating vehicle accidents (supervisor cars, co. trucks, vehicles operated by mechanics, vandalism)
81 Other alleged
82 Other alleged
88 Bicycle
90 Employee accidents
99 Public accidents on company property - not defined
100 Striking and injuring or killing animal
101 Wheelchair: Falls boarding
102 Wheelchair: Door hit
103 Wheelchair: Miscellaneous boarding
104 Wheelchair: Lift stand
105 Wheelchair: Lift WC PAX
106 Wheelchair: Fall alighting
107 Wheelchair: Fall alighting
108 Wheelchair: Fall alighting
109 Wheelchair: PAX start
110 Wheelchair: PAX stop
111 Wheelchair: PAX curve (turning)
112 Wheelchair: PAX straight
113 Wheelchair: PAX door
114 Wheelchair: PAX window
115 Wheelchair: On board
116 Wheelchair: Tie down
117 Wheelchair: Tie down
118 Wheelchair: Lift

Violation (code 119, 120)

119 Civil right
120 ADA violation

Appendix IV: Accident Data as Shown in Bar Charts

Fig. 1.9 Claim and cost distributions for collision accidents with cost less than 10K

The percentages shown in black are actual cost data, and that shown in blue are generated by the statistics from Agency IV and V.

Agency	Total claim	Total cost	Percent of claims				Percent of costs			
			F	S	R	N	F	S	R	N
I	324	\$665,044	29.0	55.2	11.1	4.6	36.1	49.5	11.1	3.4
			26.0	48.7	13.7	11.6	35.1	44.4	10.7	9.8
II	1,109	\$1,108,053	13.3	40.8	6.3	39.5	18.5	36.6	4.0	40.9
			19.5	54.4	13.8	12.4	27.5	50.8	9.9	11.8
III	346	\$263,970	16.2	46.2	24.3	13.3	20.7	51.1	15.9	12.3
			18.7	44.7	23.9	12.7	25.3	45.3	16.8	12.6
IV	243	\$343,870	27.6	35.4	25.5	11.5	34.4	32.4	22.7	10.5
			24.0	37.6	26.0	12.4	30.9	36.9	22.0	10.2

Fig. 1.10 Claim and cost distributions for all collision accidents

The percentages shown in black are actual cost data, and that shown in blue are generated by the statistics from Agency IV and V.

Agency	Total claim	Total cost	Percent of claims				Percent of costs			
			F	S	R	N	F	S	R	N
I	353	\$2,904,763	31.7	52.4	10.2	5.7	70.6	22.4	2.5	4.4
			29.0	46.4	12.6	12.1	70.4	21.3	2.4	5.9
II	1,146	\$6,319,107	14.7	40.2	6.2	38.9	20.5	45.0	0.9	33.6
			20.6	53.3	13.4	12.7	22.1	47.5	1.9	28.5
III	358	\$997,982	17.3	45.3	23.7	13.7	22.4	17.5	5.7	54.5
			19.7	43.8	23.4	13.1	23.6	15.9	5.9	54.6
IV	261	\$1,032,796	29.9	34.1	24.9	11.1	61.4	19.6	14.3	4.7
			26.6	36.1	25.4	12.0	60.2	21.1	14.0	4.6

Fig. 1.15-transit agencies: General collision accident costs by initial point of impact

Agency	Total claim	Total costs	Percent of claims				Percent of costs			
			F	S	R	N	F	S	R	N
I	348	\$1,186,535	31.0	52.9	10.3	5.7	45.2	37.8	6.2	10.7
II	1,137	\$1,826,183	14.4	40.4	6.2	39.0	31.2	31.8	3.0	34.0
III	357	\$543,490	17.4	45.4	23.8	13.4	41.1	32.1	10.4	16.4
IV	260	\$796,180	29.6	34.2	25.0	11.2	49.9	25.5	18.5	6.1
V	1,731	\$3,098,536	25.2	48.1	16.2	10.6	18.4	18.8	1.8	20.0
CalTIP(30)	1,391	\$3,339,754	22.5	43.4	19.0	15.1	38.2	29.4	8.5	24.0
All (35)	5,224	\$10,790,680	22.2	44.6	15.3	17.9	40.2	33.4	8.2	18.1

Fig. 1.19-transit agencies: General collision accident costs by collision object

Collision object	Total claims	Total costs	Percent of claims				Percent of costs			
			F	S	R	N	F	S	R	N
Vehicle	4,762	\$9,313,621	22.6	46.0	16.2	15.2	41.3	34.6	9.2	14.9

Pedestrian	184	\$1,027,244	26.3	17.5	1.6	54.6	37.2	21.4	0.2	41.2
Stationary object	278	\$449,815	12.4	38.8	9.5	39.2	24.7	35.7	6.7	32.9
Total	5,224	\$10,790,680	22.2	44.6	15.3	17.9	40.2	33.4	8.2	18.1

Fig. 1.20-transit agencies: General vehicle collision costs by accident scenario

Accident scenario	Total claims	Total costs	Percent of claims				Percent of costs			
			F	S	R	N	F	S	R	N
S1	668	\$1,697,209	31.5	49.0	5.1	14.4	40.2	43.1	4.9	11.9
S2	461	\$2,174,890	100.0	0.0	0.0	0.0	100.0	0.0	0.0	0.0
S3	486	\$432,289	0.0	0.0	100.0	0.0	0.0	0.0	100.0	0.0
S4	852	\$1,243,354	12.0	55.8	5.8	26.5	22.7	52.0	4.5	20.8
S5	752	\$935,215	0.0	100.0	0.0	0.0	0.0	100.0	0.0	0.0
S6	230	\$340,937	25.2	49.3	4.5	20.9	31.5	50.4	6.2	11.9
S7	432	\$407,126	19.6	48.4	22.8	9.1	13.8	44.8	23.8	17.5
S8	382	\$873,890	12.6	42.1	12.9	32.3	28.2	34.8	5.3	31.7
S9	499	\$1,208,711	22.0	31.0	9.0	38.1	18.9	28.3	9.8	43.0
Total	4,762	\$9,313,621	22.6	46.0	16.2	15.2	41.3	34.6	9.2	14.9

Fig. 1.24-transit agencies: Passenger injuries by bus movements

Bus movement	Claim	Cost	Percent of claims	Percent of costs
Boarding	499	\$1,013,907	11.6	7.5
Alighting	770	\$1,816,013	18.0	13.4
Starting	168	\$567,644	3.9	4.2
Stopping	849	\$3,820,606	19.8	28.1
Turning	115	\$387,192	2.7	2.9
Going straight	136	\$521,322	3.2	3.8
Moving (others)	561	\$2,259,218	13.1	16.6
Others	1,187	\$3,199,336	27.7	23.6
Total	4,285	\$13,585,239		

Appendix V: Development of Data Acquisition System (DAS)

In evaluating the data acquisition needs, an evaluation of existing DAS's was conducted. It was determined through the study that no commercial or government developed system (including DASCAR) was available that would meet all the performance requirements. PATH therefore designed a system that is composed of two distinct systems - one system records engineering data and the other records video data. The engineering data is recorded with a PC based computer. The computer used is an Industrial Computer Systems 9300™ series bench top computer using ISA/PCI architecture. This computer records the output from a variety of sensors. The sensors selected by PATH to capture the environment around the bus include commercially available mono-pulse millimeter-wave radars and scanning infrared lasers. Both the radar and scanning laser measure distance and azimuth angle for multiple targets. The radar units are mounted on the front bumper, one on each end, pointing forward. Ultrasonic sensors were originally used as corner sensors, however they did not work well for two reasons. Firstly, the ground was being picked up as a target as the sensitivity was adjusted to a high level. Secondly, as ultrasound transceiver surface was not water proof it was decided that they were not appropriate as corner sensors. It was then decided that Denso LIDAR sensors would be better for this role, so several of these were acquired from Denso. Three lidar units are mounted on the bumper. The units mounted at each end of the bumper are pointing out 20 degrees and the one mounted near the center is pointing straight ahead. Other sensors record the driver inputs to the bus, such as steering wheel angle, brake line pressure, throttle position, and turn signal activation. Other sensors include an accelerometer and a GPS system. The radars, lidars, and GPS data are recorded using RS232 communication protocol. The remaining sensors are recorded using an analog to digital board and anti-aliasing filters.



Fig. V.1 Sensors Installed on a Bus

Video data is recorded using a commercially available digital video system. The first digital video recording system implemented saved the video as a series of still images in an encrypted proprietary format. This limited the level of compression and allowed only three days of data to be collected before the removable hard disks had to be changed. This also required that the video data first be converted to a standard still-picture format, and then be converted to a standard moving-picture format (MPEG-1). This was a very time consuming manual process. The video recorder was not reliable such that it crashed the flash-ROM system several times. A Loronix™ video system was found that offered several improvements over the previous system. This system records video in a standard still format (AVI) and allows for automated conversion to MPEG-1 format. Much less time is required to convert the video data now that the process is automated. The system also has greater storage capacity than the previous one, allowing one week of data collection before the removable hard disks need to be changed. This system was retrofitted on the first bus and has proven to be much more reliable and easier to use. The video cameras in the originally developed system were too obtrusive, and easily damaged or moved by passengers. A different style of video camera was selected to replace them. These cameras have a form factor that allowed them to be installed in the destination window of the bus. This makes them less obtrusive and prevents them from being tampered with. This system records up to six cameras in AVI format onto a PC hard drive. Four miniature “board cameras” capture video images around the bus. The cameras capture the front road scene, the left and right front corner road scene, and the passenger compartment of the bus. The video streams from the four cameras are combined into one video stream by a quad image combiner to extend the hard drive storage capacity.

Synchronization between engineering and video data is very important for later playback. The first item of information for synchronization is the time stamp recorded in the video frame as a title. This time stamp is generated by a title generator which receives the clock time from the engineering computer. This title allows for manual synchronization. The engineering computer also sends three synchronization signals to the video recorder through the alarm inputs. These signals and their triggering time stamps are recorded separately by both the engineering computer and the video recorder. The signals are triggered every one minute, 15 minutes and 60 minutes respectively. By matching the signal records in the engineering data with the records of alarms in the video recorder, time difference between the two computers can be determined. Once the computer time difference is matched, the video clips can be synchronized with the engineering data streams. The synchronization occurs as part of the process of transferring the data from the removable hard disks to a permanent data base storage system. The permanent data base storage system is composed of a Redundant Array of Inexpensive Disks (RAID). Once the data base has been synchronized and broken into small data clips each set of data clips is saved in one folder for easy access.

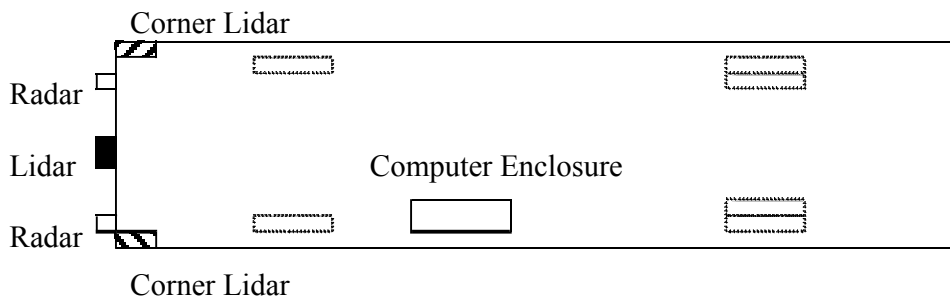


Fig. V.2 System layout on the bus

The data acquisition system has been installed on three buses in the SamTrans fleet. A fourth system has been prepared for installation on a yet to be determined bus from another agency in the Bay Area. The first system started collecting data in August 2000. The second system started collecting data in April 2001. After the second system started running, the first system was updated with the new design. The third bus started collecting data in January 2002.

Calibration of DAS

The location and direction of some sensors will influence the system performance. Before running the bus out to collect data, the sensors and the entire system must be calibrated. The calibration process involves the following three tasks: 1) measure the location and direction of the sensors, 2) correct the location and direction of some sensors, and 3) examine the system alignment.

This section describes the calibration process of the first DAS on the first bus and gives the results. The 1st section gives the measurements of location and sensor direction. The 2nd section describes the laser radar calibration procedure and results. The 3rd section describes the calibration approaches for cameras. Calibration of system alignment is given in the 4th section. Calibration of other sensors is given in the 5th section. The DAS design was changed after the first DAS was calibrated. However, the calibration process and the techniques presented in this document were conducted to calibrate all the systems. For convenience, the following abbreviations are used.

<i>Sensor Name</i>	<i>Abbreviation</i>
passenger side corner camera	P-CAM
front-looking camera	F-CAM
driver side corner camera	D-CAM
passenger side upper ultra-sensor	UP-SONAR
passenger side lower ultra-sensor	LP-SONAR
passenger side radar	P-RADAR
laser radar	LIDAR
front-looking ultra-sensor	F-SONAR
driver side radar	D-RADAR
driver side upper ultra-sensor	UD-SONAR
driver side lower ultra-sensor	LD-SONAR
Interior-looking camera	I-CAM
rear-looking camera	R-CAM
rear radar	R-RADAR
global positioning system	GPS

Sensor position

Coordinate systems

To locate the sensors, two reference frames were built on the bus. One is the Front Coordinate System (FCS) and the other is the Rear Coordinate System (RCS). Locations of front sensors, including P-CAM, F-CAM, D-CAM, UP-SONAR, LP-SONAR, P-RADAR, LIDAR, F-SONAR, D-RADAR, UD-SONAR, LD-SONAR and I-CAM, are measured in the FCS.

Locations of rear sensors, including R-CAM, R-RADAR and GPS are measured in the RCS. The reference points of the coordinates and the positions of the sensors are illustrated in the following figures. The positive x-axis is horizontally to the left, the positive y-axis is vertically upward, and the positive z-axis is horizontally to forward.

The basic dimensions of the bus are:

length = **12200** mm, width = **2750** mm.

Front Sensors

The reference point of the FCS and the locations of the front sensors are illustrated in Fig. V.3.

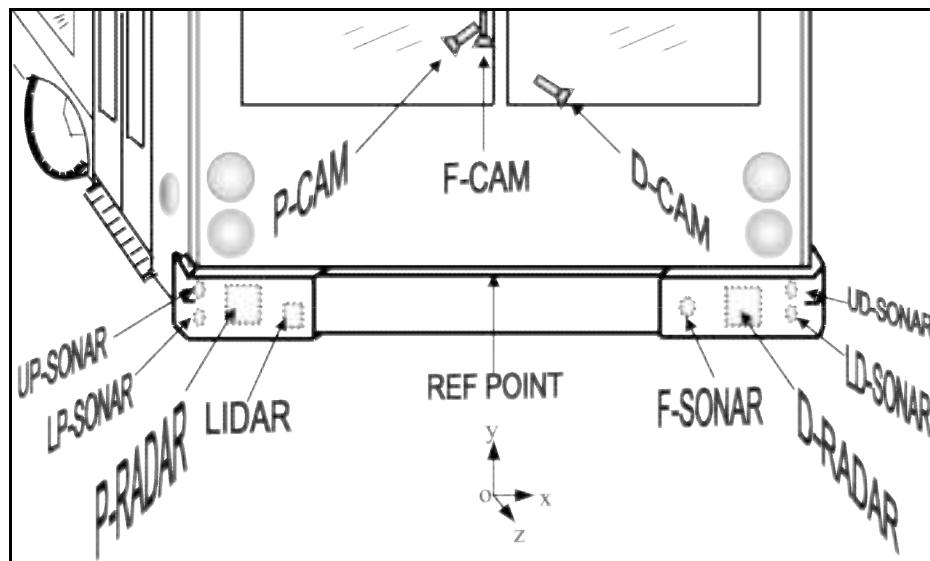


Fig. V.3 FCS and front sensors

The reference point is on the front center of the bus. The height of the reference point from the ground is **585**mm. The coordinates of the front sensors are listed in the following table.

Front sensor locations

Sensors	x (mm)	y (mm)	z (mm)	Angle (Deg)
LIDAR	-836	-195	78	¹ N.A.
P-RADAR	-1050	-132	70	N.A.
UP-SONAR	-1201	-97	64	² -36
LP-SONAR	-1201	-176	64	² -26
D-RADAR	985	-135	67	N.A.
UD-SONAR	1190	-95	64	² 35
LD-SONAR	1190	-175	64	² 26
F-SONAR	790	-161	61	N.A.
D-CAM	396	991	-80	³ 14
F-CAM	-69	1653	-61	³ 13
P-CAM	-109	1563	-95	³ 25
I-CAM	-409	2186	-365	N.A.

1: N.A. = Not available;

2: These are azimuth angles;

3: These are tilting angles.

Rear Sensors

The reference point of the RCS and the locations of the rear sensors are illustrated in Fig. V.4.

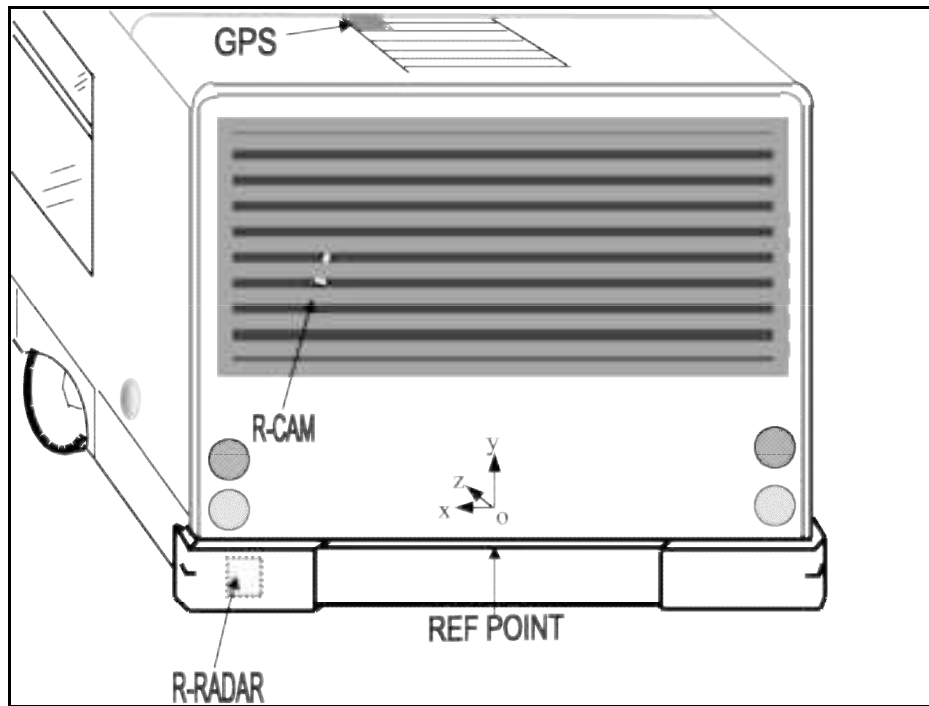


Fig. V.4 RCS and rear sensors

The reference point is on the rear center of the bus. The height of the reference point to the ground is **790mm**. The coordinates of the rear sensors are listed in the following table.

Rear sensor locations

Sensors	x (mm)	y (mm)	z (mm)	Angle (Deg)
R-RADAR	950	-154	-39	¹ N.A.
GPS	590	2220	800	N.A.
R-CAM	500	1500	140	² 16

1: N.A. = Not available;

2: Tilting angle.

LIDAR calibration

Optical axis orientation

The LIDAR beam is scanning in 2D by rotating a hexagon mirror. The equivalent detection scope is 16 degrees in horizontal and 4.4 degrees in the vertical direction. The equivalent optical axis is defined to originate from the LIDAR lens extending to the center of the detection scope, i.e. eight degrees to both the left and the right margins and 2.2 degrees to both the top and the bottom margins. There are two adjustable screws on the front face of the LIDAR, which can be rotated to adjust the optical axis in 2D (both horizontal and vertical directions). As the LIDAR has been mounted on the passenger side on the 1st bus, to calibrate the LIDAR, we must first adjust the optical axis to an appropriate direction [2].

The LIDAR optical axis is set horizontally to the point on the bus's longitudinal center line, 50 meters away from the bus front reference point, and vertically 2.2 degrees up with respect to the horizontal plane. The geometric relationship is illustrated in Fig. V.5.

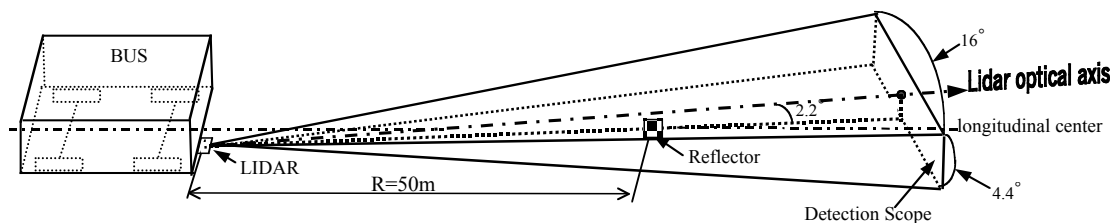


Fig. V.5 LIDAR calibration geometry

LIDAR calibration procedure

LIDAR calibration was done by the following procedure.

1. Measure LIDAR lens vertical position (height to ground) $H = \underline{0.425}$ (m).
2. Measure $R = \underline{50m}$ from bus front reference point along the longitudinal direction.
3. Set the reflector at $R = \underline{50m}$ with vertical position = H .
4. Adjust both the lower and the higher screws simultaneously, make reported "lateral position" = $\underline{0}$. Change lateral position to check the adjustment.

LIDAR lateral position test

Actual lateral position	Expected report number	LIDAR report (5 th col)
6m Left	-60 *.1m	<u>-61</u>
3m Left	-30 *.1m	<u>-30</u>
3m Right	30 *.1m	<u>30</u>
6m Right	60 *.1m	<u>61</u>

5. Adjust the lower screw, make reported "Vertical Position" changing from smaller to larger numbers thru $\underline{12}$.
6. Adjust the lower screw to "– direction" $\underline{0.3-0.5}$ rev, make sure that the LIDAR keeps detecting the reflector.
7. Change distance to check the adjustment:

LIDAR range test

Actual distance	Expected report number		LIDAR report (1 st -2 nd col)	
40m	31*1.28m	32*.01m	<u>31</u> *1.28m	<u>98</u> *.01m
30m	23*1.28m	56*.01m	<u>24</u> *1.28m	<u>14</u> *.01m
20m	15*1.28m	80*.01m	<u>16</u> *1.28m	<u>48</u> *.01m
10m	7*1.28m	104*.01m	<u>8</u> *1.28m	<u>46</u> *.01m

8. Put the reflector at $R=10m$, with vertical position changing, check the adjustment:

LIDAR vertical position test

Actual vertical position	Expected report number	LIDAR report (9 th col)
H+0.76m	2	<u>2</u>
H+0.57m	3-4	<u>4</u>
H+0.38m	6-7	<u>5</u>
H+0.19m	9-10	<u>6</u>
H+0m	12	<u>8</u>

Camera calibration

Rough adjustment

Three different options of focal length are available: 3mm, 4mm, and 7.5mm. Lenses with different focal length were fitted on the camera heads. By comparing the field of view and selecting the one that best matches the area of interest around the bus, the optimal fitted focal length was chosen for each camera, as is listed in the following table.

Camera	Focal length
D-CAM	4mm
F-CAM	7.5mm
P-CAM	4mm
I-CAM	4mm
R-CAM	7.5mm

Image plane rotation and optical axis direction of each camera was roughly adjusted by monitoring the video output. The factors of interest while adjusting are: range coverage, azimuthal direction of interest, and consistency between adjacent cameras. The tilting angle of each camera was measured with a level and an angle measure.

Intrinsic and extrinsic parameters calculation

Control points

To calibrate the cameras, 20 control points arranged in 4 lines with 5 points in each line were made on a vertically standing black screen. The adjacent lines are 50 centimeters apart. The distance between adjacent points in each line is also 50 centimeters. The screen was put in front of each camera with the points facing the camera. A picture was taken and stored in the computer. The screen was then moved 25 centimeters (for F-CAM and R-CAM) or 20 centimeters (for D-CAM and P-CAM) closer to the camera. This process was repeated until five pictures were taken for each camera. Fig. V.6 is an example of pictures taken from the front camera (F-CAM). Every time a picture was taken, the position of the screen in the bus coordinate system was marked on the ground and measured later to calculate the control point coordinates.



Fig. V.6 Pictures taken from F-CAM

The pictures were opened in Microsoft Photo Editor™ to read the image coordinates of the control points. We get the coordinates of the control points in the bus coordinate system and their corresponding image coordinates in the picture. Each control point and its image are called a calibration pair. By substituting the coordinates of the calibration pairs in the camera model described below, two equations for each pair were obtained. We can solve the unknown camera parameters from the equations for all pairs in the sense of Least Square Error (LSE).

Camera model

Let $P = (X, Y, Z)^T$ represent the coordinates of a point in the bus coordinate system (FCS or RCS), $P_C = (X_C, Y_C, Z_C)^T$ represent the coordinates of the point in the camera coordinate system, (x_U, y_U) and (x_D, y_D) represent the undistorted and distorted image coordinates of the point respectively, and (i, j) represent the coordinate read in Microsoft Photo Editor™, i.e. the pixel location with respect to the top-left corner in the image, viz. the computer image coordinate. The relationship between the bus coordinate system and the camera coordinate system is given by [3]:

$$P_C = RP + T \tag{1}$$

where $R = \begin{Bmatrix} r_{ij} \end{Bmatrix}$ is a 3×3 ortho-normal rotation matrix defining the camera orientation and $T = (t_1, t_2, t_3)^T$ is a translation vector defining the camera position. The camera coordinate

system is transformed to the undistorted image coordinate (2D) system according to the pin-hole model:

$$\begin{cases} x_U = f \frac{X_C}{Z_C} \\ y_U = f \frac{Y_C}{Z_C} \end{cases} \quad (2)$$

where f is the focal length. The distortion of image coordinates can be modeled by [5]:

$$\begin{cases} \Delta x = 2p_1x_Uy_U + p_2(r^2 + 2x_U^2) + k_1x_Ur^2 \\ \Delta y = p_1(r^2 + 2y_U^2) + 2p_2x_Uy_U + k_1y_Ur^2 \end{cases} \quad (3)$$

where $r^2 = x_U^2 + y_U^2$, p_1, p_2 are coefficients of tangential distortion, and k_1 is the coefficient of radial distortion. The distorted image coordinates are then obtained:

$$\begin{cases} x_D = x_U + \Delta x \\ y_D = y_U + \Delta y \end{cases} \quad (4.1)$$

or

$$\begin{cases} x_D = x_U + 2p_1x_Uy_U + p_2(r^2 + 2x_U^2) + k_1x_Ur^2 \\ y_D = y_U + p_1(r^2 + 2y_U^2) + 2p_2x_Uy_U + k_1y_Ur^2 \end{cases} \quad (4.2)$$

The relationship between the distorted image coordinates and the computer image coordinates is given by:

$$\begin{cases} x_D = \Delta x (i - i_0) \\ y_D = \Delta y (j - j_0) \end{cases} \quad (5)$$

where $\Delta x, \Delta y$ are the distance between the adjacent imaging sensor elements in rows and columns, respectively, (i_0, j_0) represents the computer image coordinate of the principal point of the image coordinate system.

The model itself is a nonlinear one. The unknown parameters can be categorized into intrinsic and extrinsic, or linear and non-linear parameters, as follows:

	Linear	Nonlinear
Intrinsic	$f, \Delta x, \Delta y, (i_0, j_0)$	k_1, p_1, p_2
Extrinsic	$R = \{r_{ij}\}_{i,j=1,2,3}, T = (t_1, t_2, t_3)^T$	

Calibration procedure

It is hard to solve all the parameters simultaneously from the complete nonlinear camera model. However, if the nonlinear distortion can be neglected, the model becomes linear. Once the linear parameters are known, the nonlinear parameters can be solved from linear equations (3). These properties of the camera model help us to simplify the calibration procedure into the following steps [4]:

step 1: Assume no distortion, calculate linear model parameters

Step 2: Calculate distortion using the linear parameters estimated in Step 1

Step 3: Calculate nonlinear parameters using the distortion and linear parameters estimated in Step 2

Step 4: Calculate distortion using the linear and nonlinear parameters estimated in Step 2 and 3

Step 5: Subtract the distortion estimated in Step 4 from the image coordinates, loop to Step 1 or terminate

The procedure is terminated when it is convergent. As noise exists in the calibration pair coordinates, the distortion used in Step 5 was multiplied with a positive fraction to confirm convergence. The positive fraction used in our calculation is 0.999.

Calibration results

Control point images

Control point image coordinates estimated with linear-only and nonlinear-plus models together with the actual image coordinates read in Photo Editor™ are illustrated in the following plots, where the ‘o’ signs represent the actual images read in Photo Editor™, the ‘+’ signs represent the images estimated only with linear model, and the ‘x’ signs represent the images estimated with linear plus nonlinear model.

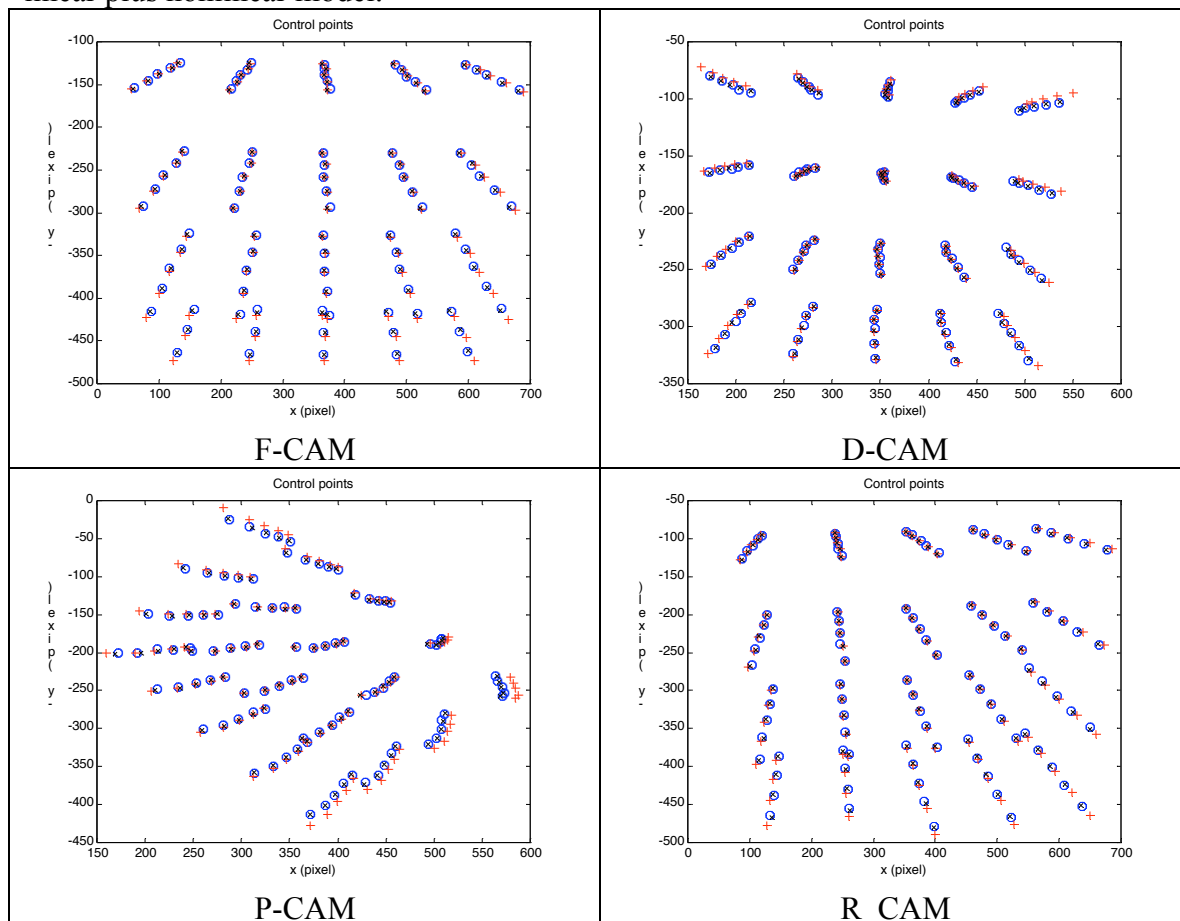


Fig. V.7 Control point images

Distortion

Distortion is calculated and plotted in the following plots.

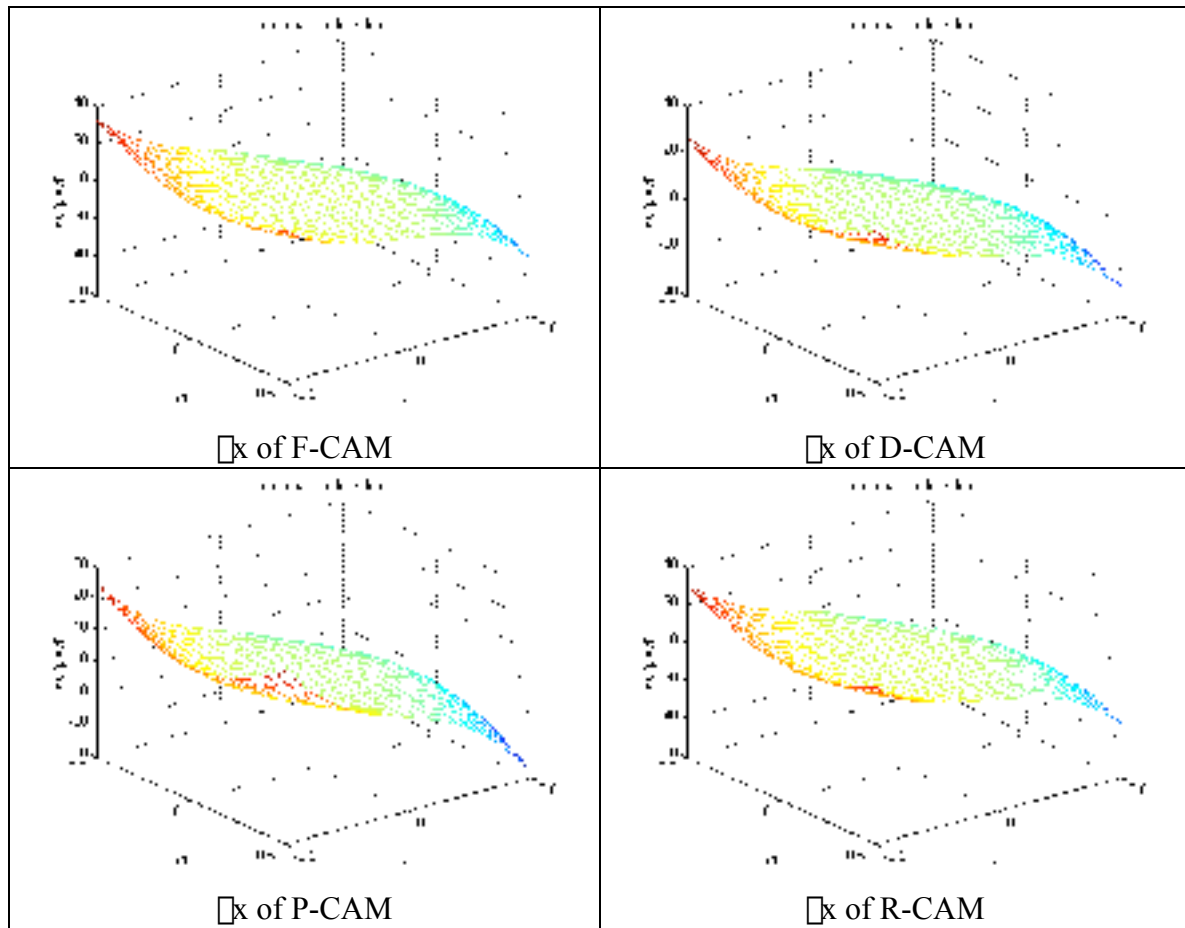
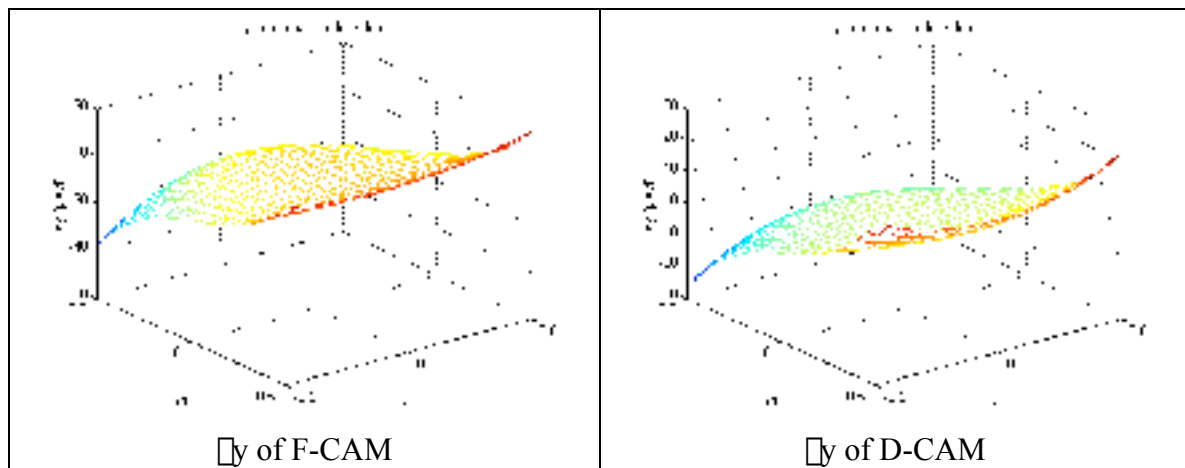


Fig. V.8 \square x of four cameras



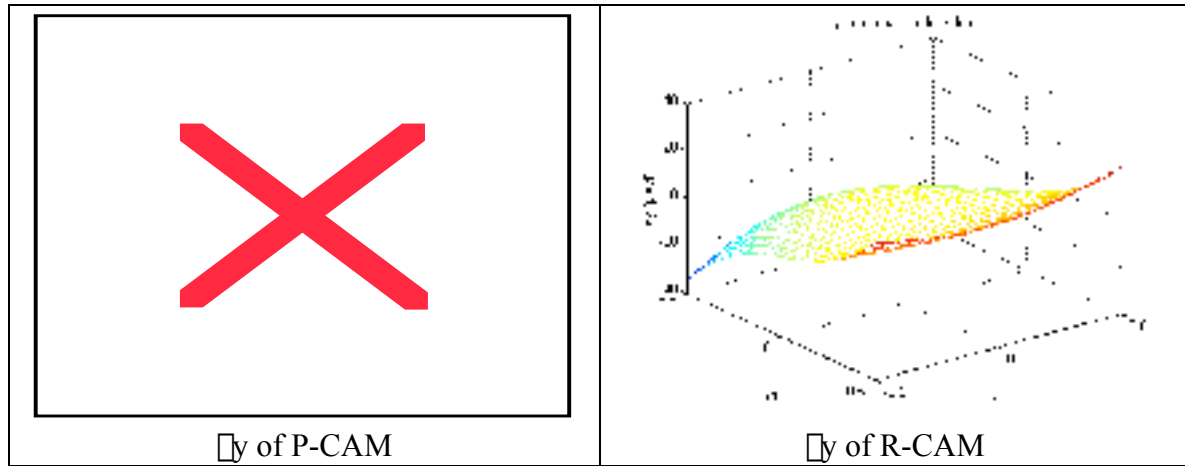


Fig. V.9 \square_y of four cameras

Intrinsic and extrinsic parameters

The intrinsic and extrinsic parameters for different cameras were calibrated and are listed in the following table.

Intrinsic and extrinsic parameters

Parameters	F-CAM			D-CAM			P-CAM			R-CAM		
	R_1	R_2	R_3	R_1	R_2	R_3	R_1	R_2	R_3	R_1	R_2	R_3
R^T	-1.0000	-0.0042	-0.0035	-0.7018	-0.1878	0.6877	-0.7390	-0.3102	-0.5965	0.9921	-0.0326	0.1207
	-0.0011	-0.9743	-0.2252	0.0535	-0.9763	-0.2092	0.6001	-0.7109	-0.3714	-0.0037	-0.9678	-0.2518
	-0.0038	-0.2252	0.9743	0.7103	-0.1080	0.6952	-0.3063	-0.6312	0.7115	0.1257	0.2496	-0.9602
T^T (m)	-0.0658	1.6280	0.5324	0.3428	1.0512	0.0723	-1.1015	1.0498	0.5364	-0.5286	1.4410	0.4298
(i_0, j_0)	359.79, 222.63			348.61, 226.08			366.81, 216.45			361.05, 206.93		
$(f/w_x, f/w_y)^t$	860.83, 790.62			461.00, 419.96			438.66, 403.40			841.70, 771.48		
$(p_1, p_2, k_1)/f$	-0.0146	-0.0056	-0.1434	-0.0064	-0.0044	-0.2342	-0.0006	-0.0048	-0.2447	-0.0108	-0.0055	-0.1486

- The imaging element size parameter \square_x, \square_y can not be determined in the calibration procedure. These parameters can be found in camera manufacturer's specifications. The cameras mounted on bus No.1 are from ELMO. The camera head model is MH42H. The effective image area is 6.54mmx4.89mm. Effective image pixels are 768 x 494. By simple calculation, the size parameters are: $w_x=0.0085\text{mm}$ $w_y=0.0099\text{mm}$

Derived parameter verification

Some parameters can be derived from the calibrated parameters. Location of the cameras can be derived by [6]:



Focus length of the cameras can be calculated by simply multiplying f/\square_x with \square_x or multiplying f/\square_y with \square_y . Angles of the cameras can be calculated from the rotation matrix R:

Tilting angle = - ;

Azimuth angle = $-\arctan(r_{31}/r_{33})$

Image rotation = $\arctan(r_{12})$

These derived parameters are listed in the following table.

Derived parameters

	F-CAM		D-CAM		P-CAM		R-CAM	
	Measured	Calculated	Measured	Calculated	Measured	Calculated	Measured	Calculated
Location X (mm)	-69	-57	396	388	-109	-168	500	523
Location Y (mm)	1653	1706	991	1023	1563	1607	1500	1501
Location Z (mm)	-61	-152	-80	-180	-95	-56	140	111
Focus fx (mm)	7.5	7.32	4.0	3.92	4.0	3.73	7.5	7.15
Focus fy (mm)	7.5	7.83	4.0	4.16	4.0	3.99	7.5	7.64
Tilting Ang (Deg)	13	13.01	14	12.1	25	21.8	16	14.6
Azimuth Ang (Deg)	N.A.	0.20	N.A.	-44.7	N.A.	40.0	N.A.	7.2
Image Rotation Ang (Deg)	N.A.	-0.06	N.A.	3.06	N.A.	31.0	N.A.	-0.21

System alignment

The purpose of system alignment is to determine the inter-relationship of multiple sensors in the system. Three sensors, LIDAR, P-RADAR and D-RADAR, are considered. Thirteen locations were marked on the ground in front of the bus. A microwave reflector and a laser reflector were used as targets for the sensors. Both reflectors were held by a person moving from location to location in the order of the numbers illustrated in

Fig. V.10. When the person moved to one location, he stayed there for about six seconds, with the microwave reflector swinging forth and back to simulate a moving target. Data was collected in the on-bus computer. This is plotted in Fig. V.11 thru Fig. V.13.

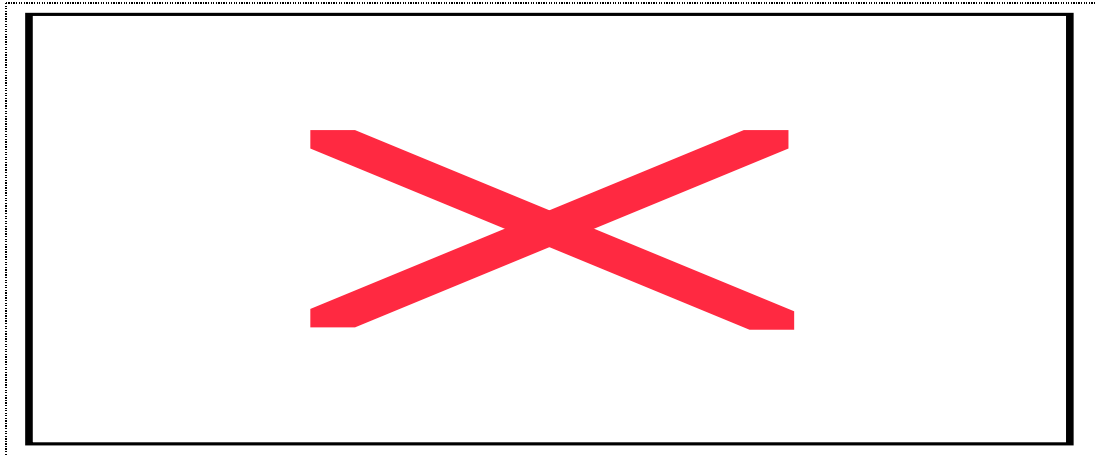


Fig. V.10 Object locations for system alignment

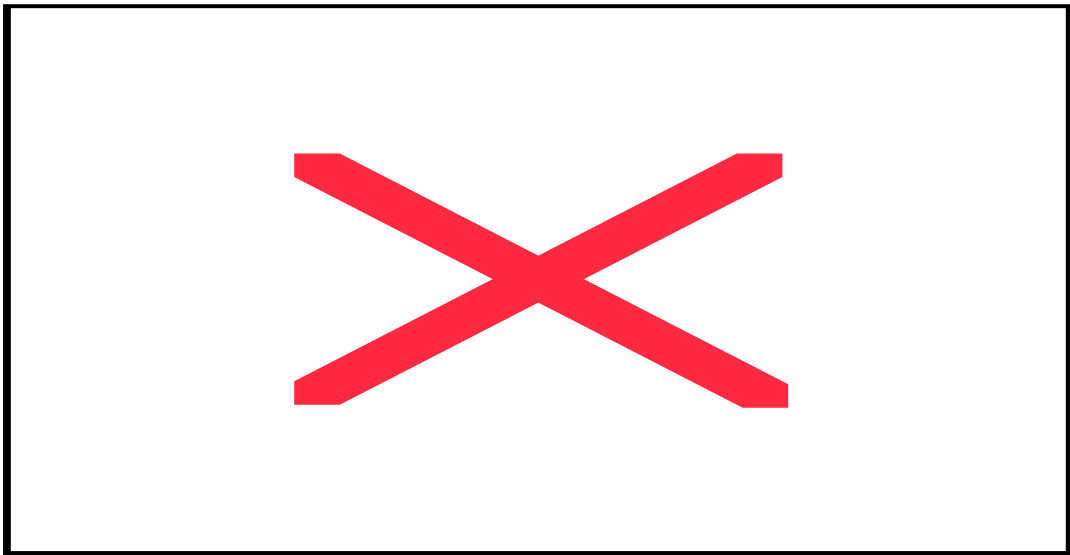


Fig. V.11 PRADAR data for system alignment

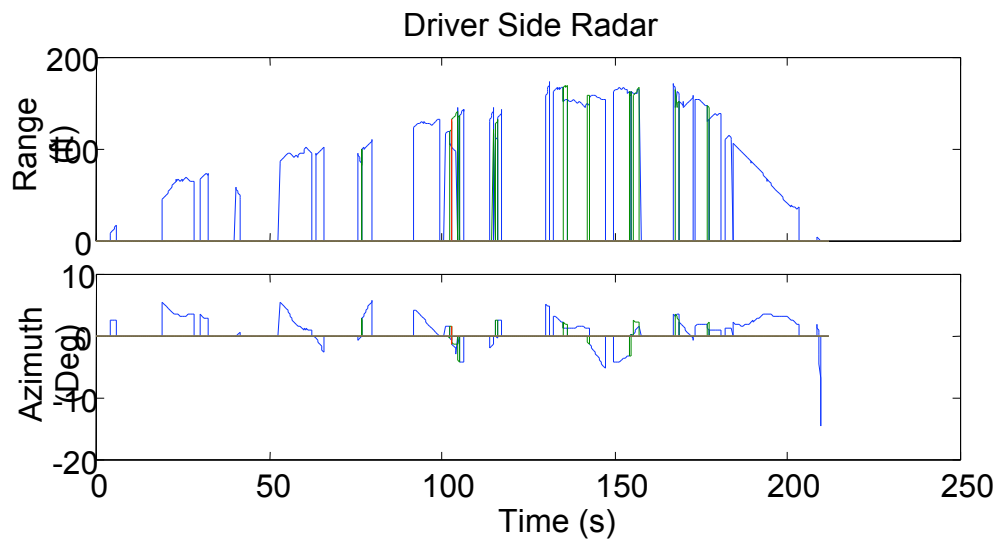


Fig. V.12 DRADAR data for system alignment

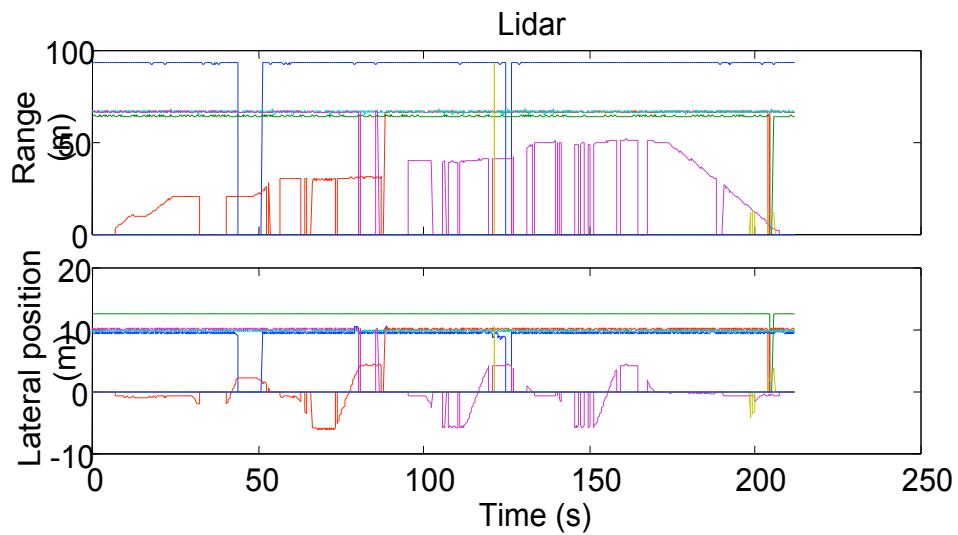


Fig. V.13 LIDAR data for system alignment

The target parameters on the marked locations were extracted from the data and transformed to the bus coordinate system (FCS). Deviations are then calculated with the assumption that the marked locations are precise. The deviations are listed in the following table and plotted in Fig. V.14. The average deviation of both distance and lateral position is less than 1m. This indicates the sensors are aligned well.

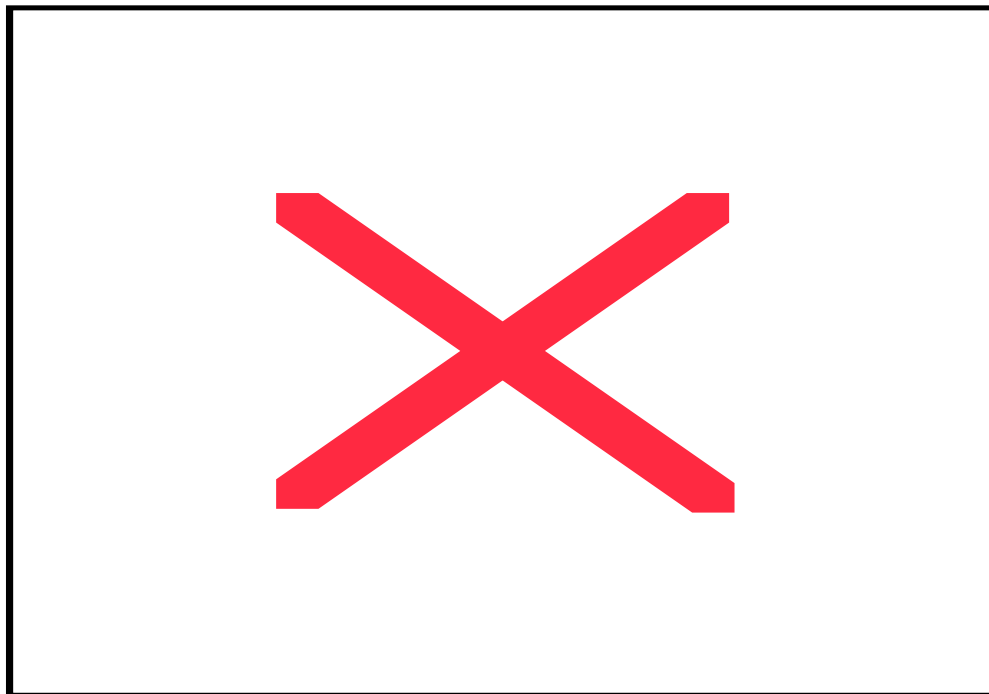


Fig. V.14 Object locations reported by sensors

Object locations reported by sensors

Locat. #	LIDAR				Passenger Side Radar				Driver Side Radar			
	Report		System (m)		Report		System (m)		Report		System (m)	
	R(H/L) ¹	L ²	Ds ⁵	Ls ⁵	R ³	□ ⁴	Ds ⁵	Ls ⁵	R ³	□ ⁴	Ds ⁵	Ls ⁵
1	8/00	-9	10.32	0.23	340	-19	10.43	-0.66	Missed			
2	16/29	-9	20.85	0.40	690	-11	21.10	-0.59	680	30	20.76	-0.26
3	Missed				Missed				Missed			
4	16/30	23	20.86	-2.80	Missed				Missed			
5	24/00	-8	30.80	0.46	910	-5	27.81	-0.77	930	18	28.4	-0.04
6	23/33	-58	29.85	5.46	Missed				Missed			
7	24/29	42	31.09	-4.54	860	45	26.17	-3.41	Missed			
8	31/88	-7	40.56	0.53	1253	-3	38.26	-0.82	1290	12	39.38	0.04
9	30/90	-57	39.38	5.53	Missed				1442	-37	43.90	4.23
10	32/40	43	41.44	-4.47	1375	41	41.84	-4.48	Missed			
11	39/30	-7	50.22	0.7	1680	-7	51.27	-0.33	1680	22	51.23	-1.27
12	38/80	-57	49.44	5.7	Missed				1628	-38	49.55	4.75
13	40/20	43	51.4	-4.3	1752	27	53.39	-3.53	Missed			
Deviation Range	-	-	-0.62 1.44	0.23 0.7	-	-	-3.83 3.39	-0.77 1.59	-	-	-1.60 3.90	-1.27 0.04
Average Deviation	-	-	0.52	0.49	-	-	-0.09	0.05	-	-	0.54	-0.43

1. Range. 'H/L' are two bytes of Lidar report. The LSB of H-byte is 1.28m and that of L-byte is 0.01m.
2. Lateral position.
3. Radar range is an integer, multiples of 0.1ft.
4. Azimuth angle. Radar azimuth angle is an integer, multiples of 0.002rad.
5. Distance and lateral position in bus coordinate system.

Host vehicle parameter

Offset

The following host vehicle (bus) parameters are biased in the collected data: steering angle, acceleration, brake pressure and wheel speed. The biased values were measured when the bus was stationary and are listed in the following table.

Host vehicle parameter biased values

Parameter	Biased Value(V)
Steering Angle	7.36
X Acceleration	2.40
Y Acceleration	2.45
Z Acceleration	2.45
Brake Pressure	1.02
Wheel Speed	0.038574

Sensitivity

Steering angle sensor

The bus hand-wheel was turned counterclockwise as far as it would go, held for five seconds, then turned clockwise step by step. For each step the hand-wheel was rotated 120 degrees and held for five seconds (the last turn was less than 120 degrees). The steering angle sensor outputs when the hand-wheel was held are listed below:

```
8.715820 (anticlockwise end)
8.525391
8.374023
8.198242
8.012695
7.822266
7.631836
7.441406
7.255859
7.070312
6.894531
6.723633
6.562500
6.406250
6.254883
6.201172 (after the last turn)
```

Average sensitivity factor is 1.5 mV/degree. Average angle-to-voltage ratio is 687.6148 degrees/V. The Steering ratio is 20.42:1 (for every degree of road wheel change requires 20.42 degrees of handwheel input). The wheel base is 279 inches.

Accelerometer

The accelerometer sensitivity is given by Summit Instruments[] as (unit: mV/g):

Accelerometer sensitivity

	To X Acceleration	To Y Acceleration
X Sensitivity	1302.31	8.76
Y Sensitivity	-13.07	1299.00
Z Sensitivity	-3.25	2.97

The accelerometer was not calibrated on the bus.

Brake pressure

The brake pressure transducer output is proportional to the pressure. The sensitivity factor is 50mV/psi. The pressure range is 0-100psi. The corresponding output range is 1-6V.

Data storage

This project has generated large amounts of data. Currently there are over 200 gigabytes of video and sensor data. The data was initially stored on one computer with three large hard drives but soon the data storage reached its maximum capacity. A new storage solution was therefore developed. This new storage method is built using a RAID. It currently has 800 gigabytes of

storage capacity which will allow this project to collect full data from three buses for one year. The RAID can be expanded to 1.5 terabytes if necessary. Later in the project we expect to perform more selective data collection which will reduce the rate of data collection. This will be done by only collecting data when the warning algorithm has given an alert. The new storage system is connected through the internet to allow users obtain data online. The RAID-based storage system has proven to be the most convenient and economical solution to our data storage needs.

References

2. Denso Lidar documents, Denso Inc.
3. Lenz, R.K.; Tsai, R.Y. Techniques for calibration of the scale factor and image center for high accuracy 3-D machine vision metrology, *Pattern Analysis and Machine Intelligence*, IEEE Transactions on , Volume: 10 Issue: 5 , Sept. 1988, Page(s): 713 -720.
4. Bacakoglu, H.; Kamel, M.S. A three-step camera calibration method. *IEEE Transactions on Instrumentation and Measurement*, vol.46, (no.5), IEEE, Oct. 1997. p.1165-72.
5. Weng, J.; Cohen, P.; Herniou, M. Camera calibration with distortion models and accuracy evaluation. *IEEE Transactions on Pattern Analysis and Machine Intelligence*, vol.14, (no.10), Oct. 1992. p.965-80.
6. Wu, L.D., *Computer Vision*, Fudan University, China, Dec.